A Study of the Effect of In-Cylinder Flow on Auto-Ignition Behavior of HCCI Combustion

筒内流動が HCCI 燃焼の自着火挙動に及ぼす影響に関する研究

千葉大学大学院融合理工学府

基幹工学専攻 機械工学コース

鐘 芸文

A Study of the Effect of In-Cylinder Flow on

Auto-Ignition Behavior of

HCCI Combustion

筒内流動が HCCI 燃焼の自着火挙動

に及ぼす影響に関する研究

千葉大学大学院融合理工学府

基幹工学専攻 機械工学コース

鐘　芸文

TABLE OF CONTENTS

ABSTRACT

To meet the increasingly stricter environmental standards for automobiles, reducing engine-out emissions and increasing thermal efficiency have been hot issues during the recent decade. Homogeneous charge compression ignition (HCCI) is well-known as the state-of-the-art combustion mode to decrease emissions and fuel consumption. With the benefits of a greater compression ratio and lower combustion temperature, HCCI can achieve a favorable thermal efficiency even higher than diesel engines and ultra-low emissions. Since HCCI is greatly determined by the chemical reaction rather than the mixing process, the combustion duration is very short, making it difficult to control the ignition timing well. Moreover, the strict demand for in-cylinder conditions during HCCI combustion greatly limits its possible operating window. Especially under high load conditions, the engine cylinder is prone to suffer from significant damage due to the sharp increase in pressure rise rate. Therefore, optimizing the in-cylinder conditions is crucial to extend the HCCI operating window with stable combustion. Thermal stratification is considered one of the most effective ways to mitigate pressure rise rate under high load conditions. However, the effects of in-cylinder conditions, such as flow motion and turbulence intensity, are still not clearly understood. Therefore, this study aims to investigate the thermal stratification varied with different turbulence levels and in-cylinder flow under HCCI combustion. A newly developed rapid compression and expansion machine (RCEM) was employed to reproduce the typical HCCI high load condition. In-cylinder turbulence was created by the special piston equipped with a flow guide plate. Meanwhile, the ambient temperature distribution in the cylinder was determined by the wall temperature controlling system, which was controlled by the independent coolant passages. Additionally, high-speed imaging was carried out to provide a deep insight into HCCI combustion. The numerical simulation using large eddy method coupled with a detailed chemical reaction was conducted as well. The results show that the HCCI mode is potential to be improved under high load conditions with full consideration of in-cylinder turbulence.

NOMENCLATURE

HCCI	Homogeneous Charge Compression Ignition
RCEM	Rapid compression and expansion machine
EGR	Exhaust Gas Recirculation
PM	Particulate Matter
TDC	Tom Dead Center
BDC	Bottom Dead Center
LES	Large Eddy Simulation
LTO	Low Temperature Oxidation
HTO	High Temperature Oxidation
A/F	air-fuel ratio
RON	Research Octane Number
PRF	Primary Reference Fuel
CA50	Crank Angle of 50 % mass burned
CA10-90	Combustion duration
SI	spark ignition
CI	compression ignition
NA	natural aspirated engine
BSFC	brake specific fuel consumption
Tt	total temperature
Ts	static temperature
Td	dynamic temperature
PIV	Particle image velocimetry
PLIF	Plane laser induced florescence
HC	Hydrocarbon compounds
CO	Carbon monoxide

Chapter 1　　Introduction

1.1 Background

With the world facing one of the most widespread and severe energy crises of modern times, energy efficiency has become increasingly valuable in addressing issues such as energy security, affordability, and climate change. As the main power source for various transportation devices such as motor vehicles, marine transport, and aerospace transport, internal combustion engines are major consumers of petroleum resources and significant contributors to air pollution emissions. In recent years, these engines, primarily running on oil, face the immediate threat of oil resources being depleted. This reality, coupled with the growing concern over global warming caused by greenhouse gas (GHG) emissions from human activities, has underscored the necessity of maximizing power output with the least amount of fuel. Thus, fuel efficiency has emerged as a critical challenge in the development of internal combustion engines since reducing fuel consumption can significantly decrease CO_2 emissions.

Although current internal combustion engines have achieved a commendable level of thermal efficiency, there is still potential for significant improvement. Figure 1.1shows Global CO2 emission and fuel consumption regulations for passenger vehicles. As global warming garners more attention, major countries around the world have been gradually setting their sights on a target of around 100g/km for passenger-car CO2 emissions since 2020. As a result, fuel efficiency regulations are likely to become even more stringent, necessitating further research focused on optimizing the combustion process to improve these engines' thermal efficiency.
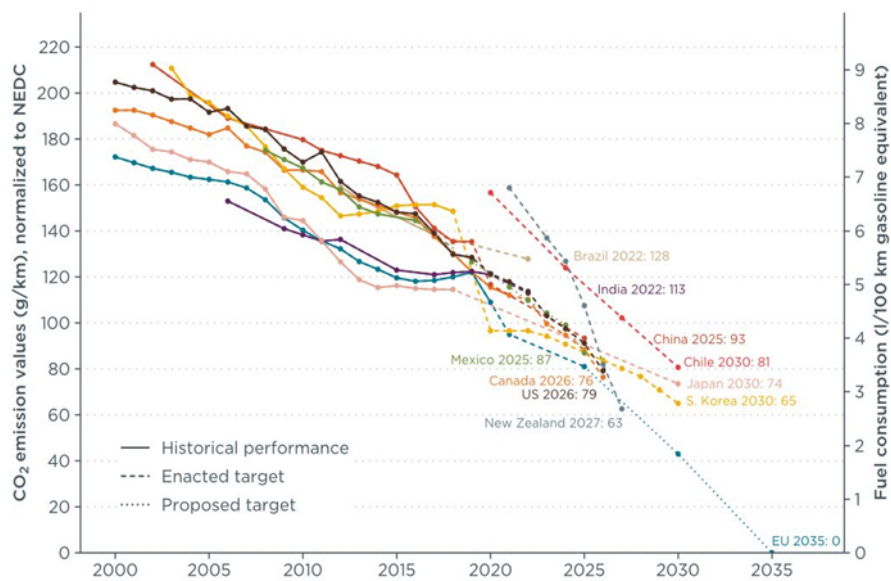
Figure 1.1 Global CO_2 emission and fuel consumption regulations for passenger vehicles

Although countries around the world have been making great efforts to develop electric vehicles in recent years, the traditional fuel-fired internal combustion engine will not disappear from the landscape in the coming decades. In its Energy Technology Perspectives 2012, the IEA (International Energy Agency) published an outlook on the number of EVs and PHVs in several scenarios, Figure 1.2. The graph shows that even though EVs and FCVs are gaining popularity as the next generation of vehicles, improving the thermal efficiency of the vehicle's internal combustion engine is becoming more important. Contemporary research on internal combustion engines focuses on reducing emissions and improving fuel economy to meet stricter regulations and compete with electric vehicles. In recent years, a new advanced combustion method, Homogeneous Charge Compression Ignition (HCCI), has gained significant attention in the global industry of fuel-powered cars and vehicles due to its significant fuel-saving performance and low emission output. Compared to conventional gasoline engines using spark ignition, HCCI combustion can significantly reduce NOx emissions and improve fuel efficiency by 15% to 20%. This type of combustion makes it possible to solve one of the most challenging problems in terms of NO_x and soot emissions. HCCI combustion has become one of the most popular research areas in the global internal

combustion engine industry due to its energy-saving and pollution-reduction features.
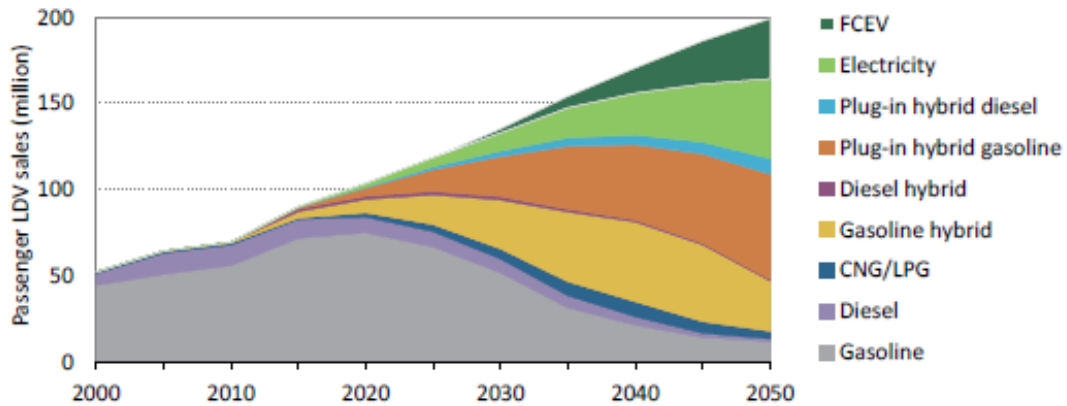
Figure 1.2 Global portfolio of technologies for passenger LDVs

1.2 An Advanced Combustion Mode – HCCI

Internal combustion engines can be divided into petrol and diesel engines depending on the fuel used. Gasoline is highly volatile, diffuses quickly, and is easily ignited by high-temperature heat sources, but it has a high self-ignition temperature, so it is suitable for ignition by spark plugs; diesel is less volatile and less easily ignited but has a long and unstable carbon chain and a lower self-ignition temperature, so it is suitable for spontaneous combustion caused by the rise in temperature of the gas in the cylinder through the compression process. Therefore, the difference between petrol and diesel leads to different ways of utilization. So, another fundamental difference between petrol and diesel engines is that they have very different modes of combustion, with gasoline engines having pre-mixed flame spread combustion and diesel engines having mainly diffusion combustion. As a result of the different combustion modes, the efficiency and pollutant emissions of petrol and diesel engines can differ significantly. The HCCI engine combines the characteristics of "diesel compression combustion" and "gasoline homogeneous mixing." Compared to conventional petrol engines, the throttle and spark plugs are no longer required. Compression ignition allows the mixture to fire at multiple points simultaneously, resulting in a shorter combustion duration and a higher

thermal efficiency comparable to that of a compression ignition engine; In contrast, compared to conventional diesel engines, the mixture is formed in a homogeneous state, resulting in better mixing, simultaneous combustion reactions, lower combustion flame temperatures, and lower NOx and soot emissions. Figure1.2 shows the differences among SI, CI and HCCI engines.
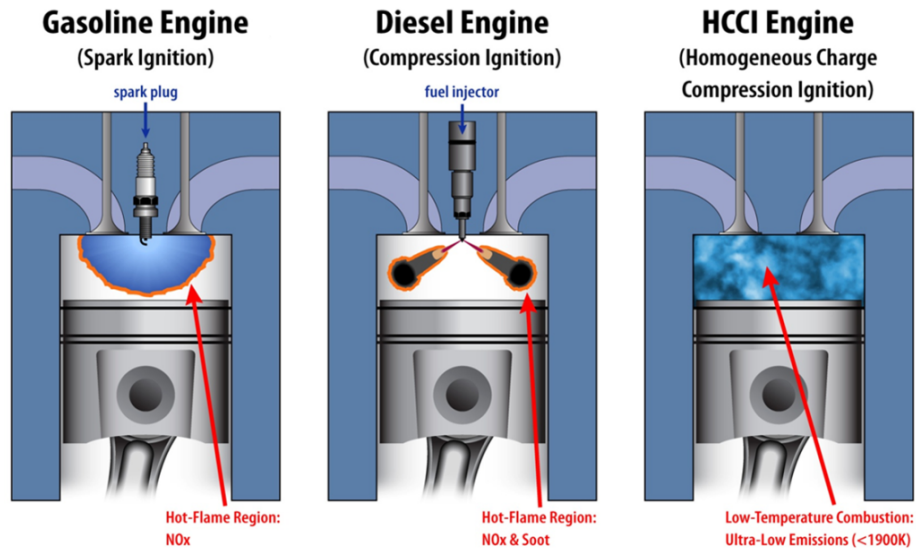
Figure 1.3 The differences among SI, CI and HCCI engines

Subsequently, many researchers have gradually expanded the concept and implication of this combustion mode (HCCI) and evolved from the initially completely homogeneous compression ignition. Its central aspect is a controlled premixed low-temperature combustion process characterized by multi-point ignition, high thermal efficiency, ultra-low NOx, and PM (Particulate Matter) emissions.

1.2.1 Brief History of HCCI

HCCI is a technology that has been around for a long time. From (Onishi et al., 1979) the concept of uniform charge compression ignition (Active Thermo-Atmosphere Combustion, ATAC) was introduced in gasoline-fueled two-stroke engines [1]. They found that the two-stroke engine could run smoothly without spark plugs and had a wider air-fuel ratio range for smooth operation than the original engine, as well as improved stability, lower fuel consumption and NOx, HC, and CO emissions. It was then known under a different name,

ATAC [1], and was officially called HCCI first time in 1989[2]. (Thring, 1989) first presented the concept and carried out an experimental study of the HCCI engine using a gasoline fuel mixture. This was a milestone for internal combustion engines, as he determined the air-fuel ratio and EGR operating MAP for HCCI of a single-cylinder, four-stroke engine.

HCCI is a combustion technology that has been around for several decades. The concept of HCCI was first introduced by Onishi et al. in 1979, who developed a gasoline-fueled two-stroke engine that could run smoothly without spark plugs and had a wider air-fuel ratio range for smooth operation than the original engine [1]. This technology was initially called Active Thermo-Atmosphere Combustion (ATAC). Later, in 1989, Thring [2] presented the concept of HCCI and conducted an experimental study using a gasoline fuel mixture. His study was a significant milestone for internal combustion engines as it determined the air-fuel ratio and EGR operating MAP for HCCI of a single-cylinder, four-stroke engine. This is the origin of the concept of HCCI.

HCCI combustion, on the other hand, uses petrol but uses compression to make the mixture ignite automatically.   In an HCCI engine, the fuel and air are completely pre-mixed, and the mixture is lean. The mixture is compressed in the cylinder and as it compresses the temperature and pressure of the mixture rises rapidly to a critical point where the mixture spontaneously ignites (auto-ignition). Because the mixture is homogeneous and the temperature of the gases in the cylinder is almost the same, the autoignition occurs rapidly in all parts of the cylinder and the combustion is completed quickly. But The moment of auto-ignition and the rate of combustion of the gases are determined by the thermodynamics and chemical kinetics of the mixture and there are no external factors that can directly control them.

1.2.2 The Benefits of HCCI Combustion

The Combustion mode of traditional SI engine (Flame propagation). In an SI engine, the air-fuel mixture temperature during compression is so low that it never spontaneously catches fire. At the right time, the spark plug discharge, and combustion starts. The combustion releases heat and raises the local temperature in the area around the spark plug. The high-temperature

flame then raises the temperature of the unburnt area of the gas to reach the ignition point and start to burn, and the flame spreads on. However, the unburned gas temperature in the distance is still very low, so it does not ignite on its own. During combustion, the gas expands and compresses those not burning gases. Hence, the temperature of the unburned gas body rises slightly but is still below the self-ignition temperature until combustion is complete. Exceptionally, suppose the combustible gas mixture is already at a high temperature before combustion. In that case, the unburned gas may be compressed above the spontaneous ignition temperature during flame propagation so that the unburned gas can burn together instantaneously and knock.

In HCCI engine, the gas temperatures in the cylinder are very high due to the high compression ratio, some gases are a little warmer, and some are a little cooler. The highest temperature gas burns first and releases heat, while the lower temperature gas is above the ignition limit and, therefore, also starts to ignite. This is a very fast process. To take an extreme example, if the temperature of the gases in the cylinder is high enough, then in a moment, all the gases will spontaneously ignite and finish burning. At this point, it would be exactly the same as the ideal Otto cycle. However, as the cylinder wall is cold, the air-fuel mixture will be in different temperatures. Hence, the ignition times are slightly sequential because the gases that lean towards the cold side need to be a little bit of heat to ignite, and the hot spots burn, and the ones that are a little bit around them burn quickly rather than spreading outwards from the center, as in the SI engines.

The combustion mode of HCCI results in two major advantages of HCCI high combustion efficiency and low emissions.

The main reasons for the high efficiency of HCCI are.

1. Lean mixture

2. High compression ratio

3. High speed near isovolumetric combustion close to the ideal Otto cycle

4. Low-temperature combustion

5. No pump gas losses.

And among the above, the main reasons that make HCCI low emissions are 1 and 4.

The low combustion temperature of HCCI (<1800K) reduces heat transfer as well as the NOx emission even under oxygen-enriched conditions, which is even lower than the NOx emission level of a normal spark-ignition gasoline engine with a triple-effect catalytic converter. It can fully meet the most stringent emission regulations in the world. Because of the pre-mixed combustion, there is no phenomenon of diffusion combustion similar to diesel engines, which makes the PM emission nearly zero. The simultaneous ignition of multiple points makes the combustion speed higher than the turbulent flame propagation speed of a normal spark ignition gasoline engine, making the engine closer to the equivalent Otto cycle and thus further improving thermal efficiency. In addition, reducing the combustion temperature can also effectively reduce NOx emissions. The following picture, Figure 1.4, is very famous. The horizontal axis is the air-fuel ratio; the definition of the air-fuel ratio is different in different places, the air-fuel ratio is thin when it is less than 1, and it is thick when it is more than 1. Soot emission is carbon soot. Obviously, soot will only be produced in the case of a rich mixture; the temperature is not high or low. NOx will be produced at high temperatures with rich oxygen, so both SI and CI engines will produce NOx. Then, if using low-temperature combustion and keeping the in-cylinder temperature below 2000K, NOx emissions will be completely negligible. Of course, the temperature should not also be too low, there is a CO-CO_2 critical conversion temperature of 1450K, therefore, the temperature is too low is not a good thing, the combustion will be incomplete, reduce the combustion efficiency and improve CO emissions.
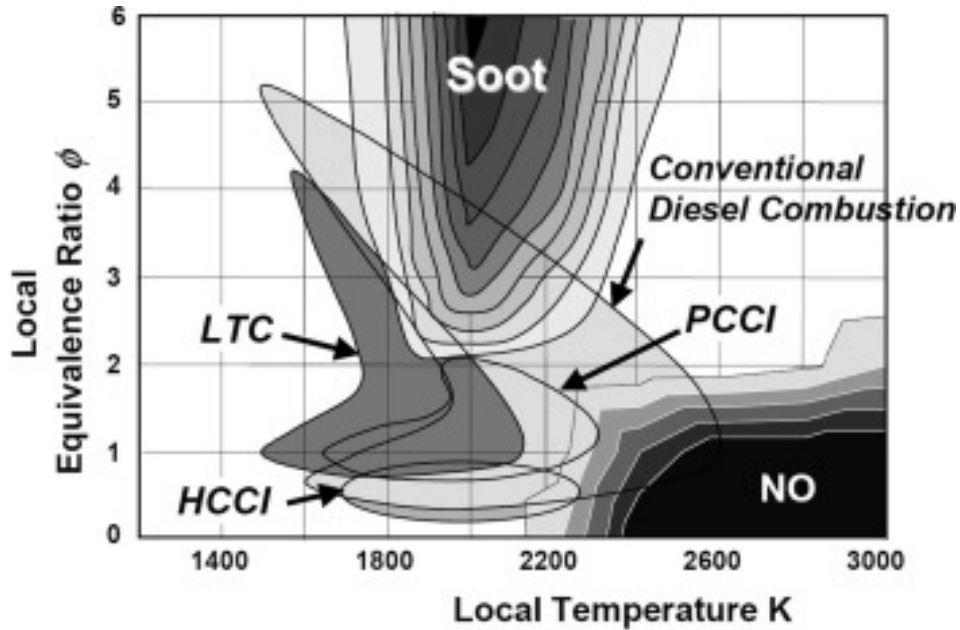
Figure 1.4 Operating range of various combustion concepts on the Φ–T Soot and NOx

generation map [3]

Although HCCI combustion has such an attractive prospect, there are still many technical difficulties that have not been solved, thus affecting the practical application of this combustion method.

1.2.3 Two Major Factors Restricting the Application of HCCI Combustion.

○ The ignition time of HCCI combustion is difficult to control.

To control the time of the start of combustion, SI gasoline engines can change the ignition time of the spark plug, and diesel engines can change the moment of in-cylinder injection, but the HCCI engine inhales a homogeneous mixture of gas. When the mixture is compressed, multiple points are burnt. So, the ignition time will be sooner, or later, is actually very difficult to determine, and there is no very effective way to control it. And so far, by adjusting parameters such as mixture composition, intake air temperature, and pressure, is difficult to achieve precise control.

○ The narrow operating range feasible for HCCI combustion

For many years, the biggest challenge preventing practical application was the very narrow operating range of HCCI feasibility.

At low loads, the mixture does not ignite consistently due to low temperatures, while knocking occurs at high loads. The reason for knocking is that the combustion is more rapid at high loads due to the increased fuel amount. This is due to the inability to properly control the ignition time according to the conditions. Various attempts have been made to control the ignition time by introducing boosting technology and EGR using a variable valve mechanism but with limited success.

1.3 Recent Studies on Achieving Stable Gasoline Engine HCCI Combustion and Control Strategies.

With the increasing stringency of emission regulation in the world, the contradiction between the oil supply and demand and the increasing research. And in order to break through the limits of both the lowest emissions and the highest thermal efficiency that exist in conventional internal combustion engines, internal combustion engine researchers around the world have been exploring a new generation of internal combustion engine technology. A new (HCCI) combustion technology was found to be the most promising alternative, and the theory associated with it has received increasing attention. A great deal of research on HCCI combustion, low temperature combustion, was carried out around the world in the late 1990s. It was found that this type of combustion discards the traditional diesel and petrol engine concept while retaining the advantages of the traditional diesel and petrol engines. Based on this theory, the cleanest and most heat-efficient combustion mode can be designed. It is broadly accepted that this is the most promising new combustion mode to meet the future ultra-low emission, or even to be able to lead to zero emission internal combustion engines. In the HCCI concept, the petrol engine meets the concept of homogenization, and as a high-octane fuel, how to perform compression ignition is a technical challenge for the petrol engine to solve. Therefore, other technologies needed to be developed to enable gasoline, which is not

susceptible to spontaneous combustion, to reach the temperatures and pressures at which spontaneous combustion occurs. Researchers at the time focused on how to create high temperature and pressure conditions in the cylinder to promote HCCI combustion in gasoline engines. Since 1989, when Thring [2] proposed the concept of homogeneous compression-ignition combustion, different methods of achievement have been proposed and carried out in great progress one by one.

1.3.1 To Achieve HCCI Combustion in Gasoline Engines

Previous studies on the realization of HCCI combustion in gasoline engines are described below.

To realize the autoignition of gasoline in HCCI combustion, it is necessary to increase the temperature of the mixture, which can be achieved through various methods. However, one of the most direct and effective ways to attain the required temperature for gasoline autoignition is through the inlet air charge heating method, which involves heating the incoming air charge to increase the temperature inside the combustion chamber without increasing fuel consumption. By raising the temperature of the mixture, this method reduces the temperature at which gasoline spontaneously ignites, thereby promoting the combustion process. Consequently, this method has garnered much attention in the field of HCCI combustion research and is widely studied. Thring [2] and Najt [4] achieved HCCI combustion by heating the inlet gas temperature to over 300°C using direct means of heating. At Brunel University, UK, Oakley and Zhao Hua et al. [5, 6] investigated the HCCI combustion of different high-octane fuels in a common inlet jet engine. To attain the required auto-ignition temperatures for gasoline at the end of the compression process and enable HCCI combustion, they utilized a heater at the inlet to raise the temperature of the inlet gas to a high temperature of 320°C. The direct heating method to achieve auto-ignition of a gasoline engine requires a high-power heating system, which makes it only suitable for research and not friendly for practical applications.

As an alternative, some researchers have proposed the use of heat exchangers to heat the

intake air using the energy from the engine's high-temperature exhaust gas for practical applications. This approach is represented by systems such as the Optimized Kinetic Process (OKP) [7, 8] and Fast Thermal Management (FTM) [9, 10] and is a viable option in the intake heating route. However, a major drawback of this solution is that factors such as temperature fluctuations in the high-temperature exhaust gas and the thermal growth inertia of the inlet air require a demanding control strategy, which may limit its performance under temporary conditions.

It is known that by increasing the compression ratio of a gasoline engine, the temperature and pressure of the mixture at the end of the compression stroke can be elevated, which aids in achieving HCCI. In contrast, conventional gasoline engines are typically limited by knocking and usually have a lower compression ratio, which is one of the primary reasons for their lower thermal efficiency compared to diesel engines [11]. However, in the earliest studies, Thring [2] found that excessively high compression ratios required dilution of the mixture to reduce the overly rapid combustion rate, thereby reducing the maximum load achieved by HCCI combustion. Subsequently, some researchers introduced variable compression ratio technology into the study of HCCI combustion and found that this technique could address the aforementioned issues.

Göran Haraldsson [12,13] carried out HCCI combustion experiments using VCR (variable compression ratio) and FTM (fast thermal management) strategies. The results show that the use of a combination of VCR (their range is from 9 to 21) technology and fast thermal management is one of the very effective ways to achieve HCCI combustion. Their study achieved a large operational range for HCCI combustion. Christensen et al. [14] studied the relationship between HCCI combustion and compression ratio for various blended fuels at different inlet temperatures on a Volvo TD100 diesel engine. The results show that the intake air temperature required to achieve HCCI combustion decreases as the compression ratio increases. Variable compression ratio technology (VCR) is not a very well-established technology, as it is not the best choice in view of the large range of compression ratio variations required for HCCI combustion and the fact that variable compression ratio technology is

currently too slow to develop and expensive. Therefore, some researchers propose modifying the fuel's composition and chemical properties to achieve suitable auto-ignition characteristics for HCCI combustion in gasoline engines. Studies [15-18] have shown that the fuel's properties significantly impact the HCCI combustion process. Modifying the fuel's properties can expand the range of HCCI combustion and improve emission and noise issues.

Exhaust Gas Recirculation (EGR) is another technology that can achieve HCCI combustion and is the most viable method for four-stroke gasoline engines. The basic idea behind EGR is to retain a portion of the high-temperature exhaust gas in the cylinder by changing the valve timing and using the energy from the exhaust gas to heat the fresh charge, enabling the charge to reach the conditions for auto-ignition. This simple solution utilizes the exhaust gases' thermal energy without requiring an intake heater. It also directly employs the residual exhaust gases as a diluent to reduce the heat release rate. Kaahaaina [19] used an electro-hydraulic valve train to keep the exhaust valve open continuously during the exhaust and intake strokes to achieve EGR for the CAI/HCCI combustion process. Duffour et al. [20] investigated the effects of two EGR strategies using an electro-hydraulic fully variable train and found that EGR can change the in-cylinder temperature distribution and exhaust gas distribution, affecting the HCCI combustion heat release process. Yamamoto et al [21] were the first to propose simultaneous HCCI combustion using in-cylinder direct multiple injection, and Willand[22] was the first to use a negative valve overlap angle to achieve HCCI combustion.

Numerous studies have emerged since then regarding the application of EGR for achieving HCCI combustion. Yamamoto et al. [21] were the first to propose simultaneous HCCI combustion using in-cylinder direct multiple injection, while Willand [22] used a negative valve overlap angle to achieve HCCI combustion. Kontarakis [23] achieved stable HCCI combustion in a single-cylinder four-stroke gasoline engine by reducing valve lift and valve opening duration with an excess air coefficient λ in a specific speed range. Bosch [24] and Lotus [25] conducted extensive research on this topic as well. As the internal EGR strategy is currently the most acceptable method for replacing conventional gasoline engine technology in achieving HCCI combustion, it was once considered the simplest and most feasible way to

achieve HCCI combustion in four-stroke gasoline engines [26].

The temperature of the mixture must be high enough to cause spontaneous combustion, but not so high as to cause detonation or excessive emissions. So, we can see that temperature control is critical to achieving HCCI combustion in gasoline engines. All the above studies have been carried out by influencing the temperature of the mixture in order to achieve HCCI combustion. However optimal HCCI combustion performance requires precise regulation of these parameters.

1.3.2 The Main Issues of HCCI Combustion

Although HCCI combustion in gasoline engines has great potential to simultaneously reduce fuel consumption and low emissions, and several implementations have been developed to date, HCCI combustion in gasoline engines still faces many challenges on the road to practicality. Many research authorities and researchers [27-30], such as the US Department of Energy and the SAE Society of Automotive Engineers, have outlined in their publications the technical issues that need to be solved to achieve HCCI combustion.

For gasoline HCCI, the main problems can be summarized in two points: the difficulty of controlling combustion and the difficulty of extending the load range.

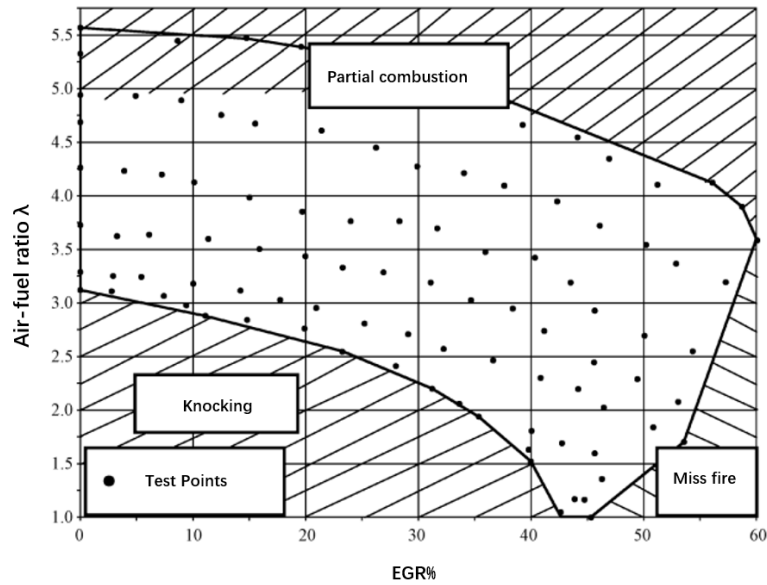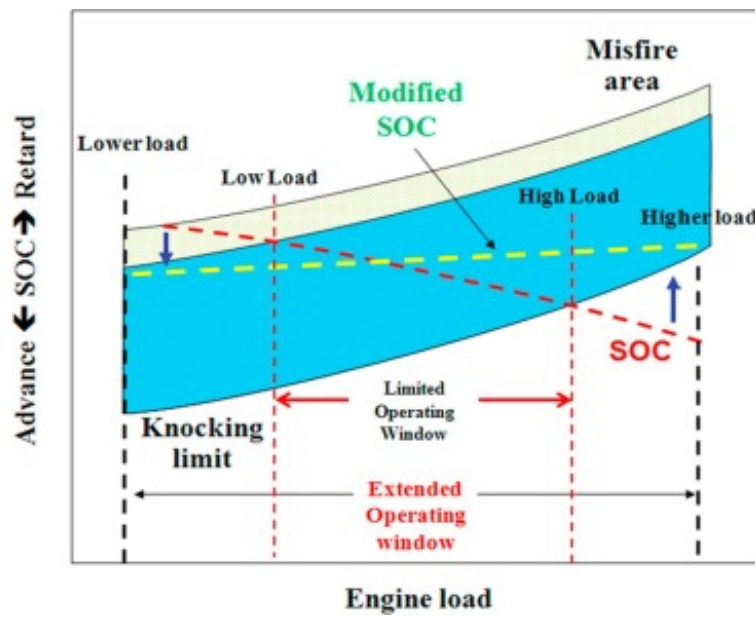Figure 1.5 Gasoline engine HCCI operating range

Figure 1.6 Limited (due to misfire and knock) and Extended (by modifying SOC) operating window of HCCI engine.

Although some auxiliary measures are generally taken to reduce the difficulty of spontaneous combustion of homogeneous mixture compression, but because HCCI combustion is controlled by chemical reaction kinetics, there is no mandatory means of ignition

control, it is difficult to control the moment of ignition and the rate of combustion, so at lower loads misfire occurs. At high loads the phenomenon of explosion occurs due to rapid pressure rise caused by rapid heat release and is still not completely avoidable. In additional, when the engine speed is too high, the chemical reactions do not take place in time and can lead to a failure of HCCI combustion. This means that HCCI can only be used at low to medium speed and under low to medium load conditions.

In recent years, many research institutes, universities and other institutions have made significant progress in the control of HCCI steady-state combustion. By controlling parameters such as inlet gas temperature, mixture concentration, in-cylinder components and compression ratio, the ignition point, and combustion rate can be effectively controlled. However, in the aspect of HCCI operating load, it is difficult to make significant progress. The reason for this is that HCCI has a significantly higher heat release rate and pressure rise rate than a normal engine due to the simultaneous ignition of multiple points. Especially at high loads, the maximum in-cylinder combustion pressure and pressure rise rate reach an unacceptable level, while the in-cylinder combustion temperature rises, leading to a sharp rise in NOx emissions and making the advantages of the HCCI combustion mode non-existent. As there is no mandatory means of ignition for HCCI combustion, control of the ignition timing and burning rate must be done indirectly by changing the in-cylinder environment, so it is important to address these difficulties to widen the load limit of HCCI.

To solve the difficulties of HCCI combustion control and the narrow load range. Fundamental research on HCCI combustion has been developing. Research on the combustion mechanism, ignition factors and testing and diagnosis methods are being carried out in many research institutes. To gain a deeper understanding of the HCCI mechanism, research into practical HCCI technology has become a top priority. Research on HCCI combustion control, both for gasoline and diesel fuels, has received a considerable amount of attention. Highly practical, studies on mode transitions of HCCI and SI combustion and the process of changing operating conditions within the HCCI mode [31-44], and in-cylinder information feedback methods [33,45,46], have made considerable progress.

Because HCCI combustion has better fuel adaptation, HCCI research for various surrogate fuels has been carried out for lots of years [47-52]. Advanced methods of optical testing have also been extensively applied to the basic study of this mode of combustion [53-61]. By means of the visualization, several questions about poorly understood combustion concepts have been clearly clarified. As well as traditional experimental methods, Numerical Simulation has been used extensively, with the development of various models based on Computational Fluid Dynamics (CFD) and detailed chemical reaction kinetic simulations [62-67].

1.3.3 Studies of The Effect of Charge Stratification on The Ignition and Combustion of HCCI

In the studies that have been conducted over these years, regardless of the research method and strategy used. In the end, the key to HCCI combustion is still boundary conditions such as temperature and the influence of chemical kinetics. Recently it has been found that although chemical kinetics plays an important role in HCCI combustion, the premixing process has an important influence on HCCI combustion. The differential fuel concentration distribution and temperature inhomogeneities that occur during the mixing process significantly affect the ignition and combustion process, and the inhomogeneous distribution of HCCI combustion still plays an important role. Sjöberg et al. concluded that thermal stratification is naturally found in all real engines, allowing him to be shown to slow down the combustion rate [68]. They also found that the introduction of 5% temperature stratification could match the measured pressure rise rate of HCCI combustion using a multi-zone chemical reaction kinetics model [69]. The chemical reaction kinetics model also showed that the highest temperature zone ignited first, with the remaining zones igniting sequentially as the temperature increased. The large temperature distribution (large thermal stratification) causes an increase in the duration of the combustion, and therefore the pressure rise rate is within an acceptable range. The latest findings of Dec et al. [70] further demonstrate that HCCI combustion is not homogeneous and that even a well-pre-mixed mixture with a strong disturbance in the outside of the cylinder is structured with a high degree of disturbance. This is mainly due to the thermal

stratification that occurs during the heat transfer and turbulent motion of the compression stroke. These thermal stratifications contribute to the non-uniformity of HCCI combustion. HCCI combustion occurs from the hottest, most suitable point for ignition towards HCCI combustion occurs from the hottest, most suitable point of ignition to the cooler regions, and processes like this can effectively reduce the rate of pressure rise.

1.4 Purpose of This Study

The objective of this paper is to investigate the mitigation mechanism of tailored in-cylinder flow on HCCI combustion heating through a combination of experiments and numerical simulations to find ways to extend the high load limit of homogeneous charge compression ignition (HCCI) combustion. We constructed an experimental system that can generate various temperature distributions and airflow patterns in the cylinder (based on a fast compression expansion device). The effect of tumbling airflow on the rate of HCCI combustion rise was experimentally investigated by combustion analysis and visual observation. Proper turbulence in the cylinder is generated by a special piston equipped with a deflector plate that allows the intensity and scale of the flow to be varied by special settings. At the same time, the ambient temperature distribution in the cylinder is determined by a wall temperature control system, which is controlled by a separate coolant channel.

Direct photographs show that as the in-cylinder flow is enhanced, multiple ignition points are formed in the combustion chamber, the heat release rate is relatively small, and the increase in the pressure rise rate is suppressed. The pressure rise rate varies with the turbulence intensity. The effects of temperature distribution and tailored turbulence on homogeneous charge compression ignition (HCCI) were also investigated numerically using large eddy simulation (LES) and detailed chemical reaction mechanisms. Comparison of numerical results with and without flow conditions shows that the combustion time is prolonged under enhanced flow conditions, which is consistent with experimental results. And the effect of turbulence on the mitigation of heat release and pressure rise varies with the type of flow and the intensity of turbulence.

1.5 Outline

In accordance with the previously described research background and objectives, a newly developed Rapid Compression and Expansion Machine (RCEM) was used in this study to reproduce typical HCCI high load conditions. The RCEM used in this study is also featured by the ability to generate specific in-cylinder flow which is generated by a special piston equipped with a flow guide plate. At the same time, the ambient in-cylinder temperature can be controlled. The temperature distribution in the cylinder is determined by the cylinder wall temperature control system. In this system the temperature distribution is controlled by separate coolant channels. It is also possible to switch from a normal metal window to a sapphire window of the same shape to achieve a visual observation of the HCCI combustion.

In this study, the combustion process, ignition mechanism and pressure rise rate of HCCI with normal no-flow and no temperature distribution condition, with temperature distribution only condition and with different in-cylinder flow (three different turbulence intensities) are investigated through a series of experiments and direct visualization conducted on this RCEM. This paper also combined with CFD numerical simulations to verify the results of enhanced in-cylinder flow on extending the HCCI combustion time, reducing the pressure rise rate, etc.

Chapter 1 (this chapter) is the introduction, which discusses the background and significance of the subject. In this chapter, HCCI combustion mode research history, progress, and status are briefly reviewed. The essential nature and characteristics of HCCI combustion are summarized, as well as the difficulties faced by this technology at this stage. In order to overcome the difficulties, the main research content and research objectives of this study are presented as a guideline.

Chapter 2 describes the use of a newly developed metal version of the RCEM with a flow generation system and a wall temperature control system to experimentally verify the effect of the HCCI heat release pattern for different flow intensities and the effect of extended combustion periods with reduced pressure rise rates.

Chapter 3 A direct photographic experiment was conducted to investigate the effect of

enhanced in-cylinder flow on the HCCI. Optical accessibility was achieved by making some changes to the RCEM presented in Chapter 2. This experiment obtained visualization results for temperature stratification, base no-flow, and previously experimentally verified combustion processes under strong flow and mid-flow conditions. Image processing of the experimentally obtained visualization results was also carried out to obtain the time evolution of the reaction zone under different conditions. To clarify the role of flow on HCCI combustion.

Chapter 4 investigates the numerical simulation of the experimental conditions of the HCCI. The experimental results are verified by comparing the simulation results with the experimental results. The results are examined and analyzed in detail by means of a combination of experiments and simulations, and some conclusions are drawn to investigate the influence of key factors. The results of these simulations agree with the experimental results.

In the final concluding chapter, Chapter 5, this thesis's main research work and results are summarized, the main innovations are summarized, and ideas for further research are presented.

Reference

[1] Onishi, S., Jo, S., Shoda, K., Jo, P. et al., Active Thermo-Atmosphere Combustion (ATAC) - A New Combustion Process for Internal Combustion Engines, SAE Paper, 1979, 790501.

[2] R. H. Thring, Homogeneous Charge Compression Ignition (HCCI) Engines, SAE Paper, 1989, 892068.

[3] E. Shim, H. Park, C. Bae Comparisons of advanced combustion technologies (HCCI, PCCI, and dual-fuel PCCI) on engine performance and emission characteristics in a heavy-duty diesel engine, Fuel, 262 (2020), p. 116436

[4] Najt P. M., Foster D. E. ， Compression-ignited homogeneous charge combustion. SAE Paper, 1983, 830264.

[5] Aaron Oakley, Hua Zhao and Nicos Ladommatos, Experimental Studies on Controlled Auto-ignition (CAI) Combustion of Gasoline in a 4-Stroke Engine, SAE Paper, 2001, 2001-01-1030.

[6] Aaron Oakley, Hua Zhao, and Nicos Ladommatos，Dilution Effects on the Controlled Auto-Ignition (CAI) Combustion of Hydrocarbon and Alcohol Fuels, Brunel University, SAE Paper, 2001, 2001-01-3606

[7] Jialin Yang, Todd Culp and Thomas Kenney, Development of a Gasoline Engine System Using HCCI Technology - The Concept and the Test Results, SAE Paper, 2002, 2002-01-2832.

[8] Jialin Yang and Thomas Kenney, Robustness and Performance Near the Boundary of HCCI Operating Regime of a Single-Cylinder OKP Engine, SAE Paper, 2006, 2006-01-1082.

[9] Joel Martinez-Frias, Salvador M. Aceves, Daniel Flowers et al, HCCI Engine Control by Thermal Management, SAE Paper, 2000, 2000-01-2869.

[10] Giran Haraldsson, Per Tunest, Bengt Johansson, Jari Hyvnen, HCCI Closed-Loop Combustion Control Using Fast Thermal Management, SAE Paper,
2004, 2004-01-0943.

[11] Heywood, J. B. (2018). Internal Combustion Engine Fundamentals. Internal Combustion Engine Fundamentals Second Edition.

[12] Göran Haraldsson; Per Tunestål; Bengt Johansson; Jari Hyvönen; "HCCI Closed-Loop Combustion Control Using Fast Thermal Management", SAE INTERNATIONAL JOURNAL OF ENGINES, 2004.

[13] Jari Hyvönen; Göran Haraldsson; Bengt Johansson; "Operating Conditions Using Spark Assisted HCCI Combustion During Combustion Mode Transfer to SI in A Multi-Cylinder VCR-HCCI Engine", 2005.

[14] Magnus Christensen, Anders Hultqvist et al., Demostrating the Multi Fuel Capability of a Homogeneous Charge Compression Ignition Engine with Variable Compression Ratio, SAE Paper, 1999, 1999-01-3679.

[15] Aaron Oakley, Hua Zhao, and Niscos Ladommatos, Dilution Effects on the Controlled Auto-Ignition (CAI) Combustion of Hydrocarbon and Alcohol Fuels, SAE Paper, 2001, 2001-01-3606.

[16] Tanet, A., Volker, S., An Investigation into the Effect of Fuel Composition on HCCI Combustion Characteristics, SAE Paper,2002, 2002-01-2830.

[17] Nicolas, J., Xavier, M., Pierre, D., Engine and Fuel Related Issues of Gasoline CAI (Controlled Auto-Ignition) Combustion, SAE Paper, 2003, 2003-01-1856.

[18] Olsson, J., Johansson, B., Closed Loop Control of an HCCI Engine, SAE Paper, 2001, 2001-01-1031.

[19] N. Kaahaaina, et al., Use of Dynamic Valving to Achieve Residual –Affected Combustion, SAE Paper, 2001, 2001-01-0549.

[20] Florence Duffour, Franck Vangraefschèpe, Vincent Knop and Loic de Francqueville, Influence of the Valve-lift Strategy in a CAI Engine using Exhaust Gas Re-Breathing – Part 1: Experimental Results and 3D Analysis, SAE Paper, 2009, 2009-01-0299.

[21] Shigeo Yamamoto, Takahiro Satou and Motoki Ikuta, Feasibility Study of Two-stage Hybrid Combustion in Gasoline Direct Injection Engines, SAE Paper,2002, 2002-01-0113.

[22] J.Willand, R-G. Nieberding, G. Vent, C. Enderle, The Knocking Syndrome-Its Cure and Its Potential, SAE Paper, 1998, 982483.

[23] George Kontarakis, Nick Collings and Tom Ma, Demonstration of HCCI Using a Single Cylinder Four-stroke SI Engine with Modified Valve Timing, SAE Paper, 2000, 2000-01-2870.

[24]Andre Kulzer, Jean-Pierre Hathout, Christina Sauer et al, Multi-Mode Combustion Strategies with CAI for a GDI Engine, SAE Paper, 2007, 2007-01-0214.

[25] J. W. G. Turner, G. Pitcher, P. Burke, The HOTFIRE Homogeneous GDI and Fully Variable Valve Train Project - An Initial Report, SAE Paper, 2006, 2006-01-1260.

[26] Wolters, P., Salber, W., Geiger, J., Duesmann, M. et al. Controlled Auto Ignition Combustion Process with an Electromechanical Valve Train[C]. SAE Paper, 2003, 2003-01-0032.

[27] U.S. Department of Energy, Energy Efficiency and Renewable Energy Office of Transportation Technologies, Homogeneous Charge Compression Ignition (HCCI) Technology- A Report to the U.S. Congress，April 2001.

[28] Fuquan (Frank) Zhao, Thomas W. Asmus, Dennis N. Assanis, et al., Homogenous Charge Compression Ignition (HCCI) Engine: Key Research and Development Issues, Society of Automotive Engineers, 2002.

[29] Christensen, M., Johansson, B., Influence of mixture quality on premixed-charge compression ignition gasoline engine, SAE Paper, 1998, 982454.

[30] Rudolf H.Stanglmaier et al., Homogeneous Charge Compression Ignition(HCCI):Benefits, Compromises, and Future Engines Applications, SAE Paper, 1999,1999-01-3682.

[31] Hans-Otto Herrmann, Rüdiger Herweg, Günter Karl. Regelungskonzepte in Ottomotoren mit homogen-kompressionsgezündeter Verbrennung// Congress „Haus der Technik"Controlled Auto Ignition, Essen, Oktober 2005.

[32] Nebojsa Milovanovic, Jamie Turner, Dave Blundell, et al. Requirements for the valve train in CAI gasoline engines// Congress „Haus der Technik" Controlled Auto Ignition, Essen, Oktober 2005.

[33] Goran Haraldsson, Per Tunestål, Bengt Johansson. Transient Control of a Multi Cylinder HCCI Engine During a Drive Cycle. SAE 2005-01-0153.

[34] Shiro Yamaoka, Atsushi Shimada, Hiromu Kakuya, et al. HCCI Betrieb in einem Mehrzylinder Ottomotor mit variablem Ventiltrie// Congress „Haus der Technik"Controlled Auto Ignition, Essen, Oktober 2005.

[35] Fredrik Agrell. Transient Control of HCCI Through Combined Intake and Exhaust Valve Actuation. SAE 2003-01-3172. 127

[36] Hongming Xu, Simon Rudolph, Zhi Liu. An Investigation into the Operating Mode Transitions

of a Homogeneous Charge Compression Ignition Engine Using EGR Trapping. SAE 2004-01-1911.

[37] Fredrik Agrell. Control of HCCI During Engine Transients by Aid of Variable Valve Timings Through the Use of Model Based Non-Linear Compensation. SAE 2005-01-0131.

[38] Petter Strandh, Johan Bengtsson, Rolf Johansson, et al. Variable Valve Actuation for Timing Control of a Homogeneous Charge Compression Ignition Engine. SAE 2005-01-0147.

[39] Nebojsa Milovanovic, Dave Blundell, Stephen Gedge. SI-HCCI-SI Mode Transition at Different Engine Operating Conditions. SAE 2005-01-0156.

[40] Yoshishige Ohyama. Engine Modeling of HCCI Transient Operations. SAE 2005-01-0158.

[41] Nebojsa Milovanovic, Dave Blundell, Stephen Gedge. Cam Profile Switching and Phasing Strategy vs Fully Variable Valve Train Strategy for Transitions between Spark Ignition and Controlled Auto Ignition Modes. SAE 2005-01-0776.

[42] Fredrik Agrell. Transient Control of HCCI Combustion by aid of Variable Valve Timing Through the Use of a Engine State Corrected CA50-Controller Combined with an In-Cylinder State Estimator Estimating Lambda. SAE 2005-01-2128.

[43] Halim Santoso, Jeff Matthews, Wai Cheng. Characteristics of HCCI Engine Operating in the Negative-Valve-Overlap Mode. SAE 2005-01-2133.

[44] Carl Wilhelmsson, Andreas Vressner, Per Tunestål. Combustion Chamber Wall Temperature Measurement and Modeling During Transient HCCI Operation. SAE 2005-01-3731.

[45] R Leithgoeb, F Henzinger, A Fuerhapter. Optimization of New Advanced Combustion Systems Using Real-Time Combustion Control. SAE 2003-01-1053.

[46] Dimistis Panousakis, Andreas Gazis, Jill Patterson, et al. Using Ion-current Sensing to Interpret Gasoline HCCI Combustion Processes. SAE 2006-01-0024.

[47] Mitsuru Konno. Ignition Mechanisms of HCCI Combustion Process Fueled with Methane/DME Composite Fuel. SAE 2005-01-0182.

[48] Kiyoshi Kawasaki, Akihiro Takegoshi, Koji Yamane. Combustion Improvement and Conrol for a Natural Gas HCCI Engine by the Internal EGR by Means of Intake-valve Pilot opening. SAE 2006-01-0208.

[49] Magnus Christensen, Anders Hultqvist, Bengt Johansson. Demonstrating the Multi Fuel Capability of a Homogeneous Charge Compression Ignition Engine with Variable Compression Ratio. SAE 1999-01-3679.

[50] Zhili Chen, Mitsuru Konno. Experimental Study of CI Natural-Gas/DME Homogeneous Charge Engine. SAE 2000-01-0329.

[51] Norimass Iida, Tetsuya Igarashi. Auto-Ignition and Combustion of n-Butane and DME/Air Mixtures in a Homogeneous Charge Compression Ignition Engine. SAE 2000-01-1832.

[52] Scott B Fiveland, Rey Agama. Experimental and Simulated Results Detailing the Sensitivity of Natural Gas HCCI Engines to Fuel Composition. SAE 2001-01-3609.

[53] Frank Beyrau, Alfred Leipertz. Laseroptische Messung von Temperatur und AGR-Rate in einem Ottomotor im HCCI-Betrieb// Congress „Haus der Technik" Controlled Auto Ignition, Essen, Oktober 2005.

[54] Adam Loch, Christian Jelitto, Jürgen Willand. Einfluss von Ladungstemperatur und AGRRate auf die Kompressionszündung in einem Ottomotor// Congress „Haus der Technik"Controlled Auto Ignition, Essen, Oktober 2005.

[55] M Richter, J Engstr M. The influence of charge inhomogeneity on the HCCI combustion

process. SAE 2000-01-2868.

[56] Anders Hultqvist. Reacting Boundary Layers in a Homogeneous Charge Compression Ignition (HCCI) Engine. SAE 2001-01-1032.

[57] Anders Hultqvist, Magnus Christensen, Bengt Johansson. The HCCI Combustion Process in a Single Cycle - Speed Fuel Tracer LIF and Chemiluminescence Imaging. SAE 2002-01-0424.

[58] Robert Collin, Jenny Nygren, Mattias Richter. Simultaneous OH- and Formaldehyde-LIF Measurements in an HCCI Engine. SAE 2003-01-3218.

[59] Richard Steeper, Shane De Zilwa. Co-Evaporative Tracer-PRF Mixtures for LIF Measurements in Optical HCCI Engines. SAE 2005-01-0111.

[60] M Weinrotter, E Wintner. Optical Diagnostics of Laser-Induced and Spark Plug-Assisted HCCI Combustion. SAE 2005-01-0129.

[61] Shane De Zilwa, Richard Steeper. Predicting NOx Emission from HCCI Engines Using LIF Imaging. SAE 2006-01-0025.

[62] Hua Zhao, Tom Ma, X Jiang, et al. Combined Experimental and Modelling Studies on CAI Combustion Engines// Congress „Haus der Technik" Controlled Auto Ignition, Essen, Oktober 2005.

[63] Zhi Wang, Jian-Xin Wang, Shi-Jin Shuai. Numerical Simulation of HCCI Engine with Multi-stage Gasoline Direct Injection Using 3D-CFD with Detailed Chemistry. SAE 2004-01-0563.

[64] Li Cao, Hua Zhao, Xi Jiang. Numerical Study of Effects of Fuel Injection Timings on CAI/HCCI Combustion in a Four-Stroke GDI Engine. SAE 2005-01-0144.

[65] Roy Ogink. Applications and Results of a User-Defined, Detailed-Chemistry HCCI Combustion Model in the AVL BOOST Cycle Simulation Code// Int. User Meeting 2003, AVL, Graz, Austria, October 2003.

[66] Roy Ogink. Computer Modeling of HCCI Combustion [Ph. D.]. Göteborg: Chalmers University of Technology, 2004.

[67] Nebojsa Milovanovic, Rui Chen. Influence of the Variable Valve Timing Strategy on the Control of a Homogeneous Charge Compression (HCCI) Engine. SAE 2004-01-1899.

[68] Sjöberg M., Dec J.E., An investigation of the relationship between measured intake temperature, BDC temperature, and combustion phasing for premixed and DI HCCI engines. SAE paper, 2004, 2004-01-1900.

[69] Sjöberg, M., Dec, J.E., and Cernansky, N.P., Potential of Thermal Stratification and Combustion Retard for Reducing Pressure-Rise Rates in HCCI Engines, Based on Multi-Zone Modeling and Experiments, SAE Paper, 2005, 2005-01-0113.

[70] Dec J., Hwang W., Sjöberg M., An investigation of thermal stratification in HCCI engines using chemiluminescence imaging. SAE Paper, 2006, 2006-01-1518.

[71 Göran Haraldsson; Per Tunestal; Bengt Johansson; Jari Hyvönen; "Transient Control of A Multi Cylinder HCCI Engine During A Drive Cycle", 2005.

[72] Jari Hyvönen; Carl Wilhelmsson; Bengt Johansson; "The Effect of Displacement on Air-diluted Multi-cylinder HCCI Engine Performance", 2006.

[73] Rafał Pyszczek; P. Mazuro; Andrzej Teodorczyk; "Compression Auto Ignition Control in A 2-Stroke Barrel-Type OpposedPiston Engine", 2016.

Chapter 2   Effect of Different Levels of In-Cylinder Flow on HCCI Combustion

2. 1 Introduction

As mentioned in Chapter 1, in high load HCCI combustion, the working area is limited due to the high pressure increase rate. It is known that stratification of the in-cylinder mixture temperature and fuel concentration is an effective way to reduce this pressure increase rate. In other words, in order to obtain design guidelines for HCCI engines that can operate over a wide operating range, it is necessary to clarify the effects of in-cylinder flow and turbulence that strongly influence premix temperature and concentration distribution, as well as the effects of in-cylinder temperature and fuel concentration distribution on heat release characteristics. Previous studies have shown, both experimentally and computationally, that increasing the turbulence intensity is an effective way to prolong the combustion period and reduce the rate of pressure increase associated with spontaneous combustion. On the other hand, the mechanism of turbulence effects on spontaneous combustion has only been partially inferred from calculations and has not yet been clarified experimentally. In this chapter of the study, the effects of mixture stratification and different in-cylinder flows on HCCI combustion are experimentally investigated to study the mechanism of heat release by enhancing in-cylinder flow to slow down HCCI combustion. The objective was to elucidate the combustion characteristics of HCCI combustion in temperature stratification and flow fields using a prototype rapid compression and expansion machine (RCEM).

2. 2 RCEM- Rapid Compression and Expansion Machine

2.2.1 Introduction of RCEM

The RCEM is a valuable tool for investigating combustion phenomena in a controlled and repeatable manner, which can help researchers to understand the mechanisms of combustion better and develop new technologies to improve engine efficiency and reduce emissions. The RCEM is designed to simulate an actual engine's compression and expansion processes. It can be used to study various combustion phenomena such as ignition, flame propagation, and emissions. Installing measurement devices such as thermocouples and pressure sensors at multiple points in the cylinder has the advantage that optical access is relatively easy and unaffected by the previous cycle. Thus, researchers can obtain detailed data on combustion processes and analyze the mechanisms of combustion phenomena. In this study, by installing a flow generation plate on the piston of the RCEM, the in-cylinder flow can be enhanced, and the mechanism of slow heat release in HCCI combustion can be studied. This demonstrates the versatility of the RCEM in studying various combustion phenomena and the potential of using it to develop more efficient and cleaner combustion technologies.

In order to investigate the mechanism of slowed heat release in HCCI combustion by enhanced in-cylinder flow, a flow-generating plate was installed through a hole in the extension piston of the RCEM to generate a tumble flow in the cylinder. The basic configuration of the rapid compression and expansion device used follows the rapid compression and expansion device developed by Murase et al. at Kyushu University, as shown in Figure 2.1.

The RCEM has the pressure reservoir unit and the cam unit to drive the piston, as illustrated in Figure 2.1. After the intake process, compressed air in the pressure reservoir unit derived the cam unit toward the left-hand side. The piston accordingly moved upward and compressed the air-fuel mixture in the combustion chamber.
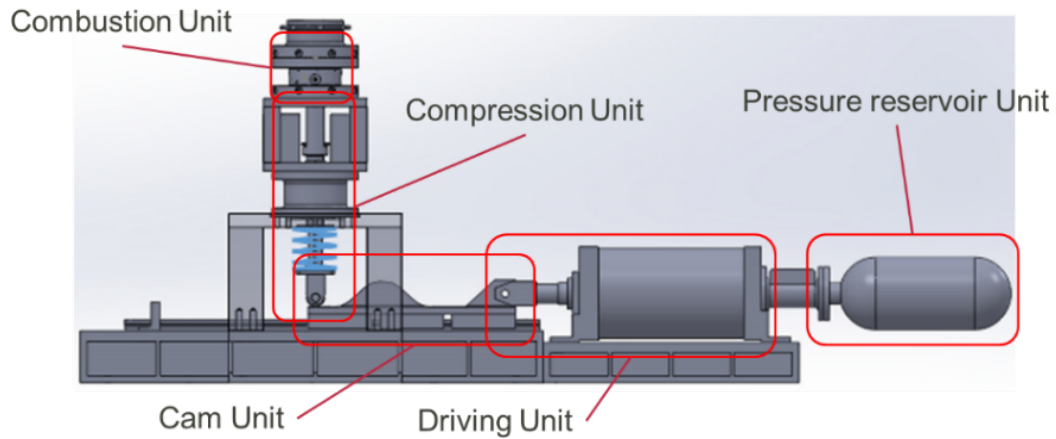
Figure 2.1   Schematic drawing of RCEM.

2.2.2 Previous Study and Superiority of RCEM

Extensive research has used RCEM to study combustion processes in internal combustion engines, including spark ignition and compression ignition engines. Researchers can gain insight into combustion's fundamental physics and chemistry by varying fuel characteristics, injection timing, and engine operating conditions.

Some of the key areas of research using RCEM include.

Studying the effects of fuel characteristics, such as fuel type, fuel mixture, and fuel additives, on combustion performance and emissions. Studying combustion processes in alternative fuel engines like hydrogen, natural gas, and biofuels. Developing and testing new combustion technologies such as homogeneous charge compression ignition (HCCI) and low-temperature combustion (LTC). Evaluating new engine designs' performance and emissions, such as depleted combustion and downsized engines. The study [12] investigated the effects of different fuel injection pressures and gasoline-biodiesel (GB) blends with varying biodiesel content (10% and 20% by volume), on a rapid compression and expansion machine (RCEM), on the ignition characteristics and performance of the engine. EL-Seesy, A. I., Kayatas, al. [13,14]   investigated the effects of blending n-heptanol with methyl oleate biodiesel fuel on combustion and exhaust emissions in a rapid compression-expansion machine (RCEM) operated under diesel engine conditions. Windarto, C al. [15] conducted experiments and

simulations using a rapid compression and expansion machine (RCEM) to investigate the combustion and performance of propane direct injection with spark discharge energy effect. Xiong Shusheng, Liu Zhentao al.: [16] measured the combustion process of a spark ignition LPG engine using RCEM. Analyses have been made of the effects of mixture concentration, ignition advance angle, compression ratio, and combustion chamber shape on the LPG combustion process.

Overall, The Rapid Compression and Expansion Machine (RCEM) is a valuable tool for studying the combustion process and improving engine performance. Its controlled environment, time and cost efficiency, flexibility, accuracy, and ability to reduce emissions make it an essential tool for developing more efficient and environmentally friendly engines.

The actual combustion, heat transfer and mixing of fuel and air in an internal combustion engine is a complex process. And as actual engine experiments are often accompanied by cycle changes, it is very difficult to obtain realistic and accurate parameters of the experimental process or to control the combustion conditions constant from cycle to cycle. Therefore, RCEM is used to simulate the combustion processes of multiple fuels and different combustion methods. is a powerful experimental tool used to study the combustion process of fuels. Combined with relevant testing and analysis techniques, RCEM is an effective tool for fundamental research into the combustion process and combustion characteristics of engines.

Here are some advantages of the RCEM:

1.   Controlled Environment: RCEM provides a highly controlled environment to study combustion processes. This allows researchers to manipulate fuel/air mixtures, ignition times, and other variables to study the effects on combustion characteristics. This control is difficult to achieve in a typical real engine, making RCEM an important tool for advancing combustion research.

2.   Time and Cost Efficient: RCEM can simulate the combustion process in a fraction of the time required to test a full-size engine. This not only saves time but also reduces the cost of research and development. Therefore, RCEM is a more cost-effective option than full-size

engine testing.

3. Flexibility: The RCEM can be used to test a wide range of fuel types, including alternative fuels and biofuels. It can also be used to test various engine configurations and operating conditions. This flexibility allows researchers to study the effects of different fuels, engine designs, and operating conditions on combustion performance.

4. Accuracy: RCEM produces highly accurate results with a high degree of reproducibility. This allows researchers to obtain reliable data for accurately modeling and simulating engine performance.

5. Emissions Reduction: RCEM can be used to develop and test alternative fuel and engine designs that produce lower emissions. This can help reduce the environmental impact of transportation and power generation.

Due to the above characteristics of the RCEM, it is ideally suited for use in this study.

2.3 Experimental Setup

A schematic diagram of RCEM is shown in Figure 2.2. RCEM can reproduce the combustion phenomena in a cylinder in a single shot by simulating the compression and expansion process of an actual engine. This section introduces the details of the experimental apparatus used in this study mainly consists of the RCEM, fuel, and mixture system, cooling system, control system, and measurement system.

2.3.1 Experimental Equipment

Table 2.1 show the specification of the RCEM used in this study. The RCEM consists of five elements, from right to left: the pressure reservoir, driving unit, cam, compression unit, and combustion unit, as shown in Figure 2.2.

Table 2.1. Specification of the RCEM

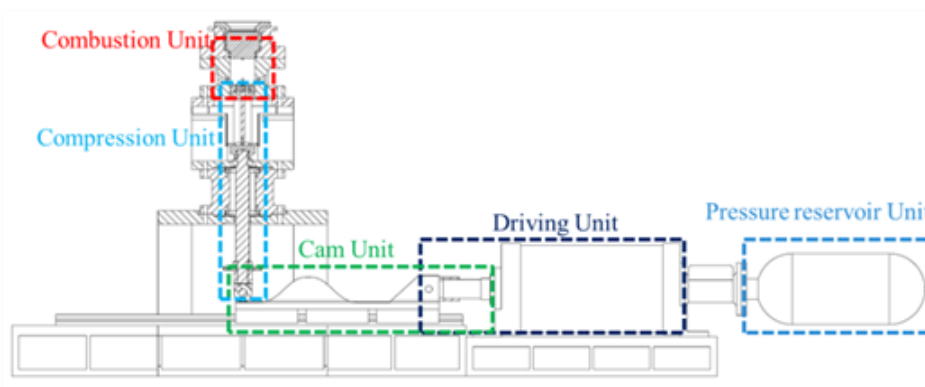| Displaced volume [cc]	306
Stroke [mm]	73
Bore [mm]	73
Compression ratio [-]	14.2:1
Average piston speed [ms/stroke]	33 (900 rpm)

Figure 2.2 RCEM assembled view.

2.3.2 RCEM Operating Principle of ThisThesis

This section describes the principle of the basic operation of the RCEM. Operation is started by filling the storage section with compressed air using a compressor and opening the solenoid valve that spatially isolates the storage section from the drive section. When the solenoid valve is opened, the filled compressed air flows into the drive unit, pushing the piston in the cam drive cylinder and pushing the cam connected to the end of the drive cylinder piston rod in a horizontal direction. Rollers are attached to the end of the piston rod in the compression section. The rollers on the rod roll along the curve of the cam and push the piston and rod vertically upwards. The piston attached to the end of the rod compresses the cylinder-filled air mixture into the combustion chamber at once. A series of actions creates a high-temperature, high-pressure field in the combustion chamber, similar to that of a real engine. Combustion then

takes place and the engine proceeds to the expansion stage. Iso-pentane, which was used as fuel, is stirred with N2 and O2 in the mixture tank. The mixture was inducted from the intake valve installed on the lower part of the combustion chamber wall. In-cylinder pressure was measured by the pressure sensor (Kistler 6052C) and acquired by the data logger (WE800) as shown in figure 2.3. The temperature of the mixture was controlled by the heater installed in the mixture tank. The RCEM has eight electric heaters or water jackets adjacent to the combustion chamber. Temperature distribution of in-cylinder mixture was created by the heaters and water flowing inside the water jackets and the temperature of the water was controlled by a cooling chiller and a heat exchanger in a hot water tank.
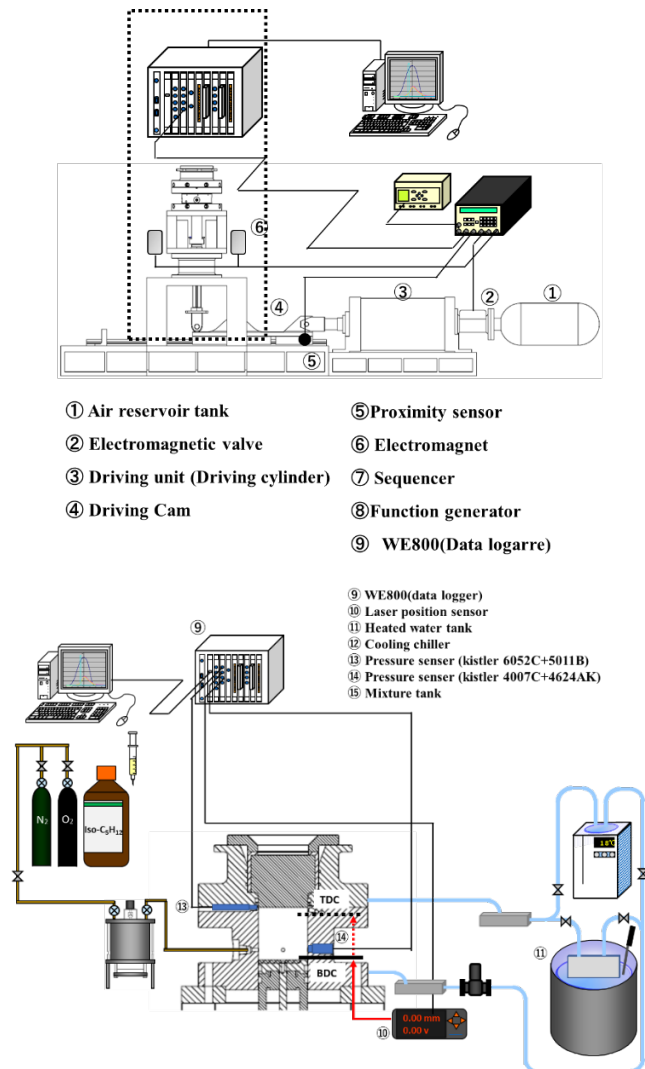

① Air reservoir tank   ⑤ Proximity sensor
② Electromagnetic valve   ⑥ Electromagnet
③ Driving unit (Driving cylinder)   ⑦ Sequencer
④ Driving Cam   ⑧ Function generator
     ⑨ WE800(Data logarre)

⑨ WE800(data logger)
⑩ Laser position sensor
⑪ Heated water tank
⑫ Cooling chiller
⑬ Pressure senser (kistler 6052C+5011B)
⑭ Pressure senser (kistler 4007C+4624AK)
⑮ Mixture tank

Figure 2.3   Experimental specification.

2.3.2 Method of In-Cylinder Turbulent Flow and In-Cylinder Temperature Distribution Generation

The following is a rough description of the system to generate the flow shown in Figure 2.4, the piston is lifted to the upper dead center by a cam, the plate support plate is hooked to a seesaw, and the piston is returned to BDC. Figure 2.5 shows the top view of the flow generation plate. The piston is then pressurized and lifted by the spring and lowered and secured by a piston-holding electromagnet. The RCEM cylinder is then evacuated, and the air mixture is sucked from the air mixture tank by opening and closing the needle valve. After the intake is completed, the piston holding electromagnet is turned off. The solenoid valve in the drive unit is opened to allow compressed air to flow into the drive cylinder, causing the drive cam to move. All these controls are performed by a program relay called a sequencer (ZEN-20C1DT-D-V2, Omron). The combination of ladders, meaning ladders, makes it easy to create arbitrary commands. A function generator (WF1646B, NF Circuit Design Block) was used to capture the trigger once, delay it for a certain period, and output the trigger again. When the cam passes the sensor, the trigger enters the plate holding electromagnet, the power is turned off, and the plate drops.

The temperature of mixture was controlled by the heater installed in the mixture tank. The RCEM has 8 electric heaters or water jackets adjacent to the combustion chamber as shown in figure 2.6. Temperature distribution of in-cylinder mixture was created by the heaters and water flowing inside the water jackets and the temperature of the water was controlled by a cooling chiller and a heat exchanger in a hot water tank.
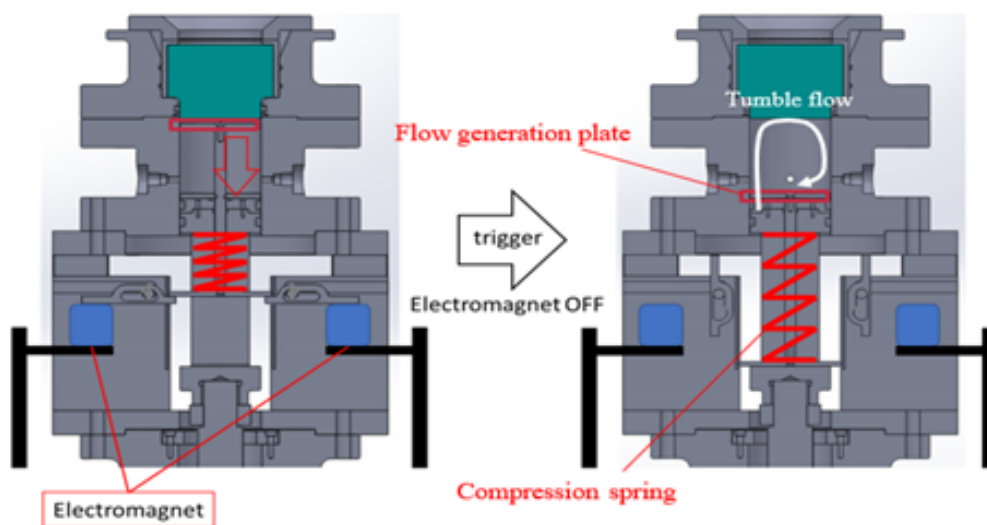

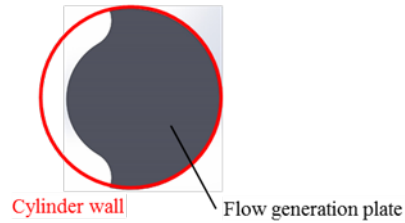Figure 2.4   Flow generation mechanism.
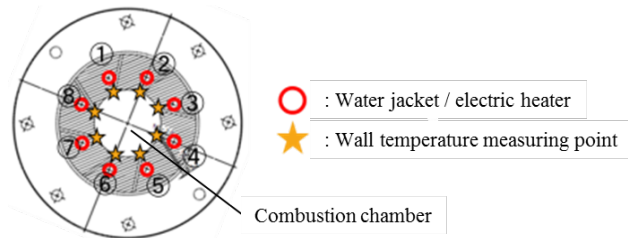
Figure 2.5　Top view of the flow generation plate

Figure 2.6 Top view of the combustion chamber and water jackets

2.4 Fuel and Air-Fuel Mixture System

2.4.1 Fuel and Octane Rating

The octane number is used to express the fuel's auto-ignition ability, and the higher the octane number, the less likely the fuel is to auto-ignite. The higher the octane number, the less likely the fuel is to auto-ignite. The octane number of the fuel is important because HCCI engines create high temperatures and pressure in the cylinder by compression and burn fuel by auto-ignition. The evaluation of octane numbers may vary depending on the operating conditions of the engine and the model used. For this reason, the octane number is determined using the Co-operative Fuel Research (CFR) engine, which is a spark-ignition engine with a variable compression ratio. The octane number of a given fuel is determined by comparing it with that of a standard fuel. Table 3.8 shows a summary of the experiment method. There are two types of octane numbers: Research Octane Number (RON) and Motor Octane Number (MON), which differ according to the experiment method: RON represents knock resistance at low speeds, and MON represents knock resistance at high speeds and high loads. First, the vehicle is run with a fuel for which the octane number is to be determined, and the compression ratio at which knocking occurs is determined. Next, the engine is operated with standard fuel,

and the octane number of the standard fuel at the time knocking occurs under the same conditions is used as the octane number of the fuel. The standard fuel is a mixture of isooctane with high knock resistance, with an octane number of 100, and n-heptane, which is prone to knocking, with an octane number of 0. The octane number of the standard fuel is the volume ratio of isooctane contained in the fuel mixture.

In this study, a fuel with an octane number of RON90, the ratio of isooctane to normal heptane of 9:1, was used for numerical analysis. Isopentane was used as fuel in the experiment. In this experiment, the fuel must be a gas to create an air-fuel mixture. Isopentane is a liquid at room temperature, but its boiling point is as low as 27.9°C. Therefore, it is possible to create an air-fuel mixture by keeping the tank at a temperature higher than the boiling point during the creation of the mixture. The octane number of isopentane is RON92.3, close to the octane number of the fuel used in the numerical analysis.

2.4.2 Air-Fuel Mixture Tank

The air-fuel mixture was prepared using a high-pressure vessel (hereafter referred to as a " container" or "air-fuel mixture tank") designed and fabricated by Kobayashi et al. in 2002. Figure 2.7 shows the vessel. This vessel can create air-fuel mixtures for both gaseous and liquid fuels. In the design, the vessel is filled with high-pressure gas, combustible gas, or vaporized fuel. The container is designed with sufficient safety measures in case of an unexpected pressure rise during the charging of the high-pressure gas or in case the high-pressure fuel in the container ignites or catches fire. First, a bursting plate called an MRK-5 (Fike Japan) rupture disk is installed at the bottom of the tank. The rupture disk shatters at the moment of an unexpected pressure rise, causing pressure to leak from the bottom of the tank. In addition, if the rupture disk does not work properly, the vessel's design is such that a part of the support column that holds the flange clamps the cylinder on the side of the vessel from the top and bottom can be broken by excessive load.

The gases, including fuel, are supplied from each cylinder to the air-fuel mixture tank via a regulator. Isopentane, the liquid fuel, is injected through a micro syringe into the silicone rubber

installed at the top of the tank. The air-fuel mixture was created using the method of partial pressure, and the pressure inside the vessel was measured with an absolute pressure gauge (4005BA5R, KISTLER) and amplifier (4618A0, KISTLER). A U-shaped mercury column made by Okano Manufacturing Co. Oxygen was used as an oxidizer, and nitrogen as a diluent for the air-fuel mixture. A needle valve was used to finely adjust the amount of each gas in the air-fuel mixture. The needle valve was used to fine-tune the amount of each gas in the air-fuel mixture. This made it possible to create arbitrary equivalent ratios, oxygen concentrations, and air-fuel mixtures. A motor-driven agitator was installed to ensure the fuel and air were sufficiently mixed. Copper piping was selected for the route from each cylinder to the air-fuel mixture tank and RCEM cylinder, considering the use under negative pressure.

When using liquid fuel, the air-fuel mixture tank and piping were wrapped with heaters to keep them warm and prevent condensation. A silicon belt heater (100 V/125 W, Sakaguchi Dennetsu) was used for the vessel. The heater was turned on and off by a temperature controller based on the output of a K-type sheathed thermocouple (φ=2.3, Sakaguchi Dennetsu) that measured the temperature inside the air-fuel mixture tank.
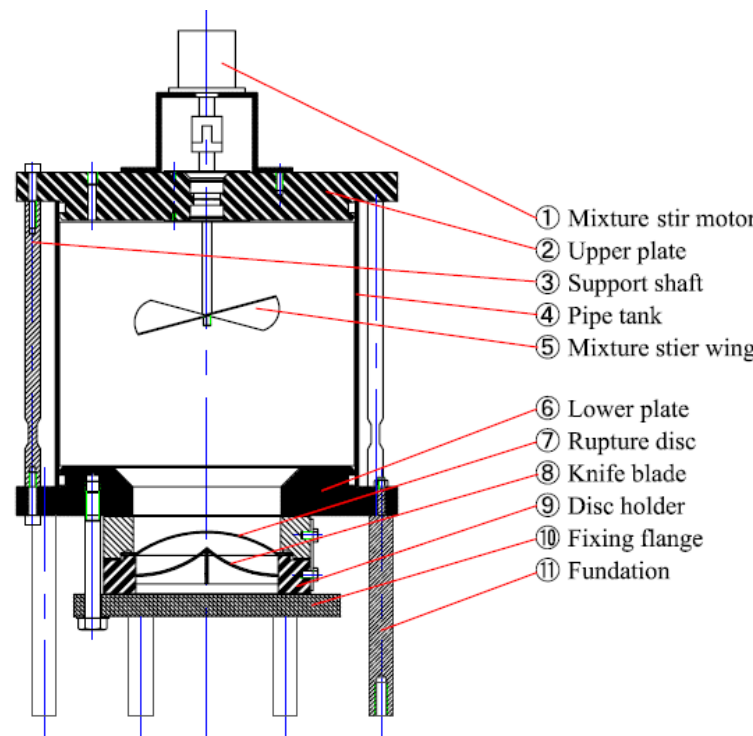

Figure 2.7 Air-Fuel mixture tank

35

2.5 Cooling System

Water was circulated through eight channels on the cylinder wall, and the wall temperature at each location was controlled using a K-type sheathed thermocouple.

The hot water temperature was controlled by measuring the wall temperature at each location with a K-type sheathed thermocouple. To control the temperature of the hot water, the temperature measured by thermocouples (K-type sheath φ2.3, Sakaguchi Dennetsu) was fed into a digital temperature controller (OMRON), and when the temperature exceeded the target temperature, a solenoid valve was activated to feed cold water into the tank with an accuracy of ±1°C. When cold water was used, the temperature was controlled by a temperature controller (OMRON) with an accuracy of ±1°C. When the temperature exceeded the target temperature, the temperature was controlled by a digital temperature controller (OMRON) with an accuracy of ±1°C. When the temperature was below the target temperature, a digital temperature controller activated by a digital temperature controller (OMRON) with an accuracy of ±1°C. When low-temperature cooling water is used, a chiller, shown in figure 2.8, (Cool Ace Model CA-1112, EYELA Tokyo Rika Kikai Kikai) is used. The temperature control range is from -20°C to 30°C and can be automatically controlled within ±2°C. Despite the circulation function of the device itself, the cooling water is not sufficient in terms of flow rate. Although the device has a circulation function, it was used only to produce cooling water due to the insufficient flow rate. A circulation pump pumps out each vessel's cold and hot water. The water was then circulated through a water flow branch box that branched into eight flow paths in the cylinder, flowing in the direction of the compression cylinder from the cylinder head and back to the tanks after being collected again at another branch box. A cartridge heater (HISD ROD 10121025) created the temperature stratification. The cartridge heater has a flange attached so it can be fixed to the compression cylinder. The heater was adjusted to the target temperature by monitoring the thermocouple-measured wall temperature with a data logger and changing the heater voltage value with a slide. When a cartridge heater and cooling water are used together, the flow path in the flow branch box connected to the flow path where the cartridge

heater is installed is plugged in.

Figure 2.8 Cooling chiller (From the website of Tokyo Rika Kiki Co.)

2.6 Measurement System

A 4-channel 100kS/s isolation digitizer module (WE7272) was installed to measure the in-cylinder pressure history, voltage output from the laser displacement meter, and triggers for the drive. The following is a brief description of each sensor.

2.6.1 Measurement of Piston Displacement

In this RCEM, a reflector is inserted in the roller follower folder, and the piston displacement is measured by a laser displacement meter. Since the cam's horizontal travel speed is determined by the pressure rise of the compressed air in this RCEM, and the roller follower, which rises in conjunction with the cam, has a constant speed, using the piston displacement as the measurement trigger is considered to be the most appropriate method for obtaining experimental reproducibility. Regarding the selection of the displacement transducer, since the combustion time is several milliseconds, the response time from the time the displacement transducer measures the distance to the time it converts it to a voltage must be in the order of milliseconds or less. Also, the displacement of the roller follower, 73mm, must be within the measurement range. Since the sensor should output a voltage value that is as accurate as

possible when setting the trigger, an analog voltage output with a voltage value proportional to the distance is useful. Therefore, a sensor head (Smart Sensor ZX-LD300, Omron) and an amplifier unit (ZX-LDA11-N, Omron) with a measurement period of 150μs were selected for the sensor. Tables 9 and 10 provide an introduction. The reflective (displacement) sensor head uses light emitting and light receiving elements to measure the distance from the sensor head to the object to be detected. The value is converted into an electrical signal and transmitted to the amplifier unit. The amplifier unit averages the input electrical signals several times and outputs the averaged values. The number of times it can be set is 1, 2, 4, ..., 2n, ..., 4096. In this experiment, the output was set to 1 V at the bottom dead center (displacement 0 mm) and 5 V at the top dead center (displacement 73 mm). The number of output calculations was set to one time to avoid response delay.

Table 2.2 Main specifications of sensor head unit

Items	ZX‐LD100L
Optical characteristic	Diffuse reflection
Light source (wavelength)	Optical wavelength semiconductor laser (650nm, 1mW Not over, Clase2)
Sensing center distance	100mm
Measurement range	±40mm
Beam form	Spot
Beam diameter	$\phi 150 \mu$m
Resolution	16μm
Linearity	±0.2%F.S. (80~120mm)

Table 2.3 Main specifications of amp unit

Items	ZX‐LDA11‐N
Measurement period	150μm
Linear output	Current output: 4~20mA/F.S. Max. load resistance:300Ω Voltage output: ±4V (±5V,1~5V variable) Output impedance:100Ω
Power supply voltage	DC12~24V±10%
Dielectric strength	AC1,000V 50/60Hz 1min

2.6.2 In-Cylinder Pressure Measurement

Depending on the application, the pressure in the combustion chamber was measured using the pressure sensors listed in Table 2.4.

A piezoelectric pressure sensor (type 6052C, KISTLER) and a charge amplifier (Dual Mode Amplifier 5010B, KISTLER) were attached to the circumferential wall of the combustion chamber to measure combustion pressure. The piezoelectric pressure sensor utilizes the piezoelectric effect, a phenomenon in which a surface potential is generated due to polarization in a crystal when stress is applied to the crystal. When a force is applied to the sensor, an electric charge is generated on the sensor surface, and the role of the charge amplifier is to convert the charge into a voltage, which is somewhat different from a normal output amplifying amplifier.

Table 2.4 Specifications of pressure transducer and amplifier

Items	Kistler 6052C + 5010B
Measurement range	10MPa
Accuracy	±0.4%F.S.
Output voltage	0 ~ 10V
Cutoff frequency	180kHz

2.7 Synchronization and Control of Each System

The following is a rough description of the system up to the start of compression in this system. To generate the "compression" shown in Figure 2.3, the piston is lifted to the upper dead center by a cam, the plate support plate is hooked to a seesaw, and the piston is returned to BDC. The piston is then pressurized and lifted by the spring and lowered and secured by a piston-holding electromagnet. The RCEM cylinder is then evacuated, and the air mixture is sucked from the air mixture tank by opening and closing the needle valve. After the intake is completed, the piston holding electromagnet is turned off. The solenoid valve in the drive unit is opened to allow compressed air to flow into the drive cylinder, causing the drive cam to move. A program relay performs these controls called a sequencer (ZEN-20C1DT-D-V2,

Omron). The combination of ladders, meaning ladders, makes it easy to create arbitrary commands. A function generator (WF1646B, NF Circuit Design Block) was used to capture the trigger once, delay it for a certain period, and output it again. Figure 2.9 shows a time chart of the entire device. Since there is a large variation of about 10~20ms in the time between the input of the trigger and the opening of the solenoid valve, the plate drop trigger is triggered by the sensor shown in Figure 2.10. When the cam passes the sensor, the trigger enters the plate holding electromagnet, and the power is turned off, and the plate drops. The time from the time the trigger is triggered to the time the electromagnet is turned off and the fall is completed was 19 ms, as measured by the high-speed camera.
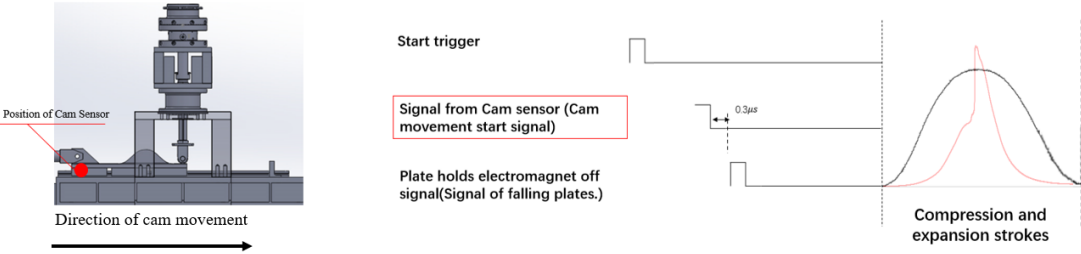
Figure.2.9 Time chart for RCEM operation

Figure 2.10 Plate trigger sensor

2.8 Analysis Method

In engine experiments, in-cylinder pressure is measured. Various evaluations are made by calculating the work done by combustion, temperature changes, and the history of heat release from the pressure data. Normally, these calculations should consider local temperature differences in the cylinder and the gas composition in the cylinder, which changes with the progress of combustion. However, many analysis methods only calculate the approximate heat release by considering the cylinder's approximate heat generated by the average temperature or by assuming that the temperature variation in the cylinder can be ignored. This is sufficient for conventional engine performance evaluation. Still, with the diversification of engine technologies, more advanced combustion analysis is required to analyze factors such as knocking that often occurs when high supercharging is used and the effect of fuel consumption improvement when Cooled EGR is used. Therefore, in this thesis a two-region combustion analysis method was used. It divides the inside of a cylinder into a combustion-ready region and a combustion-unburned region and calculates the temperatures of each unbounded region is characterized by the fact that it can be used to analyze abnormal combustion such as knocking by calculating temperatures in each region and can calculate accurate heat release and heat loss by considering temperature changes in the cylinder and changes in gas composition, enabling more advanced analysis of factors that cause changes in engine performance. This method was developed for the combustion analysis of actual engine models. The calculation method needed to be modified because it is unnecessary to consider residual gases before combustion in RCEM. Therefore, to make this method usable in this RCEM.

2.8.1 Analysis Details

1-zone combustion analysis

To perform a two-region combustion analysis, which is a feature of this method, it is necessary to calculate the combustion mass fraction using a conventional one-region combustion analysis to obtain the degree of combustion progress. This method considers the

temperature dependence of specific heat in the one-domain analysis. This one-region combustion analysis is useful for calculating the work that can be calculated from pressure and volume, the average cylinder temperature, and heat generation with conventional accuracy, as well as for their relative comparison. The formulas for these calculations are described below.

2-zone combustion analysis

The combustion mass fraction, cylinder pressure, volume, and temperature obtained in the one-region analysis are used. First, the masses of the already combusted and unburned gases are calculated from these data, and their respective temperatures and specific heat ratios are obtained. The average specific heat ratio can be calculated from the ratio of the already combusted and unburned parts in the cylinder and the specific heat ratio of each to calculate the heat generation with higher accuracy. This two-region analysis is useful when the temperature of unburned gas is needed to analyze the causes of knocking or when a more rigorous analysis of the causes is needed to examine factors that improve thermal efficiency. The formulas for each are described below.

2.8.2 Formula for 1-Zone Combustion Analysis

Cylinder Volume

In combustion analysis, the volume in the cylinder is needed to calculate various items. The volume V_t is defined as

$$V_t = V_c + X_t \cdot A_b \qquad (1)$$

V_c is the combustion chamber volume, X_t is the piston displacement, and A_b is the bore area.

In-cylinder temperature

The in-cylinder temperature can be calculated using the equation of state from the measured pressure, the initial value of the gas mixture, and the gas composition by determining the in-cylinder volume. The temperature inside the cylinder is assumed to be uniform in a one-region analysis. The in-cylinder temperature $T_t[K]$ can be expressed as

$$T_t = \frac{P_t V_t}{m R_u} \qquad (2)$$

The value of R_u is obtained by where m is the mass of the mixture [g] and R_u is the gas constant of the mixture before combustion [J/kg/K].

The gas constant R_u of the unburned mixture before combustion, which is necessary for calculating the cylinder temperature, is obtained from the universal gas constant R^* and the average molecular weight M_{mu} before combustion as

$$R_u = \frac{R^*}{M_{mu}} \qquad (3)$$

$$M_{mu} = \frac{m_{total}}{n_u} \qquad (4)$$

The mixture mass can be expressed as follows. where n_u is the number of moles of the mixture before combustion and is obtained by summing the number of moles of C, H, N_2 and O_2 before combustion as in the calculation of mixture mass.

Specific heat capacity

The specific heat and specific heat ratio are necessary to calculate heat generation, which is important for evaluating abnormal combustion. In this system, the specific heat ratio has been assumed to be a constant 1.27. However, specific heat capacity is a function of temperature and is highly dependent on temperature. Therefore, in this analysis method, the temperature dependence due to changes in the cylinder temperature is taken into account in order to calculate the heat generation with high accuracy.

The specific heat capacity $C_t[J/(kg \cdot K)]$ is given by

$$C_t = (A_u \cdot T_t^4 + B_u \cdot T_t^3 + C_u \cdot T_t^2 + D_u \cdot T_t + E_u) \cdot R^* \qquad (5)$$

The combustion coefficient is calculated where A_u, B_u, C_u, D_u, and E_u are coefficients calculated from the precombustion mixture composition and thermodynamic properties. A commercial database (CDAJ/DARS-BASIC) was used for the calculations. Tables 2.5 and 2.6 show the physical property data.

Table 2.5 DARS table (T$_t \leq$ 1000 K)

					Tt$\leqq$ 1000K
C5H12	6.12007E-12	-8.39625E-09	-1.95942E-05	5.62286E-02	-5.76903E-01
N 2	-2.44485E-12	5.64152E-09	-3.96322E-06	1.40824E-03	3.29868E+00
O 2	2.98899E-15	2.80793E-11	-5.34550E-07	1.60342E-03	3.08809E+00
CO2	-2.11728E-12	6.86669E-09	-1.04091E-05	9.92207E-03	2.27572E+00
H2O	-2.50659E-12	6.96858E-09	-6.35470E-06	3.47498E-03	3.38684E+00

Table 2.6 DARS table (T$_t$>1000 K)

					Tt$>$ 1000K
C5H12	-1.31214E-13	2.07942E-09	-1.26055E-05	0.035390742	9.0524225
N 2	-6.75335E-15	1.0097E-10	-5.68476E-07	0.001487977	2.92664
O 2	-9.23577E-15	1.32082E-10	-6.90657E-07	0.00156657	3.19345
CO2	-1.66903E-14	2.394E-10	-1.27841E-06	0.003140168	4.453623
H2O	-6.39162E-15	1.201E-10	-8.73026E-07	0.003056293	2.672145

The table coordinates used in the calculations are shown as D_{xy} for the x-row y-column values.

The following explains how to obtain each coefficient, using the calculation of coefficient A as

an example. The calculation is performed by finding the product of the physical property value

in each row and the molar ratio of the corresponding component and then summing them up.

First, the molar ratios are calculated for fuel, N_2, and O_2 in the pre-combustion mixture.

$$molR_{fuel\_u} = \frac{n_{fuel}}{n_u} \quad (6)$$

$$molR_{N_2\_u} = \frac{n_{N_2\_u}}{n_u} \quad (7)$$

$$molR_{O_2\_u} = \frac{n_{O_2\_u}}{n_u} \quad (8)$$

Then, the coefficient A_u is then calculated as follows.

$$A_u = D_{11} \cdot molR_{fuel\_u} + D_{21} \cdot molR_{N_2\_u} + D_{31} \cdot molR_{O_2\_u} \quad (9)$$

Then, by changing all the coordinates in the table to the second column, the coefficients up to

E_u can be calculated for B_u, C_u in the third column, and so on. Since the coefficients require a

change in the physical property values used around 1000K, it is necessary to decide which table to use depending on the temperature. By obtaining the coefficients $A_u \sim E_u$ in this way, the specific heat capacity can be calculated considering the temperature dependence from Equation 5.

Specific heat ratio

The specific heat ratio κ_t is calculated from the specific heat capacity obtained earlier. Since the specific heat is calculated as a function of temperature, the specific heat ratio also varies with the temperature inside the cylinder. The calculation formula is as follows.

$$\kappa_t = \frac{1}{1-\frac{R^*}{C_t}} \qquad (10)$$

Pressure rise rate and Volume change rate

The pressure rise rate dP_t and volume change rate dV_t are calculated by the following equations.

$$dP_t = \frac{P_t - P_{t-1}}{t_t - t_{t-1}} \qquad (11)$$

$$dV_t = \frac{V_t - V_{t-1}}{t_t - t_{t-1}} \qquad (12)$$

Heat release rate (dQt)

The heat release rate dQ_t is calculated based on the first law of thermodynamics, using the cylinder pressure, volume, pressure rise rate, volume change rate, and specific heat ratio obtained so far. The formula is as follows.

$$dQ_t = P_t \cdot dV_t \cdot \frac{\kappa_t}{\kappa_t - 1} + V_t \cdot dP_t \cdot \frac{1}{\kappa_t - 1} \qquad (13)$$

When calculating the heat release rate of an engine, it is usual to use a cycle-averaged pressure history in the cylinder. In a heat release rate analysis for single-shot combustion such as RCEM, the pressure history must be smoothed by a method such as moving average because differential operations amplify the noise. Here, we employed the adjacency average built into Origin 6.0J as a smoothing function and minimized the deviation from the time axis by trial and error. As a result, the heat generation rate was obtained from 100 data sets that were

smoothed by applying the adjacency averaging process.

Heat generation amount

The heat generation amount Q_t is the sum of the heat release rate dQ_t from the start of combustion. In this case, t_{CS} is the combustion start time.

Mass burnt fraction.

Mass burnt fraction MBF_t [%] is a value that indicates how many percent of the supplied fuel, except for unburned fuel, has been burned.

$$MBF_t = \frac{\Sigma_{t=t_{CS}} dQ_t}{Q_{tmax}} \cdot 100 \qquad (15)$$

MBF_t is calculated from the heat generation amount.

2.8.3 Formulas for 2-Zone Combustion Analysis

Specific heat and specific heat ratio of unburned gas

The temperature of unburned gas is one of the most important parameters in combustion analysis, and its value is necessary information in the combustion process analysis. However, it is difficult to accurately calculate the temperature of unburned gas because it changes as combustion proceeds. The temperature of unburned gas is calculated from the adiabatic compression equation. Therefore, it is necessary to calculate the specific heat ratio of the unburned gas. However, in one-region analysis, it is common to calculate the average temperature of unburned gas. However, this average temperature cannot calculate the specific heat ratio. Therefore, assuming the specific heat ratio obtained in the one-region analysis, the temperature of the unburned portion is calculated approximately. The specific heat ratio is then calculated using this temperature, and the temperature of the unburned gas is calculated again.

The tentative temperature T_{it} of the unburned gas using the specific heat ratio obtained from the average temperature is calculated by.

$$T_{it} = \begin{cases} \dfrac{P_t \cdot V_t}{m_{total} \cdot R_u} & (t < t_{CS}) \\[4mm] T_a \left(\dfrac{P_t}{P_a}\right)^{\frac{\frac{(\kappa_a + \kappa_t)}{2} - 1}{\frac{(\kappa_a + \kappa_t)}{2}}} & (t \geqq t_{CS}) \end{cases} \qquad (16)$$

This equation shows that the temperature is determined before combustion begins using the ideal gas equation of state. Then, after the start of combustion, the equation for the adiabatic process is used to calculate the temperature variation during combustion. The subscript a indicates the states of matter at the beginning of combustion.

The specific heat of unburned gas C_{ut}[J/(kg・K)] and the specific heat ratio of unburned gas κ_{ut} are calculated using these temperatures. The method for obtaining specific heat ratios is the same as that used in the one-region analysis.

$$C_{ut} = (A_u \cdot T_{it}^4 + B_u \cdot T_{it}^3 + C_u \cdot T_{it}^2 + D_u \cdot T_{it} + E_u) \cdot R^* \qquad (17)$$

$$\kappa_{ut} = \frac{1}{1 - \frac{R^*}{C_{ut}}} \qquad (18)$$

Temperature of unburned gas

Now that the specific heat ratio of the unburned gas has been calculated, the temperature of the unburned gas, T_{ut}, can be obtained using the specific heat ratio. The temperature of the unburned gas can be calculated by

$$T_{ut} = \begin{cases} \dfrac{P_t \cdot V_t}{m_{total} \cdot R_u} & (t < t_{CS}) \\[4mm] T_a \left(\dfrac{P_t}{P_a}\right)^{\frac{\frac{(\kappa_{ua} + \kappa_{ut})}{2} - 1}{\frac{(\kappa_{ua} + \kappa_{ut})}{2}}} & (t \geqq t_{CS}) \end{cases} \qquad (19)$$

Unburned Gas Volume

Now the temperature of the unburned gas has been calculated, the volume of unburned gas can be calculated using the state equation to find the mass of the unburned gas from the Mass burnt fraction. The volume of unburned gas is V_{ut}, and the mass of unburned gas is m_{ut}.

$$V_{ut} = \frac{m_u \cdot R_u \cdot T_{ut}}{P_t} \qquad (20)$$

and in this case m_{ut} is

$$m_{ut} = \left(1 - \frac{MBF_t}{100}\right) \cdot m_{total} \qquad (21)$$

Burnt gas temperature

The burnt gas temperature T_{bt} can be obtained from the state equation by calculating the burnt gas volume V_{bt} and burnt gas mass m_{bt} from the Mass burnt fraction. In other words

$$T_{bt} = \frac{P_t \cdot V_{bt}}{m_{bt} \cdot R_b} \qquad (22)$$

$$V_{bt} = V_t - V_{ut} \qquad (23)$$

$$m_{bt} = \frac{MBF_t}{100} \cdot m_{total} \qquad (24)$$

However, R_b is the gas constant of the burnt gas and must be calculated considering changes in gas composition due to combustion. Similar to the calculation of the constants for the unburned gases, R_b is calculated as

$$R_b = \frac{R^*}{M_{mb}} \qquad (25)$$

$$M_{mb} = \frac{m_{total}}{n_b} \qquad (26)$$

where, M_{mb} is the average molecular weight of the gas after combustion, and n_b is the number of moles. Since complete combustion is assumed, n_b is the sum of the number of N_2, O_2, CO_2, and H_2O moles in the post-combustion gas, including residual gas.

Specific Heat and Specific Heat Ratio of Burnt Gas

Since the composition of burnt gas differs from that of unburned gas, it is necessary to recalculate the coefficients used to determine specific heat. The main calculation procedure is like that used with unburned gas composition, but the difference is that burnt gas is assumed to contain no fuel. Each of the molar ratios of each component in the gas after combustion, which is necessary to obtain the coefficients, are

$$molR_{N_2\_b} = \frac{n_{N_2\_b}}{n_b} \qquad (27)$$

$$molR_{O_2\_b} = \frac{n_{O_2\_b}}{n_b} \qquad (28)$$

$$molR_{CO_2\_b} = \frac{n_{CO_2\_b}}{n_b} \qquad (29)$$

$$molR_{H_2O\_b} = \frac{n_{H_2O\_b}}{n_b} \qquad (30)$$

Using Tables 2.5 and 2.6, determine the coefficients A_b, B_b, C_b, D_b, and E_b necessary to calculate the specific heat capacity of the burnt gas. The first row of the DARS table is not used because it does not include fuel.

$$A_b = D_{21} \cdot molR_{N_2\_b} + D_{31} \cdot molR_{O_2\_b} + D_{41} \cdot molR_{CO_2\_b} + D_{51} \cdot molR_{H_2O\_b} \qquad (31)$$

Similarly, the coefficients up to Eb can be calculated by changing the column in the DARS table to the second column and performing the calculation, Bb is calculated in the third column, Cb is calculated in the third column, and so on.

The specific heat of the burnt gas, C_{bt}, and the specific heat ratio, κ_{bt}, can be calculated using the temperature of the burnt gas, T_{bt}, obtained in Equation 22.

$$C_{bt} = (A_b \cdot T_{it}{}^4 + B_b \cdot T_{bt}{}^3 + C_b \cdot T_{bt}{}^2 + D_b \cdot T_{bt} + E_b) \cdot R^* \qquad (32)$$

$$\kappa_{bt} = \frac{1}{1 - \frac{R^*}{C_{bt}}} \qquad (33)$$

2-domain specific heat and specific heat capacity

Two-domain analysis can calculate the average specific heat capacity and specific heat ratio from the unburnt gas and burnt gas ratio and their respective specific heat capacities during the combustion period to accurately calculate the heat generation.

The 2-region specific heat C_{2b} and 2-region specific heat ratio κ_{2b} can be calculated using the following equations.

$$C_{2t} = \frac{\left(C_{ut} \cdot \dfrac{1 - MBFt/100}{M_{mu}}\right) + \left(C_{bt} \cdot \dfrac{MBFt/100}{M_{mb}}\right)}{\left(\dfrac{1 - MBFt/100}{M_{mu}}\right) + \left(\dfrac{MBFt/100}{M_{mb}}\right)} \qquad (34)$$

$$\kappa_{2t} = \frac{1}{1 - \dfrac{R^*}{C_{2t}}} \qquad (35)$$

Where M_{mu} and M_{mb} are the average molecular weights of the gases before and after combustion, as determined by Equations 4 and 26.

Specific heat capacity

Specific heat and specific heat ratio are necessary to calculate heat generation, which is important for evaluating abnormal combustion. In this system, the specific heat ratio has been assumed to be a constant 1.27. However, specific heat capacity is a function of temperature and is highly dependent on temperature. Therefore, in this analysis method, the temperature dependence due to changes in the cylinder temperature is considered to perform the heat generation calculation with high accuracy.

2-region heat release rate

The calculation of the 2-region heat release rate dQ2t is the heat release rate calculated using the 2-region specific heat ratio. The formula is

$$dQ_{2t} = P_t \cdot dV_t \cdot \frac{\kappa_{2t}}{\kappa_{2t} - 1} + V_t \cdot dP_t \cdot \frac{1}{\kappa_{2t} - 1} \qquad (36)$$

In the second region, as in the first region, we used the smoothing function "Neighborhood Average" built into Origin 6.0J and smoothed the data from 100 data sets by applying the neighbor average process.

2nd domain heat generation amount

The 2nd domain heat generation amount Q2t is the sum of the heat release rates dQ2t from the start time of combustion based on the 2nd domain calculation, and is obtained by

$$Q_{2t} = \sum_{t=t_{CS2}} dQ_{2t} \qquad (37)$$

Q2t is obtained by Since heat loss is not calculated, it can be said to be the apparent heat generation amount including heat loss.

2.8 Pre-experiment

The operation check and reproducibility of the prototype RCEM were performed.

2.8.1 Experimental Conditions

Table 2.7 shows the experimental conditions for HCCI combustion of the homogeneous premixture. A piston with plate was used in this experiment for comparison with a later test in a flow field with plates. The experiment was conducted without dropping the plate and with no flow. Isopentane was used as fuel. The initial temperature of the mixture was equal to the wall temperature of the RCEM. The initial pressure was determined to match the temperature so that the air input mixture volume would be constant. The combustion phase was adjusted by changing the temperature of the air mixture (RCEM wall temperature). The equivalent ratio was set to 0.75, and N_2 was injected as EGR to achieve an EGR ratio of 35.5%. N_2 was added as EGR to dilute the O_2 concentration in the mixture to retard the ignition timing while the mixture temperature was kept at a certain high temperature, assuming that temperature stratification would be applied later. The combustion phase was tested at about 0.4 ms after top dead center, when the RCEM begins to expand. Four experiments were conducted under the same conditions to confirm the reproducibility of the RCEM.

Table 2.7 Experimental conditions (Homogeneous mixture)

Compression ratio ε	14.2
Fuel (RON, boiling point [℃])	iso-Pentan (92.3, 27.9)
Temperature of mixture [℃]	47
Temperature of cylinder wall [℃]	47
Initial pressure [kPa]	319
Equivalence ratio φ	0.75
EGR(N_2) rate %	35.5

2.8.2 Experiment Results - Reproduction of HCCI Combustion under High-Load Conditions Using RCEM.

The results of the four experiments are shown in Figure 2.11. The timing of CA50 for each case is shown in Table 2.8. In all cases, a 5 kPa low-pass filter was applied to the in-cylinder pressure. The pressure history and heat release rate patterns are well matched for the five cases. The variation of the maximum pressure, maximum pressure rise rate, and IMEP for each case is shown in Figure 2.12 The maximum pressure and maximum pressure rise rate decrease linearly as CA50 is slowed down.

Table 2.8 CA50 for 4 cases

Case number	CA50 ms. ATDC
1	0.34
2	0.38
3	0.37
4	0.4
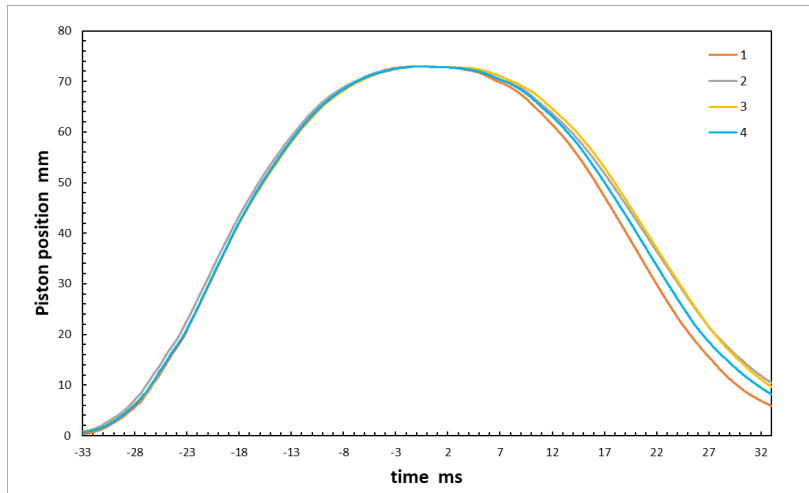
(a) Piston history
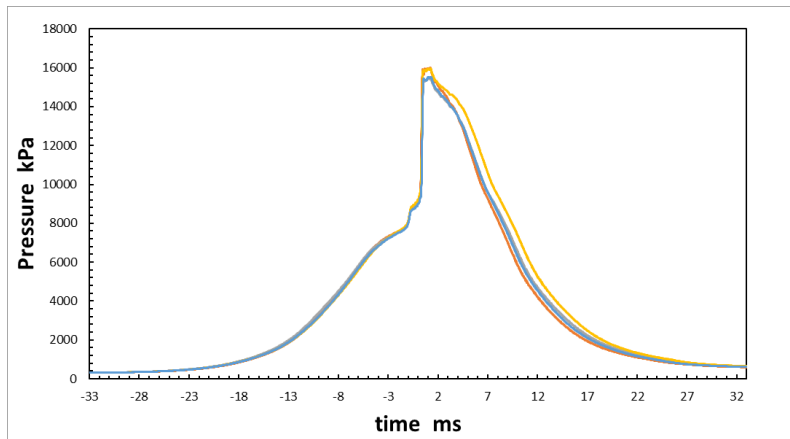
(b) Pressure
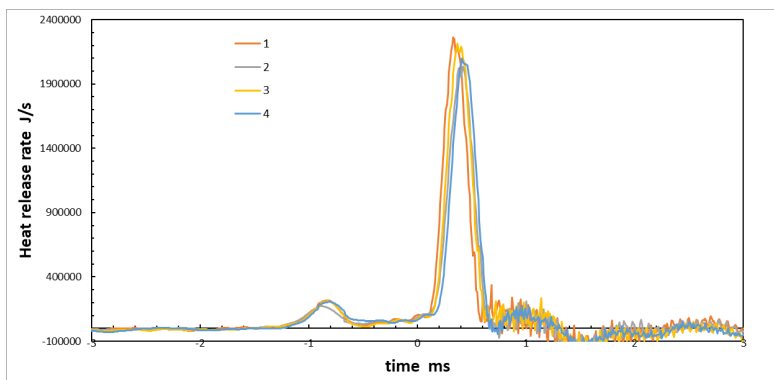
(c) Heat release rate

Figure 2.11 Comparison of 4 tests
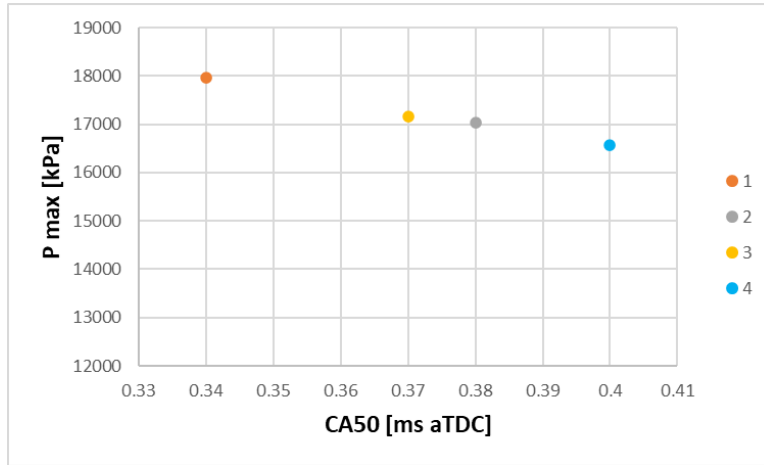
(a) Maximum in-cylinder pressure
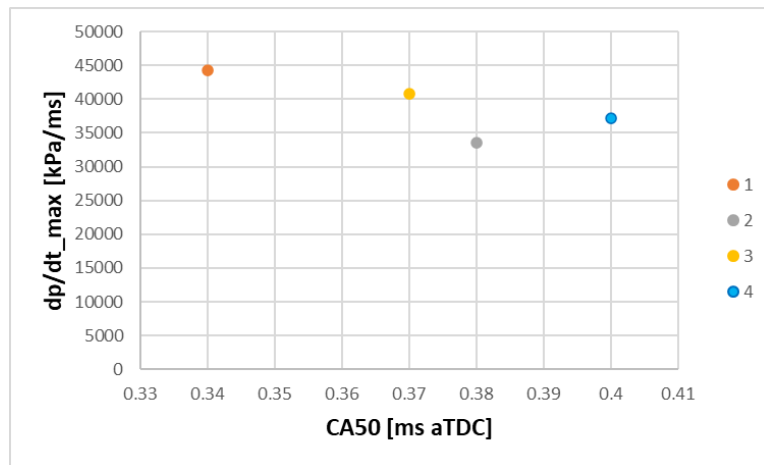
(b) Maximum pressure rise rate

Figure 2.12 Variations of 4 case

2.9 Real Experiment

2.9.1 Experimental Conditions

  The experiments for different turbulence intensities and temperature stratification conditions were carried out, as shown in Table 2.9. Case (a) represents the base condition with neither a temperature distribution on the cylinder wall nor initial in-cylinder flow. Cases (b), (c), and (d) have different turbulence intensities, which are created by the flow generation plate. These cases do not have a temperature distribution on the cylinder wall. The simulated tumble ratios in cases (b), (c), and (d) are shown in Figure 2.13. As shown in Figure 2.13, cases (b), (c), and (d) are implemented with high tumble ratio, medium turbulence ratio, and low turbulence ratio, respectively. The tumble flow was converted to turbulence as the piston compressed the mixture, which was created by the flow generation plate at the timing corresponding to BDC. Case (e) represents the case where there is temperature distribution without in-cylinder flow. The temperature distribution is created by the combination of the cylinder wall heater bar and the cooling water jacket, and the temperature difference between the highest and lowest temperatures is 60K. The temperature distribution for case (e) is shown in Figure 2.14.
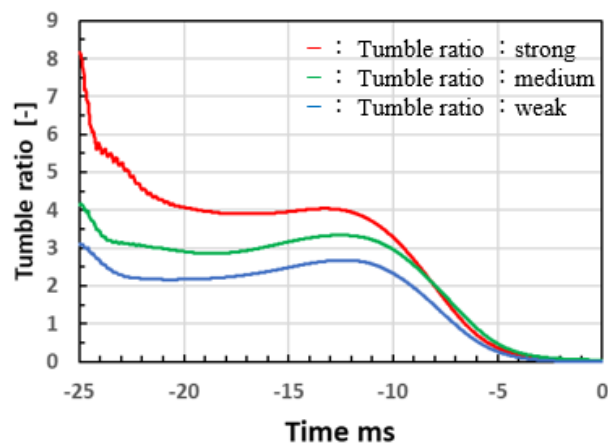
Figure 2.13 Simulated tumble ratio in case (b), (c) and (d)
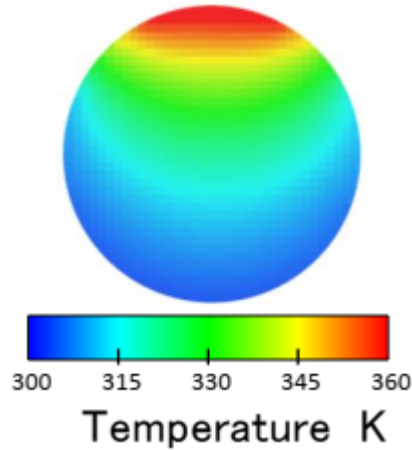
Figure 2.14 Simulated temperature distribution in case (e)

Table 2.9 Experimental conditions

Case name	a	b	c	d	e
Fuel (RON)	iso-pentane (92.3)				
Equivalent ratio φ	0.75				
Fuel mass [mg]	35.2				
Difference in temperature of wall [K]	0				60.4
The tumble ratio of initial in-cylinder flow	0	8	5	3	0
Initial mean temperature [K]	313	318	324	325	308

2.9.2 The Effect of Different Turbulence Intensity on HCCI Combustion

The effects of different turbulence intensities and previously studied temperature distribution condition on HCCI combustion were experimentally compared according to the conditions listed in Table 2.9. The results for different turbulence intensities and temperature distributions on the pressure rise rate and combustion duration under each condition are shown in Figure 2.15. The results of the temperature distribution case are a replication of the previous findings of Watanabe et al [8]. Comparison with the temperature distribution case shows that in-cylinder flow with strong, middle, and weak turbulence intensities significantly affects the reduction of

pressure rise rate. The level of the effect is as significant as the scale of influence of the temperature distribution. The results of the previous study by Watanabe et al[8] showed that the temperature distribution before ignition influenced the heat release pattern and pressure rise rate of HCCI combustion. The larger the temperature difference in-cylinder, the lower the pressure rise rate. Case (e) has a temperature difference of 60K. The mechanism by which the in-cylinder flow conditions (a), (b), and (c) affect the pressure rise rate then becomes a matter for discussion.
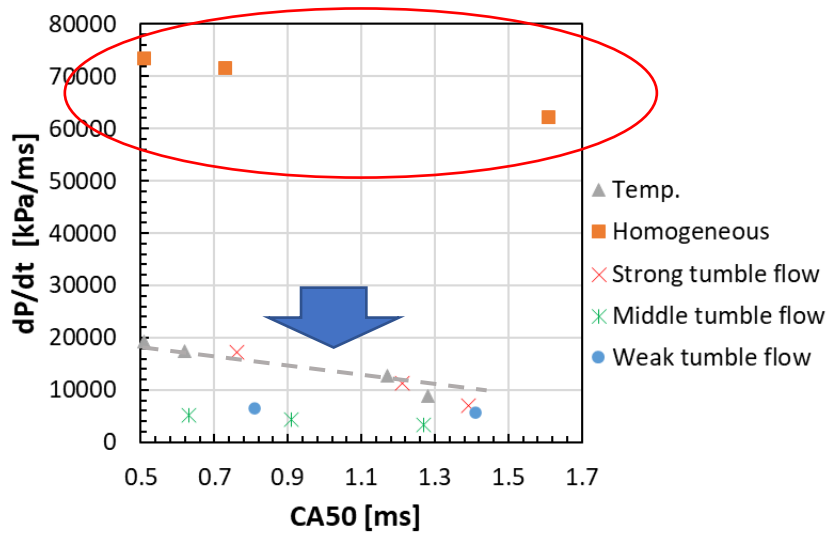
(a) Pressure rise rate vs CA50
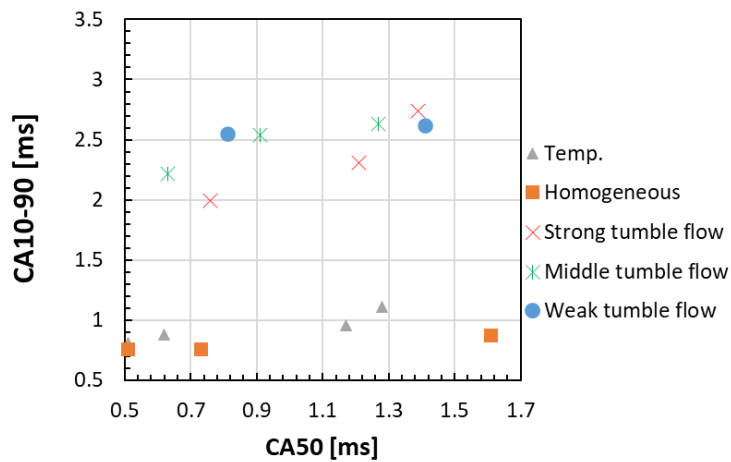
(b) Combustion duration vs CA50

Figure 2.15 Pressure rise rate and combustion duration under each condition

Next, the experimental results of each condition was compared, specifically focusing on those with closely matched CA50 values, as illustrated in Figure 2.16. As seen in Figure 2.16 (a), the homogeneous case, case (a), displays a sharp rise in pressure rate at the onset of combustion and pressure oscillation during and post-combustion. This pressure oscillation suggests that a significant portion of the mixture ignites nearly simultaneously, leading to detonation and the subsequent travel of a pressure wave within the combustion chamber. On the other hand, the temperature distribution case (e) exhibits no pressure oscillation during combustion and shows a slightly lower pressure rise rate compared to the homogeneous case. Additionally, the turbulent cases, cases (b) - (d), exhibit a lower pressure rise rate compared to both the homogeneous case (a) and temperature distribution case (e), and demonstrate no pressure oscillation. These results indicate that turbulence is effective in mitigating HCCI combustion.

Figure 2.16 (b) depicts the heat release rate for CA50 under homogeneous and turbulent conditions. The initial temperature and pressure were adjusted to regulate CA50. The turbulent cases display a lower maximum heat release rate and a later timing of the maximum heat release rate compared to the homogeneous case. These results suggest that the intensity of turbulent flow impacts the heat release rate of HCCI combustion. Furthermore, varying turbulence intensities have distinct effects on the pressure rise rate and combustion duration.

Figures 2.18(a) and (b) illustrate the heat release rate under varying flow conditions. The results reveal that cases with lower turbulence intensities have extended combustion durations and reduced pressure rise rates among the three distinct turbulence intensities tested. The maximum pressure rise rate in the cylinder is also suppressed. Figure 2.18(c) presents a comparison of the pressure rise rates under these three turbulence intensities. Within the scope of this experiment, it is observed that mid-level turbulence has the most pronounced effect on reducing the pressure rise rate.
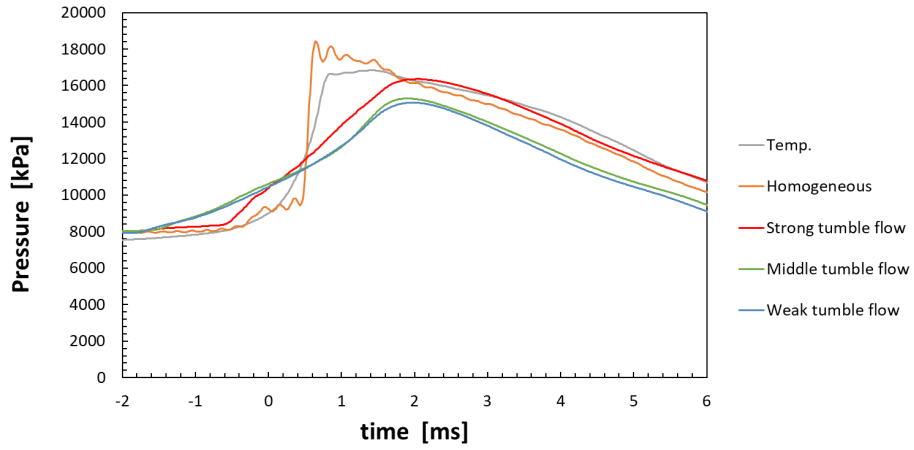
(a) In-cylinder pressure
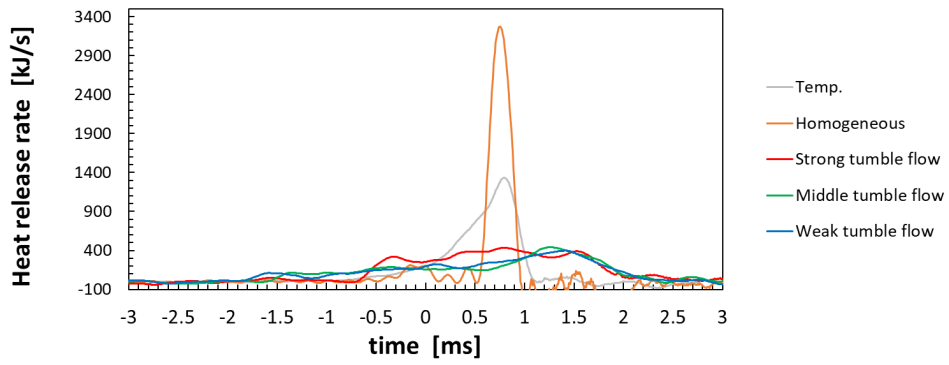
(b) Heat release rate

Figure 2.16 Experimental results of each condition with RCEM
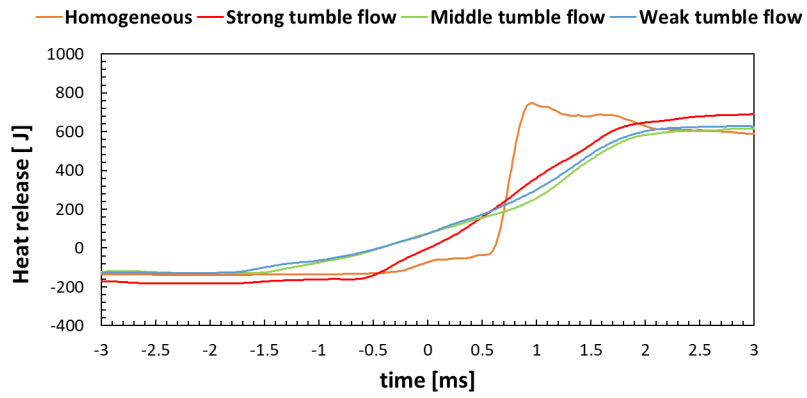
(a) Heat release
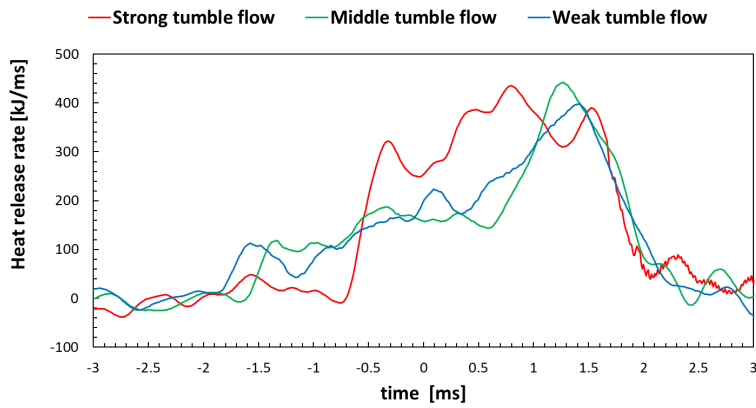
(b) Heat release rate
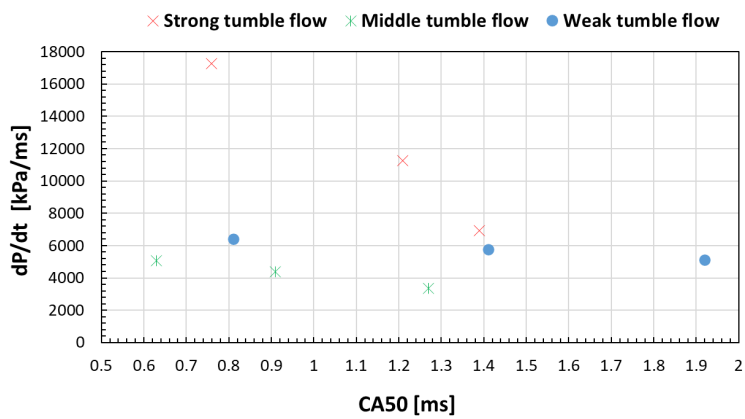
(c) Pressure rise rate vs CA50

Figure 2.17 Heat release rate and pressure rise rate under flow conditions

2.10 Summary

To investigate the effect of in-cylinder flow intensity (tumble ratio) on the combustion characteristics of HCCI, the effect of fast compression-expansion device on the heating rate and pressure increase rate of HCCI combustion at different tumble ratios was experimentally investigated.

The conclusions obtained from the above are summarized as follows.

1. An experimental study of the effect of different turbulence levels on the HCCI combustion was carried out using the newly developed rapid compression expansion.

2. The in-cylinder turbulence generated by the flow generation plate effectively mitigates the pressure oscillation and decreases the pressure rise rate of combustion. Regardless of the intensity of the in-cylinder flow, increasing the in-cylinder flow has the same effect on reducing the rate of pressure increase as the temperature stratification case examined in our previous study.

3. Turbulent flow case has a low-pressure rise rate and longer combustion duration. The influence of different flow intensities on heat release rate is also different. Lower flow intensities in the in-cylinder flow field have a greater effect on reducing the pressure rise rate in the range of this study.

Reference

[1]. K.Komura, et. al.: "Advanced Ignition Control Technology for HCCI Combustion ", Honda R&D Technical Review, vol. 26 No. 2, (2014).

[2]. T. Johansson, et. al. : "HCCI Operating Range in a Turbo-charged Multi Cylinder Engine with VVT and Spray –Guided DI", SAE2009-01-0494 (2009).

[3]. R. Yu, et. al. : " Effect of Temperature Stratification on the Auto-ignition of Lean Ethanol/Air Mixture in HCCI engine ", SAE Paper 2008-01-1669.

[4]. M. Sjoberg, et. al. : "Smoothing HCCI Heat Release with Vaporization-Cooling-Induces Thermal Stratification using Ethanol ", SAE 2011-01-1760.

[5]. K. Saijyo, et. al. : "A Numerical Analysis of the Effect of Mixture Heterogeneity on Combustion in a Premixed Charge Compression Ignition Engine ", The international symposium on diagnostics and modeling of combustion in internal combustion engines 2004(6), 239-246, 2004-08-02.

[6]. K. Yoshimura, et. al.: "Studies on the Effect of In-cylinder flow on stratified HCCI Combustion", The japan society of mechanical engineers, (2017).

[7]. K. Yoshimura, et. al.: "Studies on the Effect of In-cylinder Charge Stratifications on High Load HCCI Combustion", SAE2016-32-0010.

[8]. S. Watanabe, et. al.: "The Effect of In-Cylinder Flow and Mixture Distributions on Combustion Characteristics in a HCCI Engine", SAE2017-32-0061.

[9]. https://convergecfd.com/

[10]. T. Tsurushima. A new skeletal PRF kinetic model for HCCI combustion. Proceedings of the Combustion Institute, Vol.32 (2009), pp. 2835-2841.

[11]. T. ISHIHARA,et. al.: A DNS study of the effects of temperature non-uniformity and turbulence on an auto-ignition process in a homogeneous n-heptane/air mixture. Transactions of the JSME (in Japanese), Vol.80, No.820, (2014).

[12]. Setiawan, A., Wahono, al.: A study of combustion characteristics of two gasoline-biodiesel mixtures on RCEM using various fuel injection pressures. Energies, 13 (12). https://doi.org/10.3390/en13123265

[13]. EL-Seesy, A. I., Kayatas, al.: Combustion and emission characteristics of a rapid compression-expansion machine operated with N-heptanol-methyl oleate biodiesel blends. Renewable Energy, 147.

[14]. EL-Seesy, A. I., Kayatas, al.: Combustion and emission characteristics of RCEM and common rail diesel engine working with diesel fuel and ethanol/hydrous ethanol injected in the intake and exhaust port: Assessment and comparison. Energy Conversion and Management, 205. https://doi.org/10.1016/j.enconman.2019.112453

[15]. Windarto, C al.: Combustion and Performance Characteristics of the Spark Discharge Energy Effect on Rapid Compression and Expansion Machine (RCEM) Working with Propane and Diesel Fuel Direct Injection as Marine Fuel.

[16]. Xiong Shusheng ,Liu Zhentao al.: Study on Combustion of LPG S.I. Engine by Rapid Compression-Expansion Machine[J].Chinese Internal Combustion Engine Engineering,2002,23(3):9-12.

Chapter 3　The effect of Tailored In-Cylinder Flow on HCCI Combustion Phenomenon by Direct Photographic Analysis

3.1 Introduction

Pressure oscillation (knocking) caused by the auto-ignition of unburned gas reduces the thermal efficiency of spark-ignition gasoline engines under high-load operation. In addition, in HCCI combustion, which is expected to be a next-generation high-efficiency combustion technology, the operating range on the high-load side is limited due to the high-pressure increase rate. Therefore, establishing a method to reduce the pressure rise in auto-ignition combustion is expected to lead to the development of technology to improve the thermal efficiency of gasoline engines. It is widely known that stratification of the in-cylinder mixture temperature effectively reduces the pressure increase rate. In order to suppress knocking during high-load operation and to obtain a design policy for HCCI engines that can be operated over a wide operating range, it is essential to clarify the effects of in-cylinder flow and turbulence, which strongly affect the temperature and fuel concentration distributions of the premixture, as well as the impact of temperature distribution in the cylinder on heat release characteristics.

In the second chapter, experiments have shown that enhanced in-cylinder flow is an effective method for extending the combustion period of auto-ignition and reducing the associated pressure increase rate with auto-ignition. However, the mechanism of the effect of turbulence on auto-ignition has not been clarified experimentally. Therefore, we combine optical diagnostic techniques in this chapter to experimentally investigate how temperature distribution and in-cylinder flow affect the HCCI combustion process. The equipment used for this chapter is an RCEM with an optical pathway. We have modified the original equipment to create an RCEM with an optical pathway and obtained waveforms for each condition as well as direct visualization of combustion. Based on this, we investigated how the enhanced in-cylinder flow mitigates the heat release of HCCI combustion. The purpose of this chapter is to

63

clarify the effect of turbulence on the combustion behavior of HCCI through an optical version of the rapid compression and expansion machine (RCEM).

3.2 Equipment Setup

In this chapter, the effects of tumble flow and thermal stratification on the pressure increase rate of HCCI combustion are observed by direct imaging of the combustion chamber. A sapphire visualization window is used as the visualization window for combustion inside the cylinder. Sapphire, which has excellent transparency from the visible region to the infrared region, was used as the material of the window because it is intended for direct imaging and infrared imaging visualization.

3.2.1 Introduction of The Optical Version of RCEM

The RCEM used for this investigation is an optically accessible version of the all-metal RCEM used for the data presented and numerous previous studies from our previous works [7-10]. A sapphire visualization window was used to visualize combustion in the cylinder. The piston surface and the entire combustion chamber can be seen through a cylindrical sapphire window mounted on the cylinder head. The combustion inside of the cylinder is directly photographed with a high-speed camera. Since the thickness of the sapphire visualization window is thinner than the metal one that was previously installed for combustion experiments, we made a spacer for fixing the visualization window. Sapphire has good transparency from the visible to the infrared range and was used as window material because it is used for direct and infrared visualization. A Photron FASTCAM SA-X high-speed camera was used to take experimental combustion images. The RCEM simulates an engine's compression and expansion process and can duplicate combustion phenomena in the cylinder in a single shot. The specification of the optically accessible version of RCEM is presented in Table 3.1.

Except for the sapphire visualization window, the other components of the RCEM are the same as the metal RCEM used in chapter 2, the pressure reservoir unit, the cam unit that drives

the piston, Etc. Iso-pentane, which was used as fuel, also the same as chapter 2, is stirred with N2 and O2 in the mixture tank. The mixture was inducted from the intake valve installed on the lower section of the combustion chamber wall. After the intake process, compressed air in the pressure reservoir unit is derived from the cam unit toward the left-hand side, as indicated in Figures in chapter 2. The piston accordingly moved upward and compressed the air-fuel mixture in the combustion chamber. In this way, individual cycles of compression and expansion strokes which include combustion events, were measured with the RCEM. In-cylinder pressure was measured by the pressure sensor (Kistler 6052C) and acquired by the data logger (WE800). The temperature of the mixture was controlled by the heater installed in the mixture tank. The RCEM has eight electric heaters or water jackets adjacent to the combustion chamber. The temperature distribution of the in-cylinder mixture was created by the heaters and water flowing inside the water jackets, and the temperature of the water was controlled by a cooling chiller and a heat exchanger in a hot water tank.

Table 3.1 Specification of the optically accessible version of RCEM

Displaced volume	306 cm^3
Stroke	73 mm
Bore	73 mm
Compression ratio	14:1

3.2.2 Preparation for Direct High-Speed Photographic Measurement of In-Cylinder Combustion Phenomena.

Figure 3.1 shows the shape of the sapphire visualization window. Because the thickness of the sapphire visualization window is thinner than the metal lid for the window that has been used for combustion experiments, a spacer was fabricated to fix the visualization window. The shape of the spacer is shown in Figure 3.2. Figure 3.3 shows an assembly diagram of the sapphire visualization window and the new spacer (assembly diagram of the combustion chamber visualization component). Figure 3.4 shows the direct imaging optical setup of the high-speed camera. A FASTCAM SA-X from Photron was used as the high-speed camera as shown in Figure 3.5.
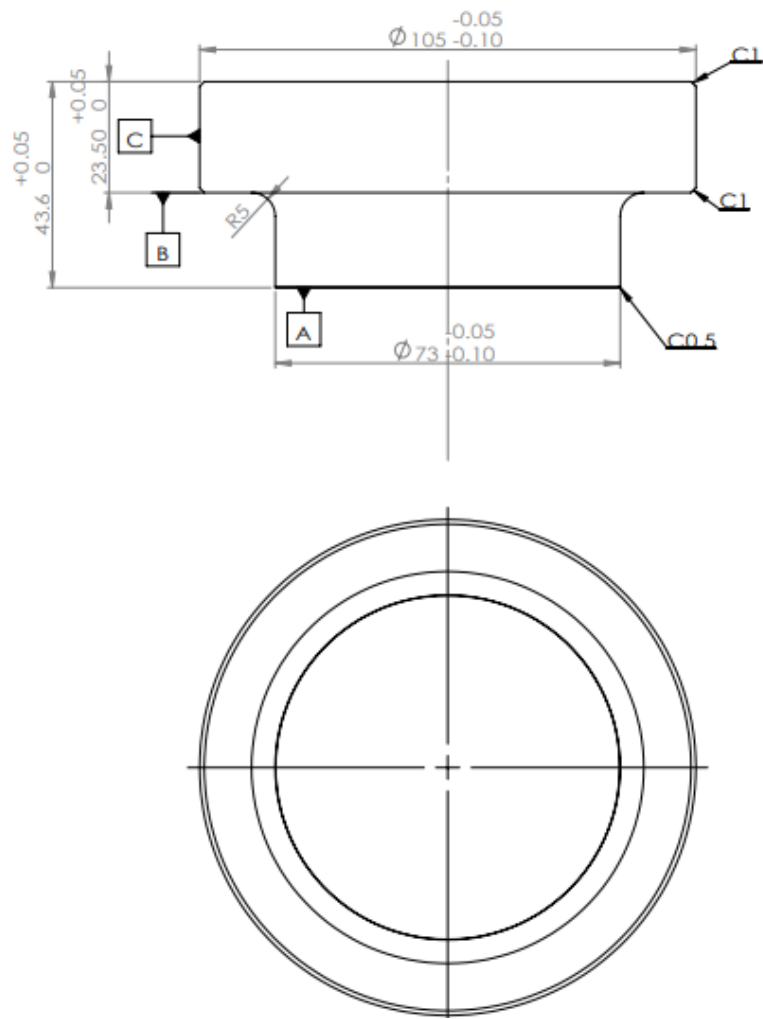
Fig. 3.1 Drawing of sapphire window
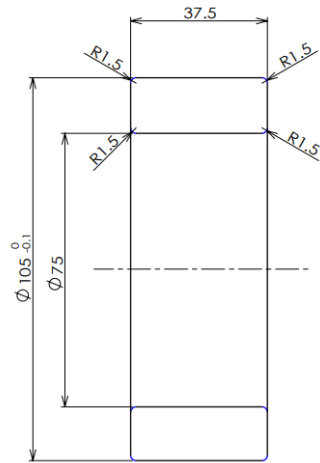
Fig. 3.2 Drawing of spacer
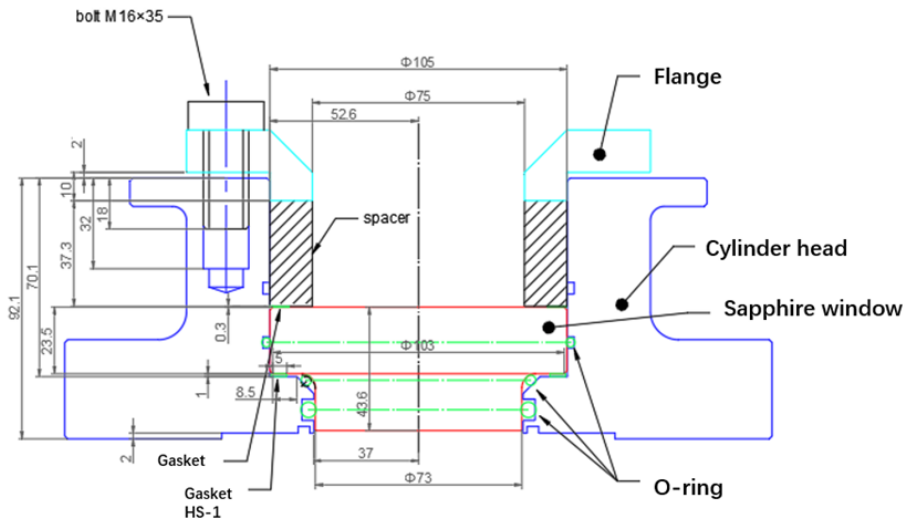
Fig. 3.3 Drawing of assembly drawing of combustion chamber visualization parts
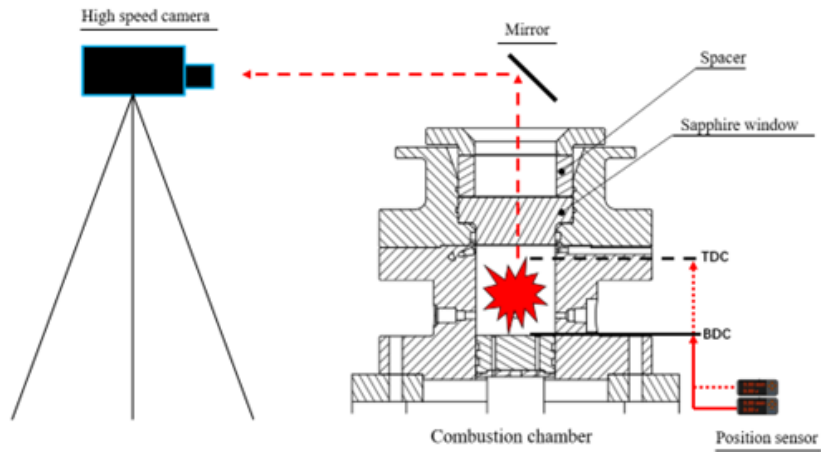
Fig. 3.4 Schematic diagram of optical system setup

Figure 3.5 Normal high-speed camera (FASTCAM SA-X)

3.3 Control and Measurement System

The following is a rough description of the system up to the start of compression in this system. To generate the "compression" shown in Figure 2.6, the piston is lifted to the upper dead center by a cam, the plate support plate is hooked to a seesaw, and the piston is returned to BDC. The piston is then pressurized and lifted by the spring and lowered and secured by a piston-holding electromagnet. The RCEM cylinder is then evacuated, and the air mixture is sucked from the air mixture tank by opening and closing the needle valve. After the intake is completed, the piston holding electromagnet is turned off. The solenoid valve in the drive unit is opened to allow compressed air to flow into the drive cylinder, causing the drive cam to move. All of these controls are performed by a program relay called a sequencer (ZEN-20C1DT-D-V2, Omron). The combination of ladders, meaning ladders, makes it easy to create arbitrary commands. A function generator (WF1646B, NF Circuit Design Block) was used to capture the trigger once, delay it for a certain period of time, and output the trigger again.

Figure 3.6 shows a time chart of the entire device. When the cam passes the sensor, the trigger enters the plate holding electromagnet, the power is turned off, and the plate drops. The time from the time the trigger is triggered to the time the electromagnet is turned off and the fall is completed was 19 ms, as measured by the high-speed camera. In this experiment, the start trigger and the trigger to the high-speed camera were combined.
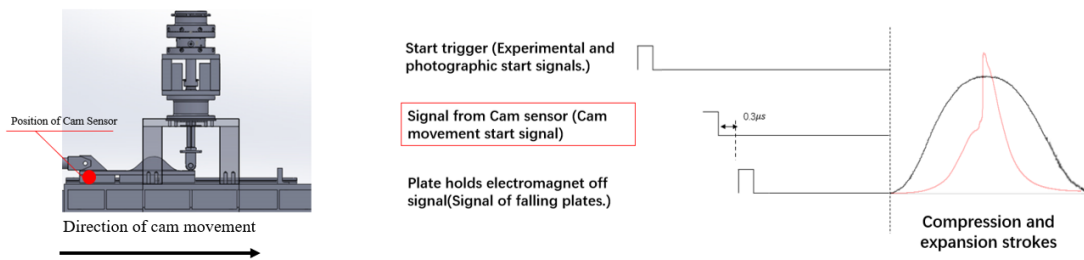
Fig.3.6 Time chart for RCEM operation

3.4 Research Method

3.4.1 Optical Diagnosis Technology and Application of Internal Engine Combustion

Optical diagnosis technology is a valuable tool for engine research, providing critical information about the in-cylinder working process through various optical test methods. Techniques such as the ripple shadow method, two-color method, extinction method, refractive index matching method, PIV, LIF, LII, PDPA, etc. can yield essential data about engine characteristics such as velocity field, concentration field, temperature field, particle size of spray droplets, morphological information, velocity, concentration distribution of various intermediate components in combustion field, flame morphology, carbon smoke generation characteristics, and more. This data can enable researchers to systematically study engine airflow motion, spray, mixture formation, combustion process, and pollutant generation and emission. Ultimately, this information provides crucial reference and support for the industrial design, performance evaluation, and independent R&D of engines. Therefore, optical engine

diagnosis technology is irreplaceable for engine research.

Some common optical diagnostics used in combustion research include.

1. The Ripple Shadow Method

    The Ripple Shadow Method is an optical diagnostic technique used to visualize the flame surface in combustion applications. It works by inducing a laser-induced perturbation of the flame surface, which causes the flame to cast a shadow on a nearby surface. The shadow is then recorded using a high-speed camera, producing a two-dimensional image of the flame surface. The Ripple Shadow Method is particularly useful for studying flame propagation and combustion instability, as it provides a detailed view of the flame front and any fluctuations that may occur. It can also be used to study the effects of various parameters such as fuel injection timing and air-fuel ratio on the flame surface. Typical applications of the Ripple Shadow Method include studying the flame propagation in engines and gas turbines, as well as investigating combustion instability in rocket engines and other combustion systems.

2. The Two-Color Method:

    Uneven mixture combustion in engines is the root cause of carbon soot. The carbon soot generation and oxidation process are very complex and still poorly understood. It requires precise time and space analysis of the in-cylinder combustion process, including the carbon fumes generated. The Two-Color Method is based on thermal radiation theory, which can simultaneously obtain the flame's two-dimensional soot concentration and temperature field distribution with high temporal resolution. This method is widely used in the study of engine combustion processes.

3. Planar Laser Induced Fluorescence (PLIF):

    This technique is particularly useful for studying flame propagation and fuel-air mixing. Planar Laser-Induced Fluorescence (PLIF) is a non-intrusive, laser-based diagnostic technique used to measure various properties of fluids, such as temperature, velocity, and species concentration. It is commonly used in fluid dynamics research and engineering

applications. The PLIF technique involves exciting a fluorescent dye or tracer that has been added to the fluid with a laser beam, which causes the dye to emit light at a longer wavelength. The emitted light is then captured by a camera, which records the fluorescence intensity in the fluid. By analyzing the recorded fluorescence intensity, the distribution of the dye and the properties of the fluid can be determined.

PLIF can be used to measure temperature by using temperature-sensitive dyes that have varying fluorescence intensity depending on the temperature of the fluid. It can also measure velocity by introducing a tracer into the fluid and tracking its movement over time using multiple PLIF images. Species concentration can be measured by adding a dye that reacts specifically to a particular species in the fluid. PLIF offers several advantages over other diagnostic techniques, such as its non-intrusive nature, high spatial and temporal resolution, and the ability to measure multiple properties simultaneously. However, it also has limitations, such as the need for fluorescent tracers, which can potentially alter the properties of the fluid being measured, and the limited depth of field of the laser.
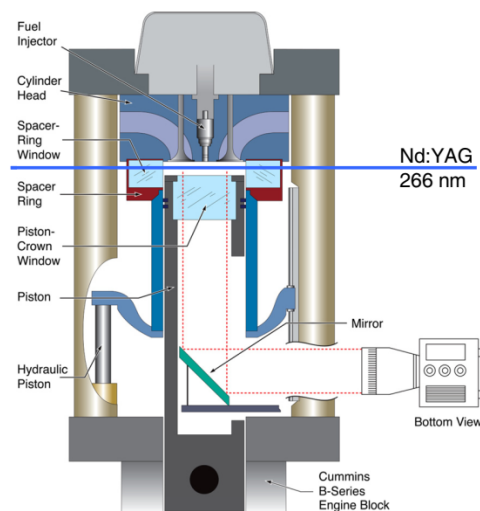
Figure 3.7 Engine schematic showing the setup for PLIF imaging. [13]

4. Laser Induced Incandescence (LII):

    Laser Induced Incandescence (LII) is a diagnostic technique used to study the size,

concentration, and spatial distribution of soot particles in combustion systems. The technique works by illuminating the soot particles with a laser pulse, which heats the particles and causes them to emit light at a characteristic wavelength. The emitted light is then detected and analyzed to determine the properties of the soot particles.LII is based on the principle of incandescence, which is the emission of visible light from a heated object. In the case of LII, the laser pulse heats the soot particles to a high temperature, causing them to emit light in the visible and near-infrared spectral regions. The wavelength of the emitted light depends on the temperature of the particles, and therefore, the technique can provide information about the temperature of the soot. LII can be used in a variety of combustion systems, including engines, gas turbines, and industrial burners. The technique provides a non-intrusive method for studying the properties of soot particles, which is important for understanding the formation and evolution of pollutants in combustion systems. LII is used to measure soot concentrations and size distributions in combustion chambers. This technique involves heating soot particles with a laser beam so that they emit light at a characteristic wavelength that can be detected and quantified.

5. High-speed imaging:

High-speed imaging is used to capture the dynamics of the combustion process, including ignition, flame propagation, and knockdown. This technique involves recording a series of images at high frame rates, allowing researchers to study the process in detail. High-speed imaging is a powerful tool that allows researchers to capture and analyze the dynamics of the combustion process in real time. This technique involves using high-speed cameras capable of recording thousands of frames per second, which enables the visualization of fast-moving phenomena such as ignition, flame propagation, and knockdown. Ignition is the process of starting a combustion reaction, and it can be triggered by various means, such as spark ignition or compression ignition. High-speed imaging can capture the moment of ignition, typically characterized by a sudden increase in temperature and pressure. Flame propagation refers to the flame front moving through the combustion chamber.

High-speed imaging can be used to visualize the shape and velocity of the flame front, which provides insight into the combustion process and can be used to optimize engine performance. Knockdown, or engine knock or detonation, is abnormal combustion occurring in engines under certain operating conditions. High-speed imaging can capture the occurrence of knockdown, characterized by a rapid increase in pressure and temperature that can cause engine damage.

6. Particle Image Velocimetry (PIV):

PIV is a powerful experimental technique used to measure the velocity field of a fluid in both two- and three-dimensional space. PIV involves the injection of small tracer particles into the fluid, which is illuminated by a laser sheet. The resulting images captured by a camera are then analyzed to determine the fluid's velocity field. Since its development in the 1990s, PIV has been refined and applied to measure velocity fields in various flow and combustion systems. PIV is also a valuable tool for studying fluid mechanics, providing a detailed and accurate measurement of instantaneous velocity fields.

Unlike traditional velocity measurements techniques, such as hot-wire anemometry and laser Doppler velocimetry, PIV can provide a two-dimensional measurement of the velocity field in a single snapshot, making it possible to study complex flow structures in detail. Additionally, PIV is a non-intrusive technique that does not disturb the fluid flow and can be used to measure the velocity field in opaque fluids. Overall, PIV is a versatile technique with a wide range of applications in fluid mechanics, including studies of turbulent flows, boundary layers, and flow-induced vibration. PIV data can also be used to validate computational fluid dynamics (CFD) simulations, which are often used to study complex fluid flows in engineering applications.

Table 3.2 Experimental conditions for direct photography of HCCI combustion

Technique	Principle	Information provided	Typical applications
Ripple Shadow Method	Laser-induced perturbation of the flame surface	Two-dimensional image of the flame surface	Flame propagation, combustion instability
Planar Laser-Induced Fluorescence (PLIF)	Laser excitation of specific molecules	Two-dimensional image of species distribution in a plane	Flame propagation, fuel-air mixing, combustion chemistry
Laser-Induced Incandescence (LII)	Laser heating of soot particles	Measurement of soot concentration and size distribution	Diesel engines, sooty flames
High-Speed Imaging	High-speed recording of the combustion process	Real-time visualization of the combustion process	Ignition, flame propagation, engine knock
Particle Image Velocimetry (PIV)	Laser illumination of particles	Two-dimensional velocity field of fluid flow	Turbulent flow, engine airflow, fuel spray characterization

3.4.2 Direct High-Speed Photographic Technology

As environmental and energy problems become increasingly serious, countries are enacting stricter emission and economy regulations one after another. The development of a new generation of combustion technology for internal combustion engines is the key to achieving efficient and clean combustion. A deeper understanding of the in-cylinder combustion process and the formation mechanisms of harmful pollutants in internal combustion engines is an important contribution to the development of new combustion technologies. Therefore, there is an urgent need for advanced technologies that enable direct visualization of in-cylinder combustion processes and the formation of pollutants. The basic principle is to obtain information about the flow field, temperature and components of the working mass during engine operation by receiving spectral or optical images, which can be used to analyze the

engine's operating process.

The combustion and emission generation process of an internal combustion engine is a very complex process, which requires the measurement of several parameter. Although laser diagnostic techniques are developing at a rapid pace as science and technology continue to advance, each measurement and diagnostic method has its own advantages, disadvantages, limitations and relevance, and the best measurement method should be selected for different measurement purposes. In this study, direct imaging techniques were used to obtain images of the combustion process under different conditions of HCCI combustion.

3.4.3 Image Processing

Once the images are obtained, the next step is to process them in a scientific manner to extract feature information. This involves using various image processing techniques such as filtering, segmentation, feature extraction, and data analysis to identify and quantify important characteristics of the combustion process, such as flame shape, temperature distribution, and pollutant emissions. These features can be used to gain a deeper understanding of the engine's performance and optimize it for better efficiency and reduced emissions.

In this research, the software ImageJ is used for processing the obtained images. First, ImageJ is a free and open-source software, which is advantageous for research with limited budgets. Second, ImageJ has a user-friendly interface that enables efficient image analysis and manipulation. Third, ImageJ is widely used and has a large community of developers who contribute to its development, creating a broad range of plugins and macros that can extend its capabilities. Fourth, ImageJ is highly customizable, allowing researchers to develop their own plugins and macros to suit their specific needs. Finally, ImageJ supports a range of image formats, making it a versatile tool for image processing and analysis. Therefore, we chose to use ImageJ to process our images, as it offers a powerful and flexible platform for our research needs.

Figure 3.7 illustrates the details of the image processing workflow used in this study. The

flowchart begins with image loading, followed by pre-processing steps such as background subtraction to remove any noise or artifacts. The image is then converted to grayscale to simplify the processing of image data. Next, the image is thresholder and binarized to separate foreground and background pixels. A region of interest (ROI) is selected within the image. In this study, the ROI is defined as the burnt zone, which is the region where combustion has taken place and where measurements will be performed. Finally, the area of the selected region is measured using ImageJ's built-in tools for quantifying and measuring image features. The resulting measurements are then exported. Therefore, it is possible to quantitatively calculate the temporal development of the burnt zone. Figure 3.8 illustrates the resulting images before and after processing using this method.
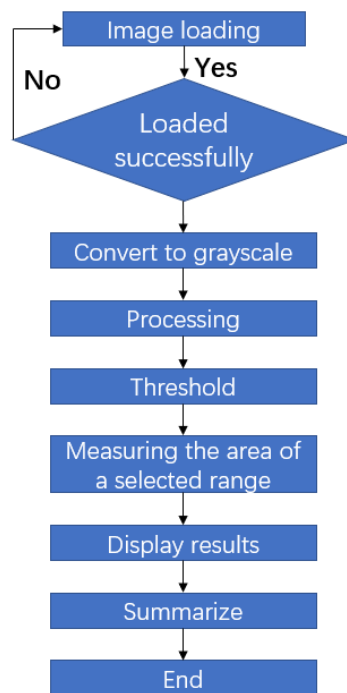
Figure 3.7 Image processing flowchart
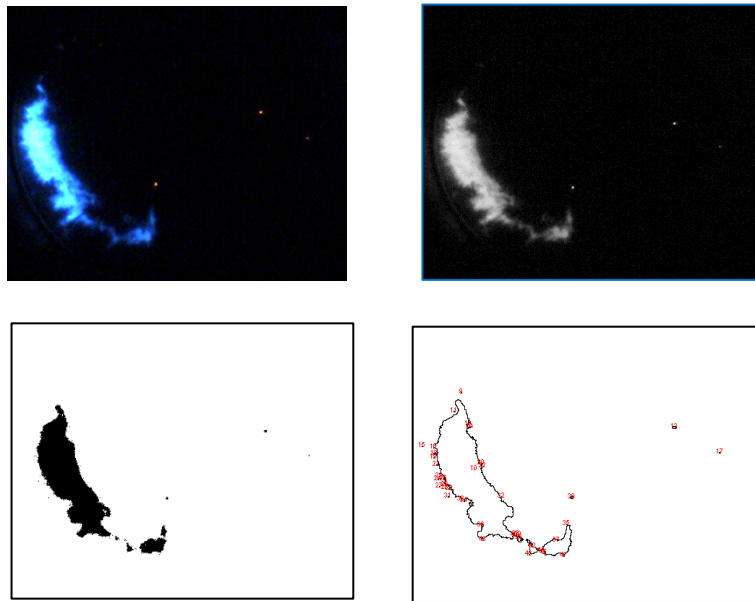
Figure 3.8 Image processing result display

3.5 Experimental Conditions

The effects of mixture stratification and in-cylinder flow on HCCI combustion were experimentally investigated to find the mechanism of slow heat release in HCCI combustion by enhancing in-cylinder flow. The heat release rate and maximum pressure increase rate in a single HCCI combustion cycle were compared when different intensities of in-cylinder flow were generated using a rapid compression and expansion device (RCEM). The effects of gas flow were also compared with the heat release rate and maximum pressure increase rate in a temperature stratified HCCI combustion cycle to verify the effects of gas flow. In this experiment, direct in-cylinder visualization was conducted to investigate the effect of tumble flow on the pressure rise rate of HCCI combustion. A high-speed camera was used to capture images inside the cylinder through a sapphire observation window mounted on the top of the cylinder head.

Optical tests of HCCI combustion under different conditions were conducted, including without flow, with different flow intensities (tumble ratio), and temperature stratification in a

homogeneous fuel mixture, using an RCEM equipped with a visibility window. The results of each cycle under these conditions were compared, with CA50 held constant. Table 3.3 presents the experimental conditions.

The in-cylinder flow intensity was altered by changing the rate at which the in-cylinder generation plate dropped. In addition to the high-intensity tumble (TR=8) and the medium-intensity tumble (TR=5) experiments, piston compression was initiated without dropping the flow generation plate, thereby eliminating the need for initial gas flow. The simulated tumble ratios in high-intensity tumble flow case and medium-intensity tumble flow case are shown in Figure 3.9. In addition, a temperature distribution visualization experiment with significant temperature differences in the cylinder was also conducted. The temperature distribution for temperature distribution case is shown in Figure 3.10, and the temperature difference between the highest and lowest temperatures is 60K.The fuel used was isopentane. Isopentane was selected as the test fuel because it has a low boiling point, vaporizes at ambient temperature, and has a research Octane Number of 92.3, which is about the same as that of regular gasoline sold on the market. The initial temperature of the mixture was set equal to the wall temperature of the RCEM. The initial gas temperature was adjusted to achieve the desired combustion phase (CA50 was used as an index). The initial pressure was varied with the initial temperature in order to keep the air input constant. The equivalent ratio was set to 0.75, and N2 was added at a dilution ratio of 35.5 % to simulate EGR. The initial temperature and dilution ratio of N2 were adjusted so that the combustion phase was from the top dead center, where the RCEM begins to expand, to CA50 at 2ms after the top dead center.
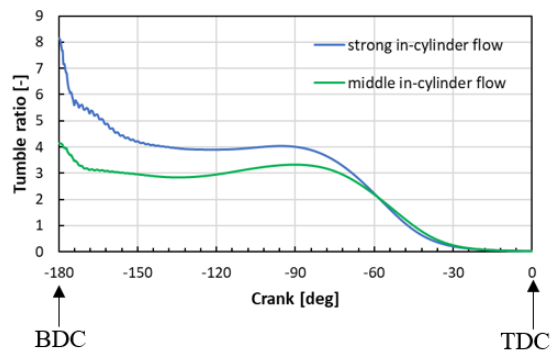
Figure 3.9 Tumble ratio of in-cylinder flow cases
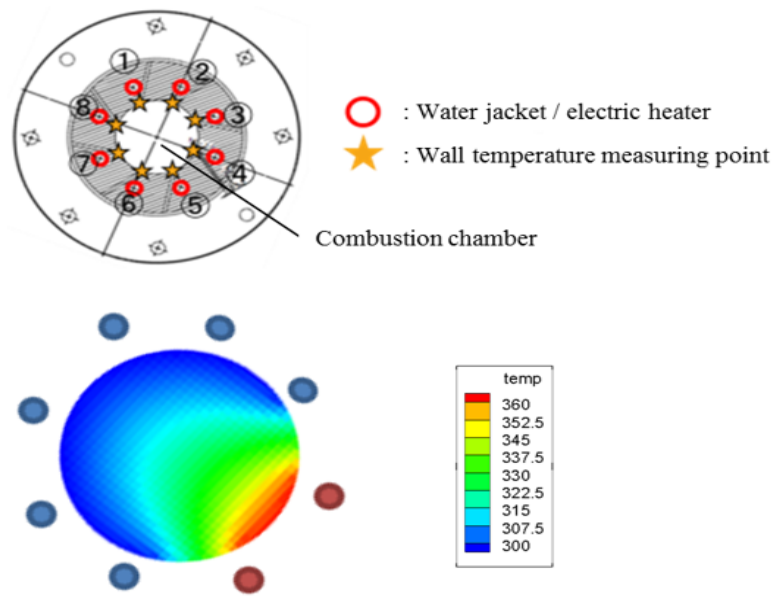
Figure 3.10 Top view of the temperature distribution of the combustion chamber (case (b))

and water jackets

Table 3.3 Experimental conditions for direct photography of HCCI combustion

Case name	Homogeneous w/o flow	High Tumble intensity （TR=8）	Mid. Tumble intensity (TR=5)	Thermal strat. w/o flow
Compression ratio ε	14.2			
Fuel (RON, boiling point [℃])	iso-Pentan (92.3，27.9)			
Compression time [ms]	33(Equivalent engine speed is 900 rpm)			
Equivalent ratio φ	0.75			
EGR(N₂) ratio [%]	35.5			
Fuel mass [mg]	35.2			
Temperature of mixture [℃]	43	71	63,65,66	43
Initial pressure [kPa]	249	271	265,267,268	250
Wall Temperature [℃]	43	71	63,65,66	43 (Mean)
1				39.4
2				87
3				77.8
4				34.5
5				26.5
6				26.5
7				26
8				27.6

3.6 Experimental Results and Discussion

3.6.1 Effect of In-Cylinder Flow (tumble) on The Tressure Rise Rate

This part presents the experimental results of HCCI combustion with internal flow enhancement using RCEM. Figure 3.11 shows the low-pass pressure history, local pressure history, and heat release rate as the results of the experiments in this chapter. Figure 3.12 displays each experimental case's pressure rise rate (dP/dt) against the combustion phase (CA50). Figures 3.13 and 3.14 show that mixture temperature stratification and in-cylinder flow can reduce the pressure rise rate by extending the period of heat release and reducing the maximum heat release rate. In the stratified conditions with in-cylinder flow and temperature distribution, heat release began 0ms before the top dead center, indicating an extended combustion period and slower combustion. Furthermore, the heat release period was longer in the flow condition than in the temperature stratification condition, indicating that combustion was slowed down. Homogeneous cases without in-cylinder flow showed pressure oscillations. Figure 3.12 also suggests that lower in-cylinder flow intensity is more effective in reducing the pressure rise rate within the range of the experimental conditions.

The waveform results from the above experiments show that the previous studies described in Chapter 2, which investigated the effect of in-cylinder turbulence on reducing the pressure rise rate and prolonging the combustion duration, can be replicated in the optically accessible version of the RCEM.
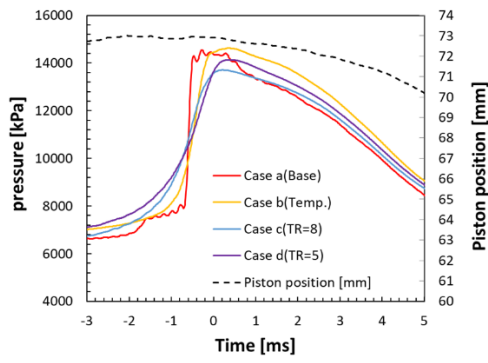
Figure 3.11 Pressure history of each case
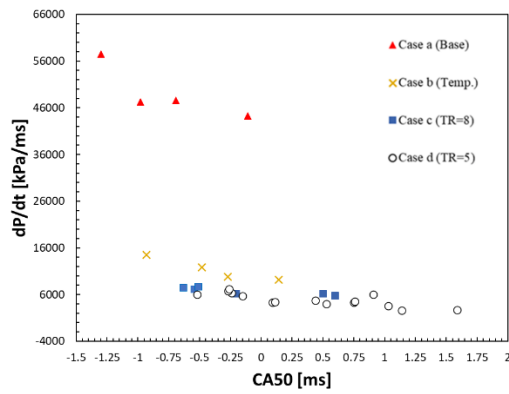
Figure 3.12 Effect of in-cylinder flow (tumble) on pressure rise rate.
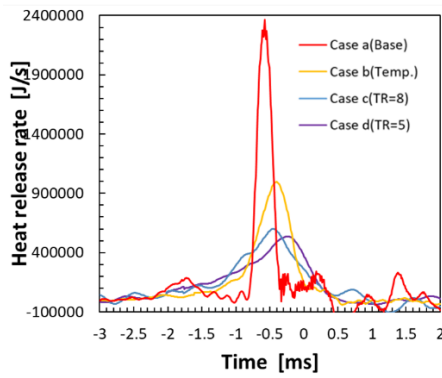
Figure 3.13 Hear release rate of each case.
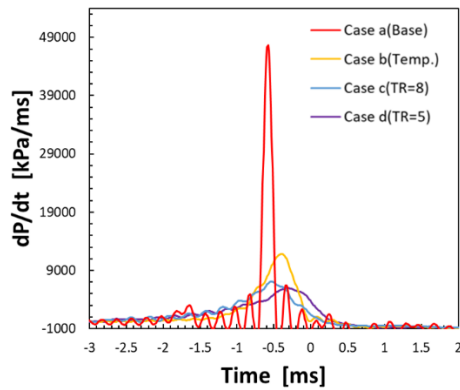
Figure 3.14 Comparison of waveform results with RCEM

3.6.2 Observation of Direct Imaging Visualization of Combustion Phenomena under Different Conditions

To investigate the mechanism of the slowdown in HCCI combustion due to the enhanced in-cylinder flow in terms of heat release, we performed high-speed imaging photography of natural luminescence using RCEM to compare the combustion phenomenon under each condition. Next, we will discuss the images of combustion under each condition obtained from high-speed direct imaging, as shown in Figure 3.15. Compared to other cases, we observed that no-flow (homogeneous w/o flow) combustion results in the shortest combustion duration, and the combustion is completed in a very short time. The combustion phenomenon is characterized by a sharp pressure rise and heat release, indicating the simultaneous ignition of the entire air-fuel mixture. In the case of the temperature stratification case (w/o flow), ignition occurs in the lower right corner of the image, corresponding to the high-temperature zone, and then spreads from the lower right corner to the upper left corner, from the high-temperature zone to the low-temperature zone, depending on the temperature stratification in the cylinder. The combustion zone then spreads from the center of the ignition zone to the periphery. The combustion time is longer than in the no-flow condition but shorter than in the in-cylinder flow conditions. In the cases of strong and medium intensity with in-cylinder flow conditions, we observed that ignition kernels were formed at multiple points in the combustion chamber. For both conditions,

83

the heat release rate was slower and the pressure rise rate was lower compared to the condition without in-cylinder flow.

Next, Figures 3.16 and 3.17 show the reproducibility of the ignition location for the strong and medium flow conditions. From the figures, we can observe that, for both intensity flow conditions, the medium intensity flow is more effective in reducing the pressure rise rate, and the latter part of the combustion shows a longer tendency.

The first ignition spot under strong flow conditions was small and appeared near the center's upper part. Because the initial autoignition point is considered to be determined by the temperature, the high-temperature zone is smaller due to the enhanced stirring caused by turbulent flow. In contrast, the first ignition point in the mid-flow condition shows a long ring and appears in the lower-left corner of the cylinder, which is far from the center of the chamber.

The combustion images of flame development after ignition under the in-cylinder flow conditions show the appearance of combustion in an intermediate stage, where the reaction starts from the auto-ignition zone formed at the location where the ignition first started. In the case of strong flow, the auto-ignition zone formed at the location where the combustion started first has a smaller auto-ignition zone, and the progress of auto-ignition from this zone is slower. After the burning zone started to develop, we observed that the number of previously burned areas formed in the strong flow was greater than in the medium flow condition, leading to accelerated spontaneous combustion around the previously burned areas. It is hypothesized that the unburned part is more easily ignited because the temperature stratification of the unburned part in the strong flow is smaller, and the initial temperature in the strong flow is higher. However, more detailed experimental and numerical analyses are needed to confirm this hypothesis.

Different levels (intensities) of in-cylinder flow influence the location of the initial ignition nucleus. Under strong flow conditions, the initial ignition invariably occurs near the upper part of the center. However, under medium flow conditions, the first ignition nucleus forms a long strip, consistently appearing at the lower left corner of the cylinder, far from the plate gap.

Figure 3.18 shows the temporal variation of the developed ignited zone area for both flow intensities using graphical processing software. The plot indicates that the combustion time is longer under medium flow conditions, as the burnt zone area increases gradually, and peaks later compared to the strong flow condition.

Base 43℃
-0.66ms~
-0.51ms
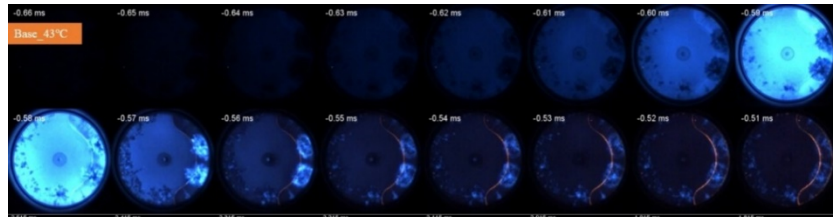
Temp. 43℃
-.515ms~
-0.015ms
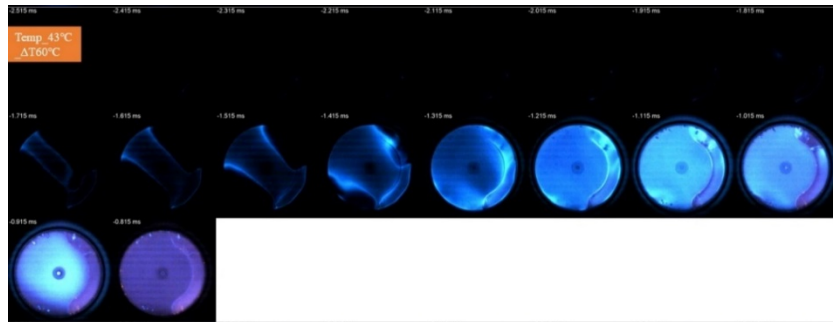
Strong 71℃
-2.81ms~
-0.010ms
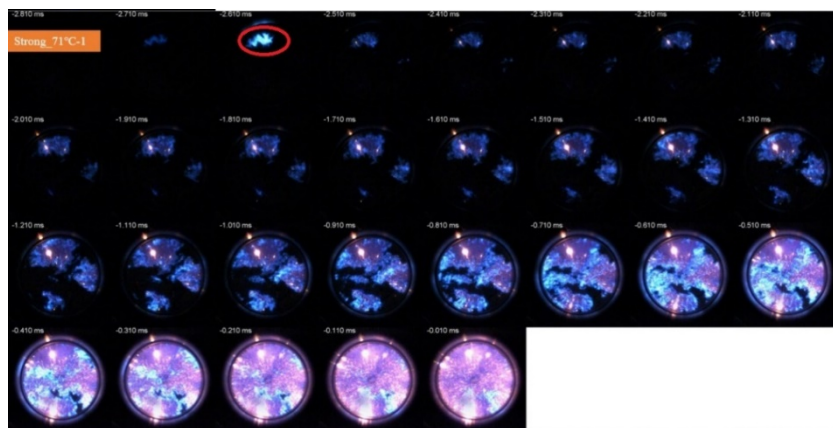
Middle 66℃
-2.645ms~
0.455ms
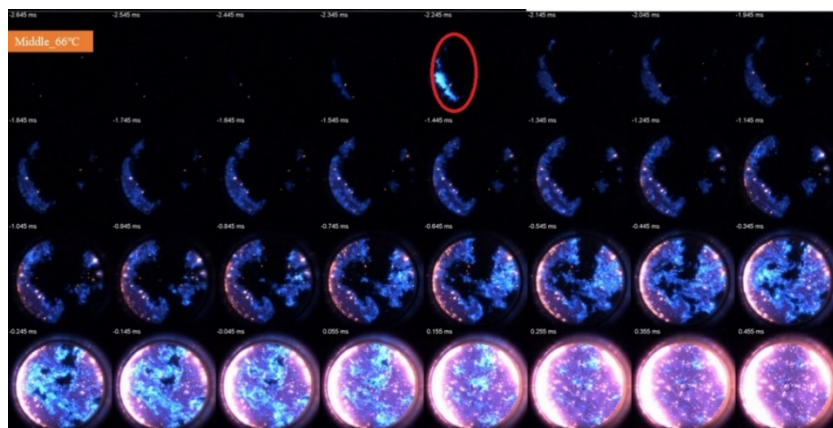
Figure 3.15 Images of combustion phenomenon under each condition
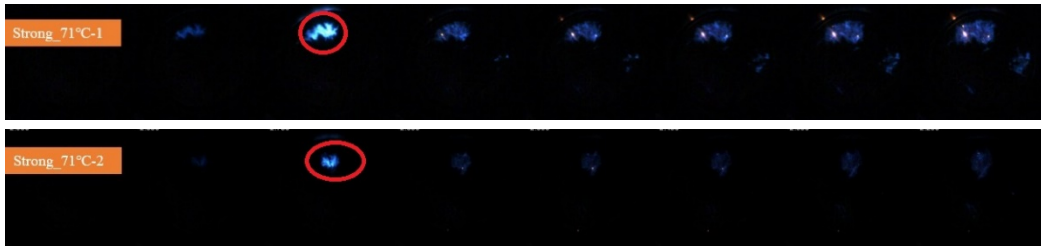
Figure 3.16 The reproducibility of the ignition location for the strong flow cases.
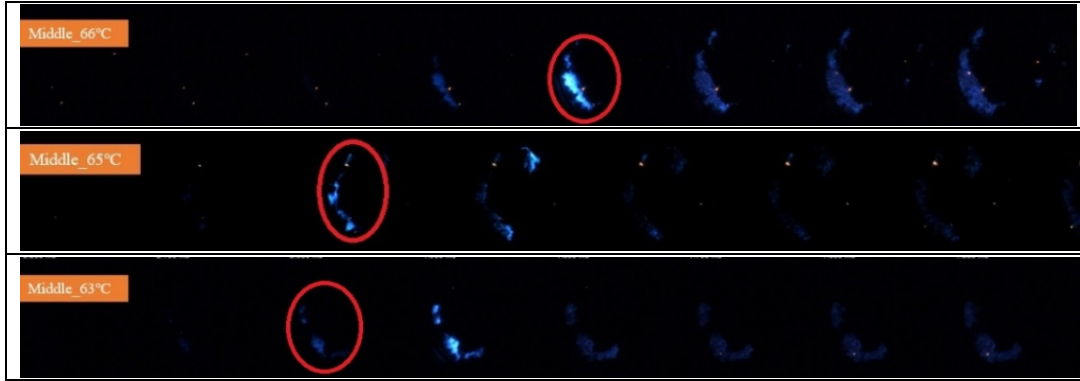
Figure 3.17 The reproducibility of the ignition location for the middle flow cases.
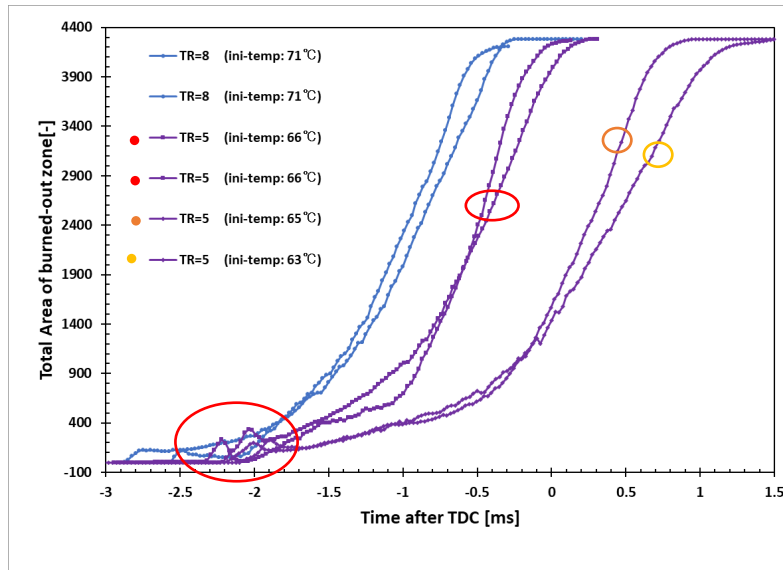
Figure 3.18 Temporal variation of the developed ignited zone area of flow cases

3.6.3 Observation of The Effect of In-Cylinder Flow (tumble) on Auto-Ignition Combustion

To investigate the mechanism of the slow heat release of HCCI combustion by enhanced in-cylinder flow, we conducted a series of visualization experiments using RCEM in order to compare the combustion under each condition. The following sections describe the results of the visualization and the measured waveforms for each observation period, including (1) immediately after ignition, (2) in the middle of combustion, and (3) in the late combustion period, using RCEM.

Figure 3.19 illustrates the appearance of combustion under the no-flow (homogeneous w/o flow) and temperature stratification conditions, as well as the appearance of combustion in stage (1) under the condition that the flow was enhanced. It is observed that combustion without flow (homogeneous w/o flow) results in the shortest combustion time compared to the other cases, with combustion being completed in a very short time. The combustion phenomenon is characterized by a steep pressure increase and heat release, indicating that the entire fuel is ignited simultaneously. In the case of temperature stratification w/o flow, ignition occurs in the lower right corner of the image, corresponding to the high-temperature region, and then proceeds from the lower right to the upper left, from the high-temperature region to the low-temperature region according to the temperature stratification in the cylinder. The combustion zone then spreads from the center of the ignited area to the outer periphery. The combustion time is longer than in the no-flow condition but shorter than in the condition with in-cylinder flow. In stage (1) of the condition with in-cylinder flow, Figure 3.19 shows the formation of ignition nuclei at multiple points in the combustion chamber, resulting in a slower heat release rate and a lower pressure rise rate compared to the condition with no flow in the cylinder. Among the two conditions with enhanced in-cylinder flow, medium flow was found to be more effective in reducing the pressure rise rate. The first ignition point is smaller for the strong flow condition. Since the initial auto-ignition point is considered to be determined by temperature, the scale of the high-temperature zone is smaller due to the stronger agitation

caused by turbulence.

To examine the mechanism of the effect of flow on auto-ignition, we compared the results of the visualization of mid- and late-stage combustion for cases with similar CA50 values for the case with the in-cylinder flow. Figure 3.20 shows photographs of the combustion in stages (2) and (3) under the conditions with in-cylinder flow, as well as the local pressure history and pressure rise rate. The local pressure history and pressure rise rate results show that strong flow slows down the heat release rate. Regarding the appearance of combustion, in the middle stage, the reaction starts from the auto-ignition zone formed in (1). In the case of strong flow, the auto-ignition zone formed in (1) is smaller, and the rate of progress of the auto-ignition starting from this zone is slower. The images of combustion during this period also indicate that the scale of flow is smaller in strong flow. In the late stage of combustion (from 0.5 ms), the number of previously combusted areas formed in strong flow was larger than that in medium flow, and auto-ignition around previously combusted areas was accelerated. It is assumed that the unburned portions are more easily ignited because of the smaller temperature stratification of the unburned portions in strong flow and the higher initial temperature in strong flow. However, more detailed experiments and numerical analysis are needed to confirm this hypothesis.

Figures 3.21 and 3.22 show the variation of reaction zone and combustion images with different levels of in-cylinder flow and without flow case. According to Figures 3.21 and 3.22, compared to the case without flow, when there is in-cylinder flow, ignition occurs dispersively, which leads to slow combustion. Consequently, the pressure rise rate also decreases. One reason could be the impact of temperature distribution caused by the flow. However, the effect of in-cylinder flow on reducing the pressure rise rate of HCCI seems larger than the effect of temperature distribution discussed in Chapter 2. Therefore, there may be other factors that need to be investigated in the future.
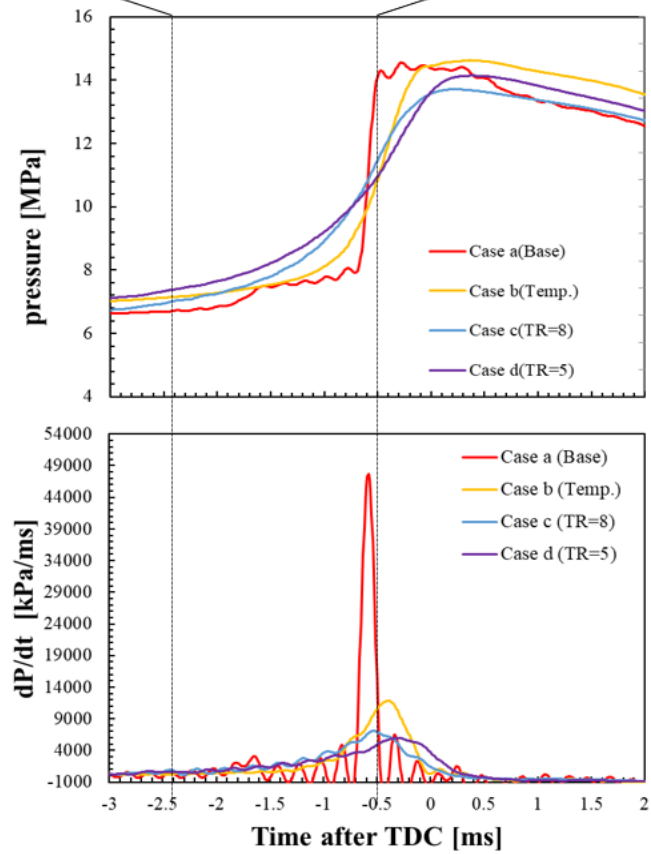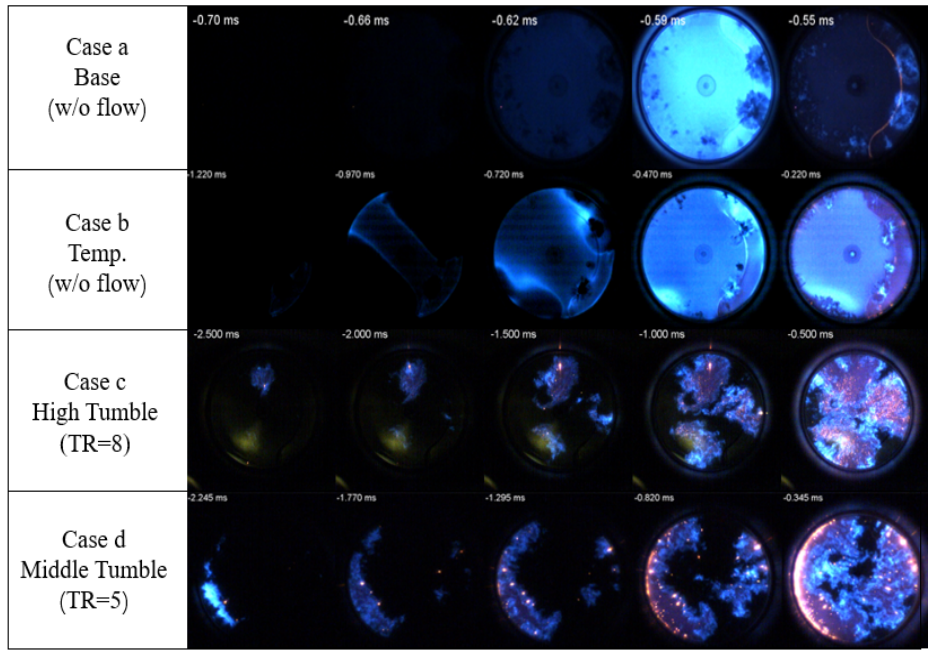
Figure 3.19 Comparison of combustion visualization results under different conditions (stage

1: early-period of combustion
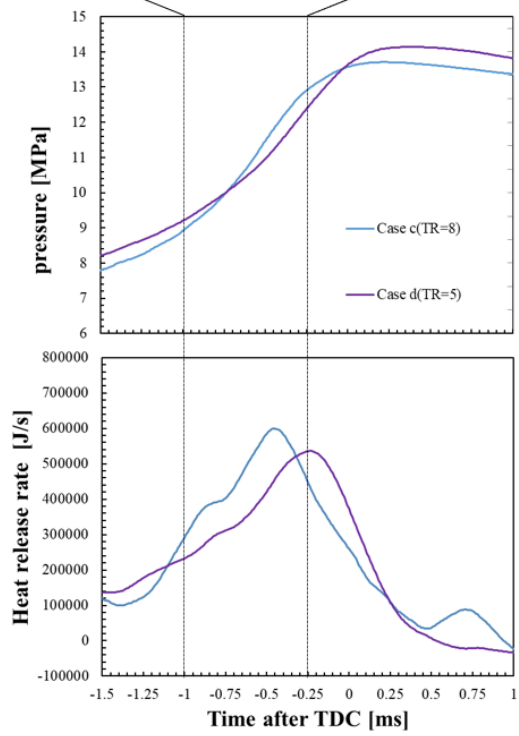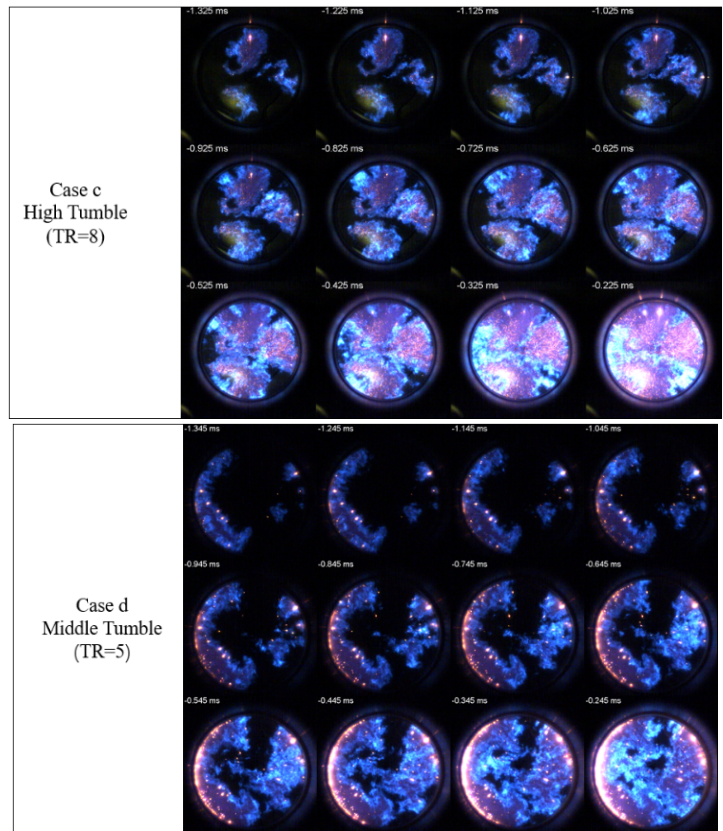
Figure 3.20. Comparison of combustion visualization results under different conditions (stage 2,3)
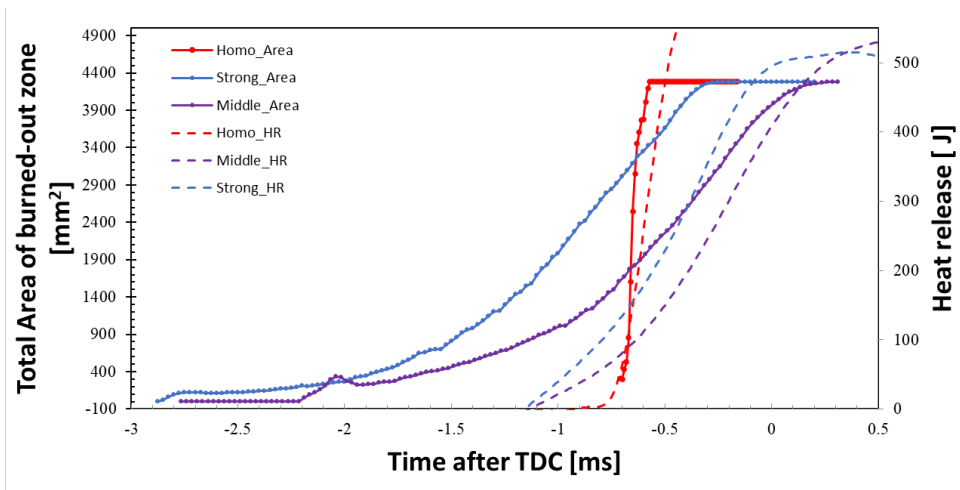
Figure 3.21 Time evolution of the reaction area (burned zone) during combustion.
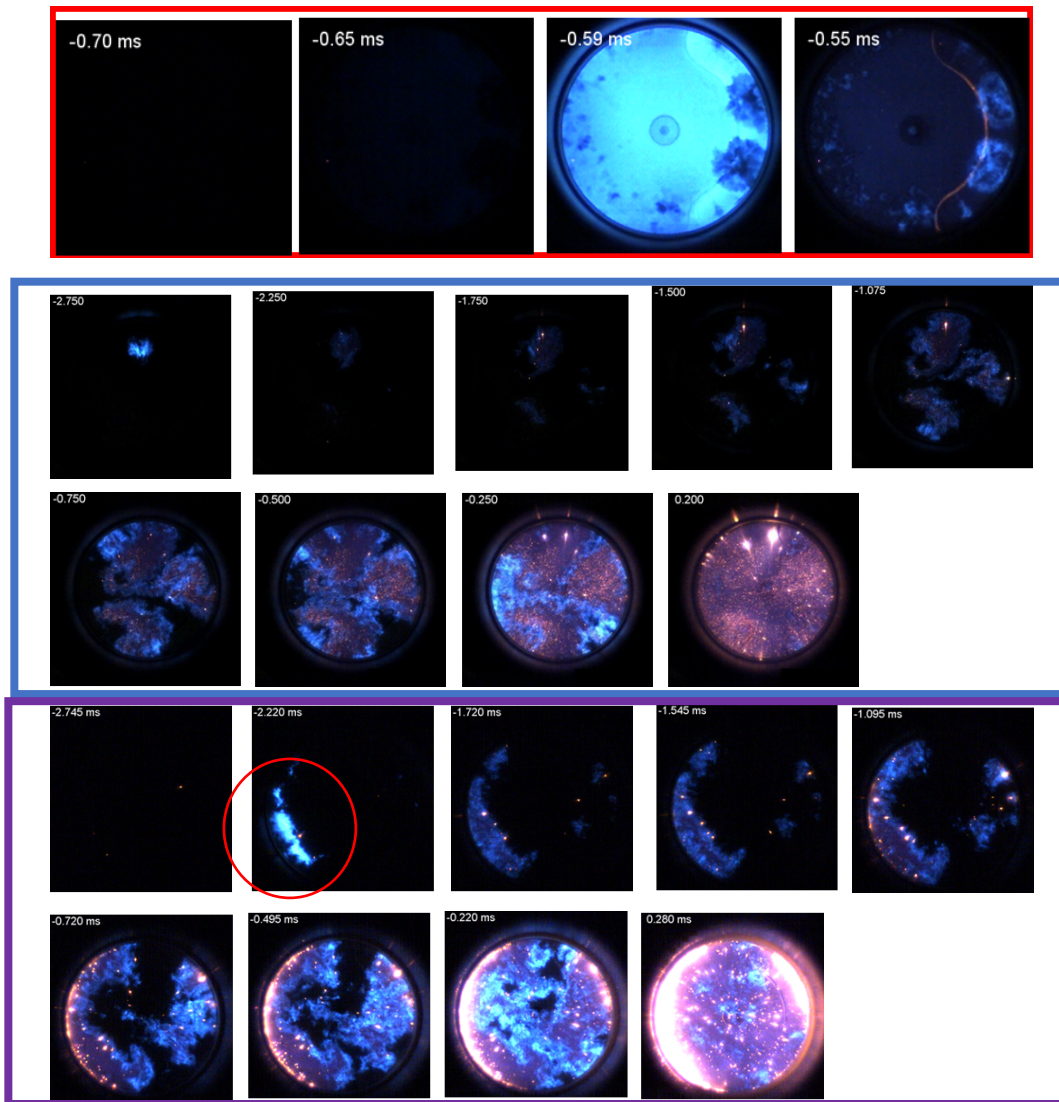
Figure 3.22 Images for with and without in-cylinder cases

3.7 Summary

We constructed an experimental system based on a rapid compression and expansion system capable of generating various patterns of temperature stratification and gas flow in the cylinder. Through combustion analysis and visualization observations, we experimentally investigated the effects of tumble flow on the pressure rise rate of HCCI combustion. The results of the optical experimental investigation of the effects of mixture stratification and in-cylinder flow on HCCI combustion using the rapid compression and expansion system showed that in-cylinder flow can extend the heat release period, reduce the maximum heat release rate, and lower the pressure rise rate. In the range of present experimental conditions, lower in-cylinder flow intensity appears to be more effective in reducing the pressure rise rate. Visualization results of HCCI combustion with enhanced flow confirmed that in the presence of in-cylinder flow, ignition nuclei are formed at multiple points in the combustion chamber, resulting in a slower heat release rate and reduced pressure rise rate compared to the case with no flow in the cylinder. The effect of slowing down the heat release rate and pressure rise rate depends on the strength of the flow and turbulence.

The experimental results can be summarized as follows.

1. In the visualization experiment, we confirmed that the combustion trend with a previous temperature distribution follows a pattern where ignition occurs in the high-temperature region and then expanse toward the low-temperature region.

2. We discovered the potential for an 'extended high load limit of HCCI combustion' due to enhanced in-cylinder flow. Under enhanced in-cylinder flow conditions, ignition points formed at multiple locations within the combustion chamber, prolonging the combustion duration. Simultaneously, the pressure rise rate decreased compared to cases without enhanced in-cylinder flow.

3. The location of ignition initiation points demonstrated good repeatability under different flow conditions. This visualization confirms the feasibility of controlling the ignition onset location through customizing in-cylinder turbulence.

4. The effect of enhanced in-cylinder flow on heat release rate and pressure rise rate varies depending on the intensity of in-cylinder flow. In the present experimental conditions, mid-intensity in-cylinder flow delays the ignition time compared to strong flow conditions. Since the more delayed CA50 resulted in a lower pressure rise rate, this led to a relatively low pressure rise rate, compared to the strong flow.

Reference

[1]. K. Komura, et.al.: "Advanced Ignition Control Technology for HCCI Combustion", Honda R&D Technical Review, vol. 26 No. 2, (2014).

[2]. T. Johansson, et.al.: "HCCI Operating Range in a Turbo-charged Multi Cylinder Engine with VVT and Spray –Guided DI", SAE2009-01-0494 (2009).

[3]. R. Yu, et. al.: "Effect of Temperature Stratification on the Auto-ignition of Lean Ethanol/Air Mixture in HCCI engine", SAE Paper 2008-01-1669.

[4]. M. Sjoberg, et. al.: "Smoothing HCCI Heat Release with Vaporization-Cooling-Induces Thermal Stratification using Ethanol", SAE2011-01-1760. 2. J. E.

[5]. Dec, W. Hwang, et.al.: "An Investigation of Thermal Stratification in HCCI Engines using Chemiluminescence Imaging," SAE Paper 2006-01-1518 (2006).

[6]. K. Saijyo, et. al.: "A Numerical Analysis of the Effect of Mixture Heterogeneity on Combustion in a Premixed Charge Compression Ignition Engine", The international symposium on diagnostics and modeling of combustion in internal combustion engines 2004(6), 239-246, 2004-08-02.

[7]. K. Yoshimura, et. al.: "Studies on the effect of In-cylinder flow on stratified HCCI Combustion", The Japan society of mechanical engineers, (2017).

[8]. K. Yoshimura, et. al.: "Studies on the Effect of In-cylinder Charge Stratifications on High Load HCCI Combustion", SAE2016-32-0010.

[9]. S. Watanabe, et. al.: "The Effect of In-Cylinder Flow and Mixture Distributions on Combustion Characteristics in a HCCI Engine", SAE2017-32-0061.

[10]. Z. Yiwen, et.al.: "Investigation of The Effect of Enhanced In-Cylinder Flow on HCCI Combustion in a Rapid Compression and Expansion Machine", SAE 2019-32-0528

[11]. https://convergecfd.com/

[12]. T. Tsurushima. A new skeletal PRF kinetic model for HCCI combustion. Proceedings of the Combustion Institute, Vol.32 (2009), pp. 2835-2841.

[13]. T. Ishihara. al.: A DNS study of the effects of temperature non-uniformity and turbulence on an auto-ignition process in a homogeneous n-heptane/air mixture. Transactions of the JSME (in Japanese), Vol.80, No.820, (2014).

[14]. HE Xu, WU Yue, MA Xiao, et al. A review of optical diagnostic platforms and techniques applied in internal combustion engines[J]. Journal of Experiments in Fluid Mechanics, 2020, 34(3): 1-52.

[15]. Dec, J. E., & Hwang, W. (2009). Characterizing the Development of Thermal Stratification in an HCCI Engine Using Planar-Imaging Thermometry. SAE International Journal of Engines, 2(1), 421–438. http://www.jstor.org/stable/26308409

Chapter 4 Numerical Simulations (Experimental conditions)

4.1 Introduction

The objective of this chapter is to examine the mechanism of the pressure rise rate reduction by numerical analysis based on the experimental results obtained by RCEM. CONVERGE, a three-dimensional calculation software for thermal-fluid analysis dedicated to engines, was used for the numerical calculations.

4.2 Engine Model

The engine model used for the three-dimensional calculations is shown in Figure 4.1 (the cylinder walls are not shown to emphasize the internal geometry). The geometry model is a cylindrical form that simulates the shape of the combustion chamber of a rapid compression and expansion machine (RCEM), and the actual compression ratio is the one obtained from actual measurements. The piston shape is a simulation of the actual piston up to the upper O-ring, and the piston history is the history of the piston during the motoring experiment of the RCEM. Table 4.1 shows the geometry model parameters.
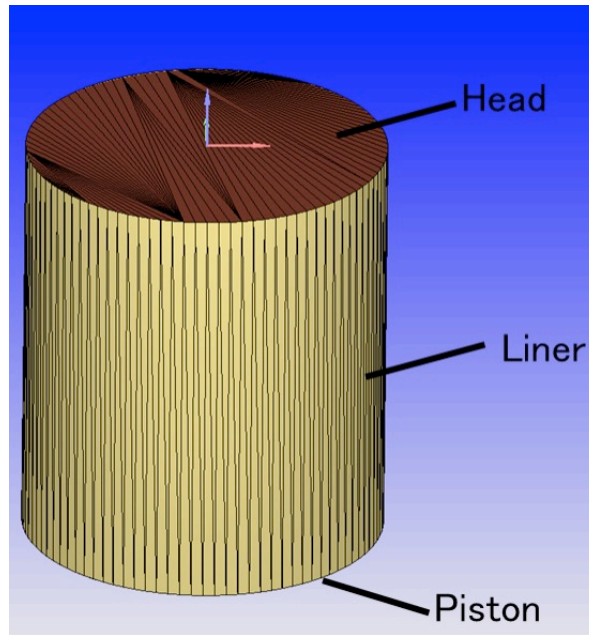
Figure 4.1　Engine model

Table 4.1　Main specification of engine model

Compression cylinder, Bore×Stroke [mm]	73 × 73
Displaced volume [cc]	306 cc
Compression ratio	14.2
Compression chamber configuration	Pancake type
Compression time [ms]	25,33 (Equivalent engine speed are 1200rpm and 900 rpm, respectively)
Base grid size [mm]	0.5

4.3 Numerical calculations for Experimental Conditions

In this study, Large Eddy Simulation (LES) is used to directly solve the unsteady Navier-Stokes equations for flow above the filter threshold to obtain the effect of turbulence on combustion. The software and models used are described in Table 4.2, and Dynamic Structure [15] from the models in CONVERGE is used as the SGS (Sub-Grid Scale) model of LES. The detailed chemical reaction model SAGE was used as the combustion model. PRF90 (isooctane,

n-heptane) was used as the fuel, and a simplified reaction mechanism for PRF (33 chemical species, 38 reactions) [5] proposed by Tsurushima was used as the chemical reaction mechanism for the three-dimensional HCCI combustion simulation.

Table 4.2   Simulation software and Simulation model

Software	CONVERGE
Turbulent model	Dynamic Structure
Wall model	O'Rourke and Amsden
Heat transfer model	Law of wall
Combustion model	SAGE
Reaction mechanism	PRF90 (33species, 38reactions)

4.3.1 Calculation Conditions

The results of the numerical calculations of with and without flows conditions performed for the simulations of the experiments are described. Table 4.3 and 4.4 show the conditions used in the calculations to reproduce the experiment.

Table 4.3 Details of implementation experiments for comparison with past experiments

(Comparison with and without in-cylinder flow, engine speed is equivalent to 1200rpm)

Case name	Without flow	Tumble_Stong
Turbulent flow	-	○
Initial average in-cylinder temperature	Adjusted to set CA50	
Initial in-cylinder pressure	Adjusted with initial in-cylinder temperature to maintain fuel mass	
Compression time	25ms (Equivalent engine speed 1200rpm)	

Table 4.4 Details of implementation experiments for comparison with experiments of Chapter 3 (Comparison different level of in-cylinder flow, engine speed is equivalent to 900rpm)

Case name	Without flow	Strong_flow	Middle_flow
Turbulent flow	-	○	○
Initial average in-cylinder temperature	Adjusted to set CA50		
Initial in-cylinder pressure	Adjusted with initial in-cylinder temperature to maintain fuel mass		
Compression time	33ms (Equivalent engine speed 900rpm)		

4.3.2 Methods of Creating Initial Flow

In the experiment, an initial flow is generated in the RCEM cylinder using a flow generation mechanism. In numerical calculations, this flow generation mechanism is replicated, and calculations are performed to generate an initial tumble flow that simulates the experiment. The method used for the three-dimensional calculation of flow generation is shown in Figure 4.2.

First, as shown in Figure 4.2(a), a combustion chamber shape model (cylindrical shape) and a plate shape model were created. The geometry model is a cylindrical shape that simulates the combustion chamber geometry of a rapid compression and expansion machine (RCEM), and the initial flow is generated by dropping the upper plate. Next, as shown in Figure 4.2(b), numerical calculations were performed by combining the plate and cylinder models and dropping the upper plate to generate an initial flow. The shapes of the piston and plate were the same as those used in the experiment. The speed of the plate's fall was the same as that used in the experiment. The piston and plate geometries are the same as those used in the experiment. The plate drop history was calculated from the spring force values used in the experiment.

Figure 4.3 shows the pathlines of the flow inside the cylinder during the compression process

after the plate falls. Figure 4.3 shows that the pathlines of the vertical vortex centered around the middle of the cylinder are drawn, and it is understood that a tumble flow similar to that inside a real engine cylinder has been generated. The data inside the cylinder after the plate falling calculation was used as the initial condition for subsequent compression and expansion calculations.
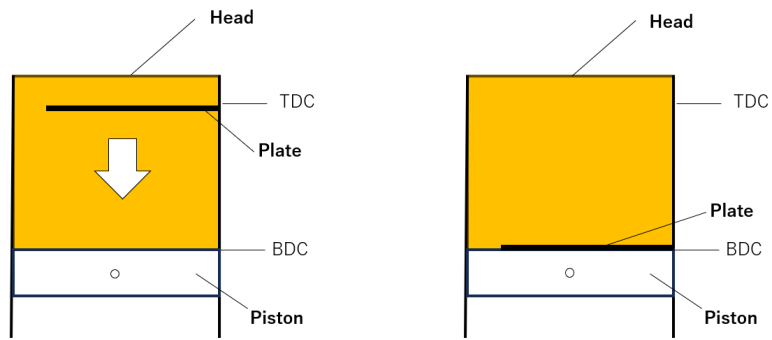
(a) Schematic diagram of the fall of the flow generating plate(Drop the flow generation plate from the TDC position to the BDC)
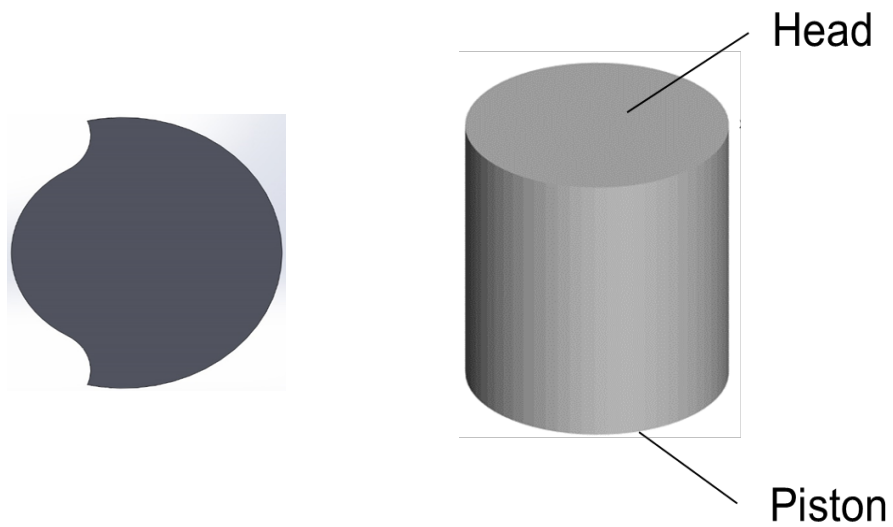
Top view of Geometry model of plate	The geometry model of combustion chamber is a cylindrical shape of RCEM

(b) Create Geometry model for plate and cylinder
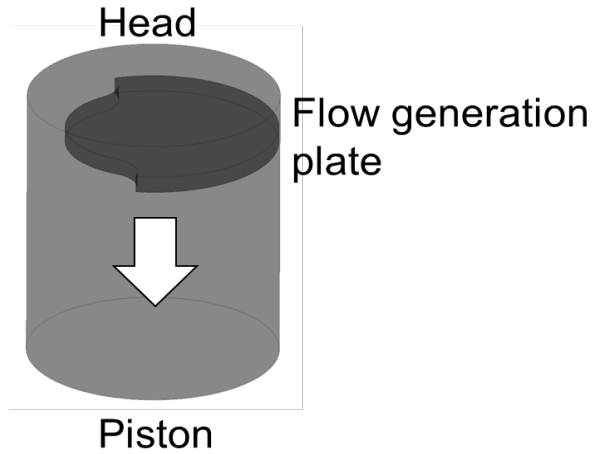
(c) Model of the plate and combustion chamber after assembly

Figure 4.2 Numerical calculations reproduce the same generation of the initial flow in the cylinder as in the experiment. In-cylinder flow is generated with the plate moving downward before compression stroke
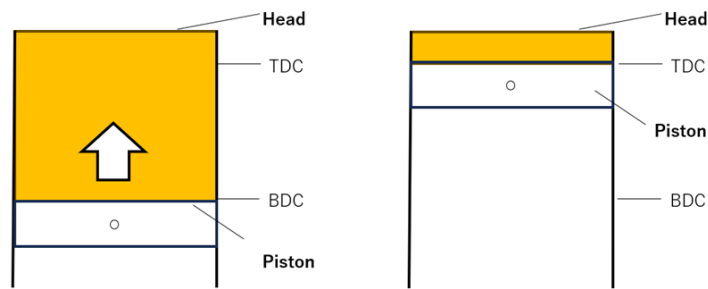
(a) Compression stroke
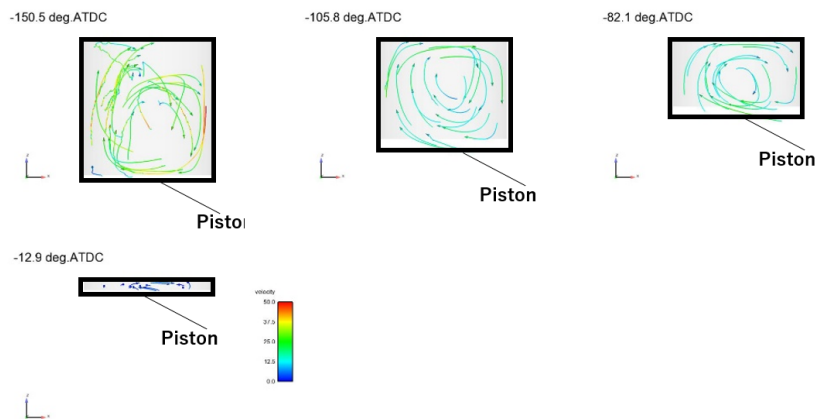
(b) Path lines of in-cylinder flow

Figure 4.3 Compression stroke is performed directly after the plate is dropped and the simulated in-cylinder flow during compression stroke.

4.4 Results and Discussion

4.4.1 Validation of Calculation

The accuracy of the numerical calculations was examined by comparing them with the experimental results. The calculation's compression time is 25ms, equivalent to the speed actual engine at 1200rpm. Table 4.5 shows the initial conditions of the compared cases. The initial conditions are adjusted to regulate the ignition timing. As the original experimental conditions would result in the ignition phenomena before the top dead center, these conditions are not used in the initial conditions for the calculation. Figure 4.4 compares the experimental and computational pressure histories, revealing a good agreement during the compression process. However, the discrepancy between the experimental and calculated results becomes more pronounced after -4 ms. This difference is attributed to the influence of leakage in the RCEM and a pressure increase caused by the effect of heat release in the calculation.

Table 4.5 Compared case.

Case name	Withour flow_Exp	Without flow_Simulation
Initial temperature [K]	325	320
CA50 [ms]	1.5	1.6
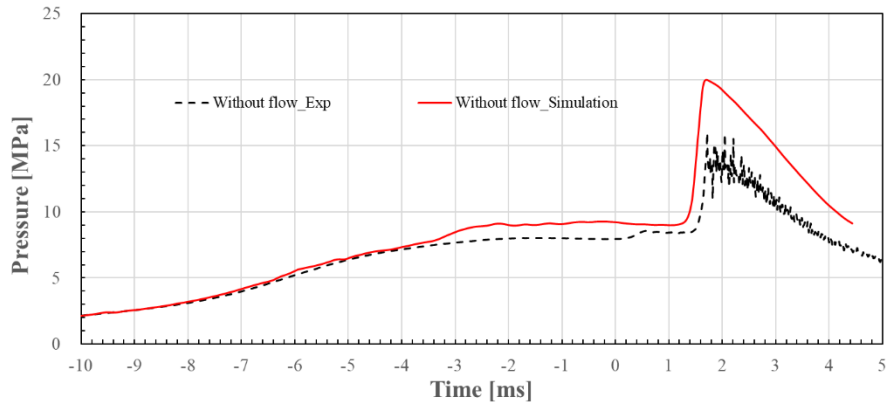
(a) Pressure history
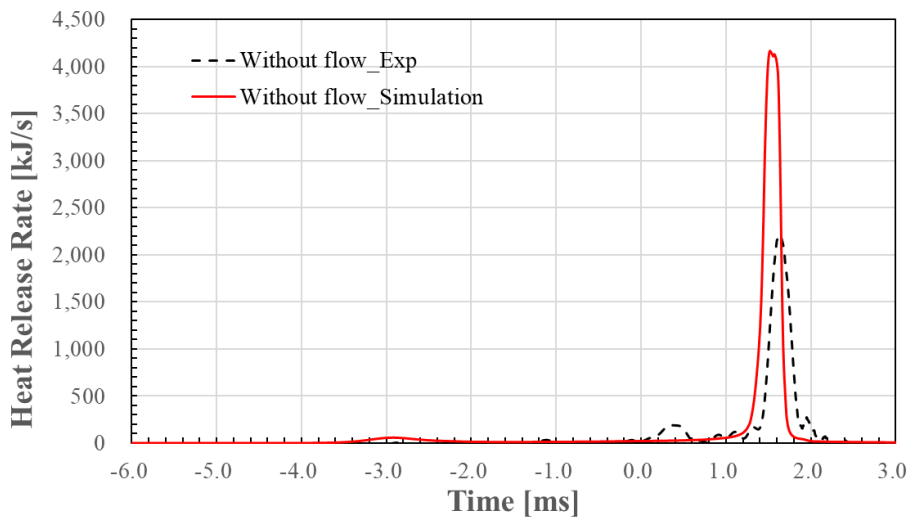
(b) Heat release rate

Figure 4.4 The pressure history and HRR of the experimental and numerical results were compared to validate the accuracy of the numerical calculations.

4.4.2 Effect of In-Cylinder Flow on HCCI Combustion

Comparison was made directly between with flow (strong flow) and without flow. The results of the numerical calculations of the strong and medium flow flows performed for the simulations of the experiments are described. First, the combustion duration (CA10-90) for the combustion phase (CA50) with and without in-cylinder flow is shown in Figure 4.5, both for experimental results (Without flow_exp, Tumble_exp) and simulation results (Without flow_simulation, Tumble_simulation). As seen in Figure 4.5, the combustion duration (CA10-90) in the Tumble_Simulation is longer than Without flow_simulation, which is consistent with the trend in the flow field in the experiments.
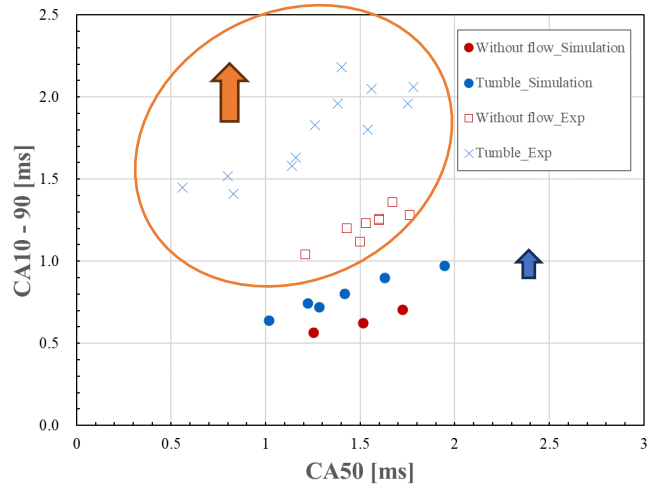
Figure 4.5　dP╱dt_Max，CA10-90 for CA50

Figure 4.6 shows that in (b) Tumble (Strong) case, compared to (a) Without　flow　case, heat release starts gradually around 0.5[ms] after heat production from the low-temperature oxidation reaction. Figure 4.7 illustrates the temperature distribution of the in-cylinder mixture before the reaction begins for cases with the flow (strong flow) and without flow. Furthermore, from Figure 4.8, it can be confirmed that combustion is spreading from the high-temperature areas. From this, it can be inferred that the combustion duration (CA10-90) was extended because the timing of the fuel's auto-ignition varied spatially due to the temperature distribution created by the flow. Figure 4.8 also confirms that combustion is spreading from the high-temperature regions. Therefore, it can be considered that the combustion duration (CA10-90) increased due to the spatial variability in the timing of auto-ignition caused by the temperature distribution resulting from the flow, which is examined in the optical experiment as shown in Figure 4.9.
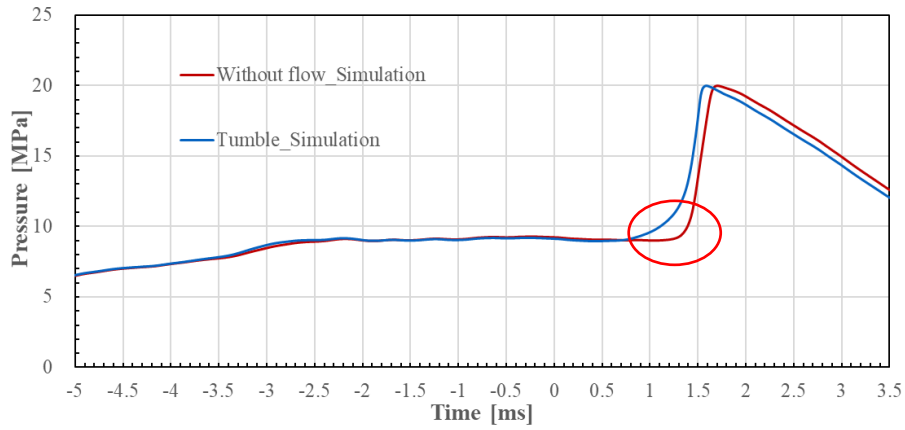
(a) Pressure
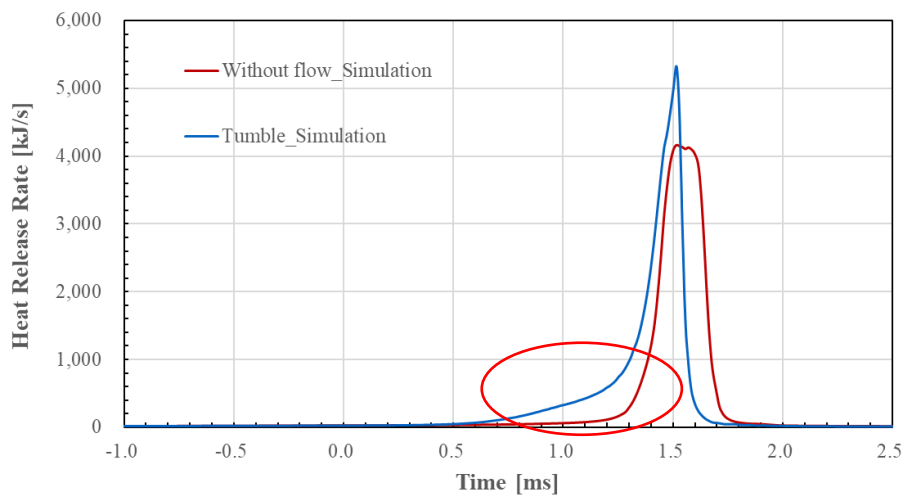
(b) Heat release rate

Figure 4.6 Simulation results
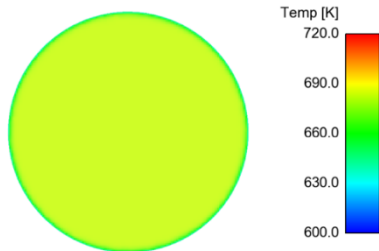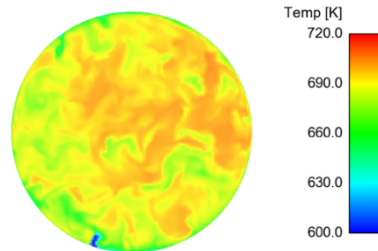
(a) Without flow 　 (b) Tumble (Strong)

Figure 4.7 Temperature distribution before beginning of reaction
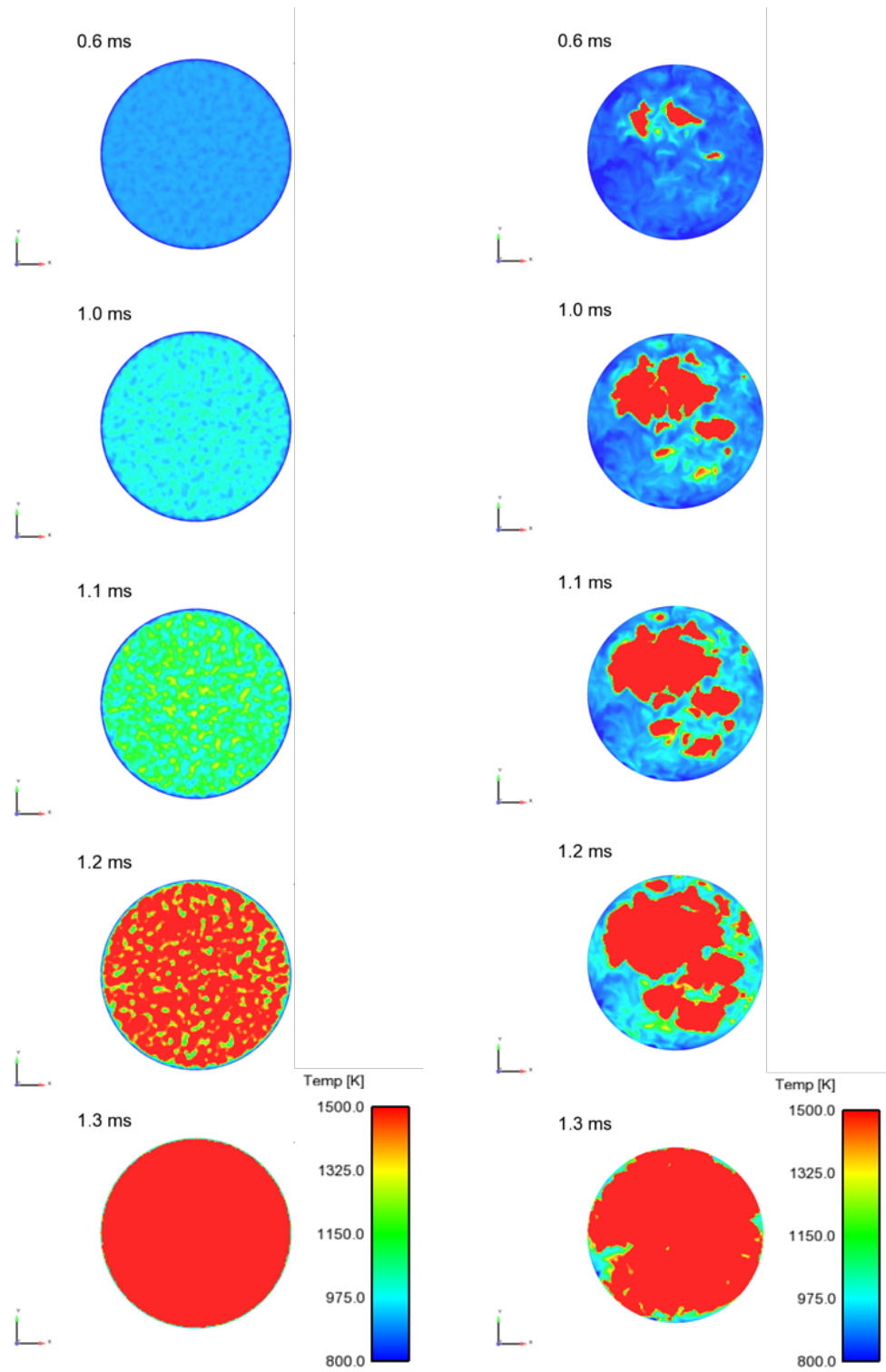
(a) Without flow   (b) Tumble (Strong)

Figure 4.8   Temperature distribution of with flow (strong flow) and without flow case

Without flow   Tumble (Strong)

Figure 4.9   Combustion process of with and without flow case

4.4.3 Effect of Different Levels of In-Cylinder Flow on HCCI Combustion

The results of the numerical calculations are depicted in the simulated flow field for the conditions of the experiments in Chapter 3.

Table 4.6 Compered cases

Case name	Without flow	Strong_flow	Middle_flow
Equivalent raio	0.75		
Fuel mass [mg]	35.8		
Initial mean temperature [K]	326.4 324.15	344.15 341.15	344.15 341.15
Initial pressure [kPa]	Adjusted with initial in-cylinder temperature to maintain fuel mass		

The results of the numerical calculations are depicted in the simulated flow field for the conditions of the experiments in Chapter 3. First, Figure 4.10 shows the pressure rise rate (dP⁄dt) and the combustion period (CA10-90) versus the combustion phase (CA50) for each calculated case. Although the rate of pressure increase (dP⁄dt) for the case with flow is not the highest this is not consistent with the experimental results. However, the combustion phase (CA10-90) is longer for all conditions in the presence of flow, which is consistent with the experimental trend in the flow field.   This means that the experimental results are not fully replicated but have the agreement with the experimental results.
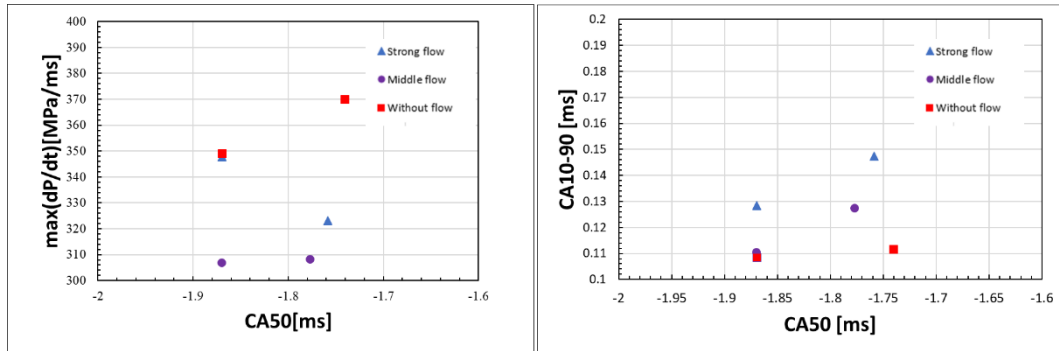
Figure 4.10 dP∕dt_max，CA10-90 for CA50

The next step is to compare the closely related CA50 values under each condition. Figure 4.11 displays the pressure rise rate. The results from Figure 4.11 indicate that not only the strong flow condition shows slower combustion before the main combustion begins (as indicated by the circled section in the figure) and a lower pressure rise rate, but also in the middle flow case. This is consistent with the experimental results. To analyze the cause of the slowed combustion speed and the reduced pressure rise rate, a temperature difference is defined in this study as the difference between the average temperature of the highest temperature region and that of the second region. The second region refers to the second lowest temperature region when the temperature frequency distribution of the in-cylinder mixture is divided into five equal-mass regions from the lowest temperature side. Figure 4.12 shows the temperature frequency distribution of the in-cylinder mixture before the reaction begins under each condition, while Figure 4.13 displays the impact of the cylinder temperature difference on the pressure rise rate change, as well as the definition diagram of the temperature difference. Figure 4.13（b） shows that in Base(without flow), the temperature distribution is somewhat formed by heat loss, and the temperature difference is around 5 [K]. On the other hand, in turbulence cases, a tumble is formed, and the initial temperature is almost the same as that of the Base case, and the temperature difference is 18[K] for medium flow case and 16[K] for strong flow case.

From the numerical results above, it can be said that not only strong flow, but also medium flow conditions are effective in slowing HCCI combustion and reducing the pressure rise rate. Moreover, the temperature difference formed by the medium flow is 1[K] larger than that of the strong flow. The larger temperature difference leads to a longer combustion period and a lower pressure rise rate.

The effects of flow were investigated in visualization experiments. Compared to no flow, flow results in a more dispersed ignition and, consequently, a different appearance of combustion. The pressure rise rate is accordingly reduced. One reason for this is the effect of temperature stratification due to flow. However, from the results of figure 4.14, shows that the effect of in-cylinder flow on pressure rise reduction appears to be greater than the effect of temperature stratification discussed in Chapter 2. Therefore, there may be other factors contributing to the effect of flow. To illustrate the above, a comparison of the reaction zones with and without different levels of flow has been added to the image processing, shown in figure 4.15.

Numerical calculations were also conducted to investigate the causes of the lower pressure rise rate when the flow is added. A figure for dP/dt with ΔT (pressure rise rate against temperature difference) has been added to the numerical calculations section still. One of the causes is the temperature stratification created by the flow. As shown in Figure 4.16, the distribution of CH_2O during low-temperature oxidation. Another factor from turbulence is the influence of the local distribution of the dominant chemical, leading to a lower pressure rise rate and longer burn times.
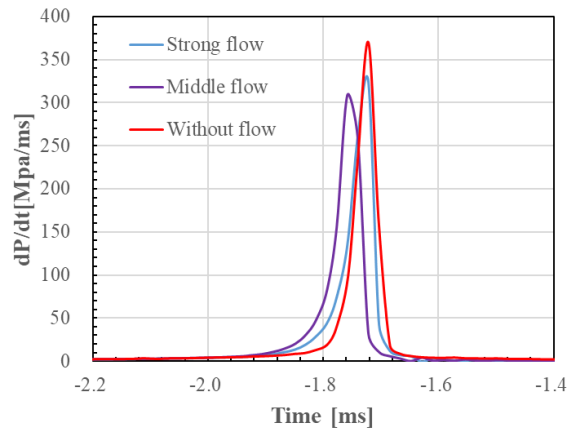
Figure 4.11 Pressure rise rate
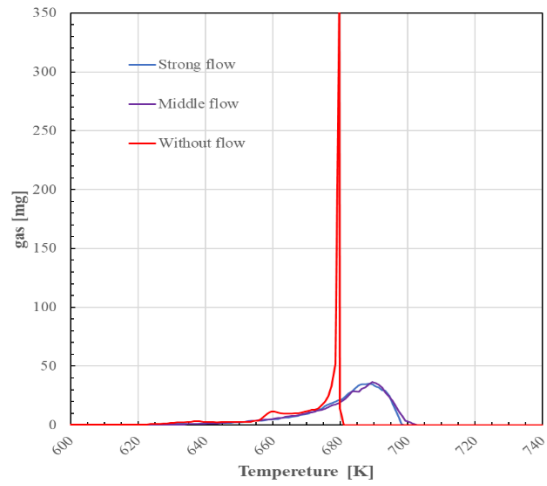
Figure 4.12 Temperature frequency distribution before beginning of reaction.
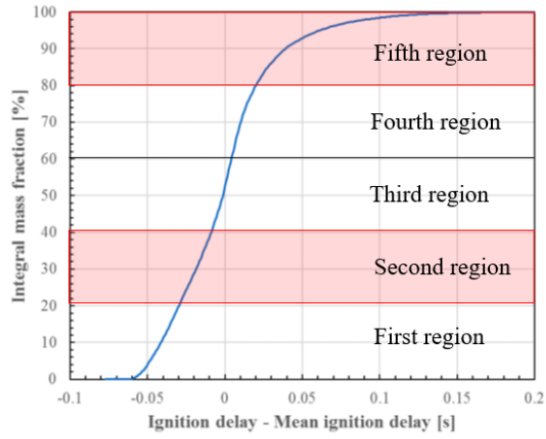
(a) Definition of five regions
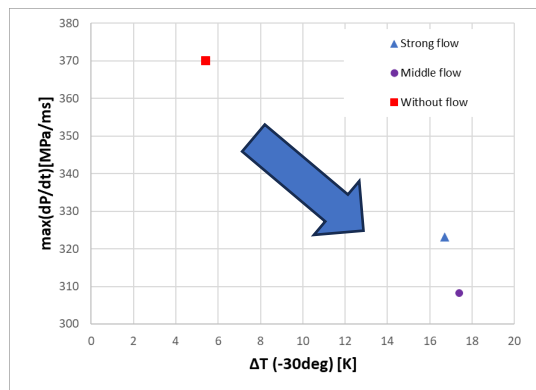
(b) Temperature difference before beginning of reaction.

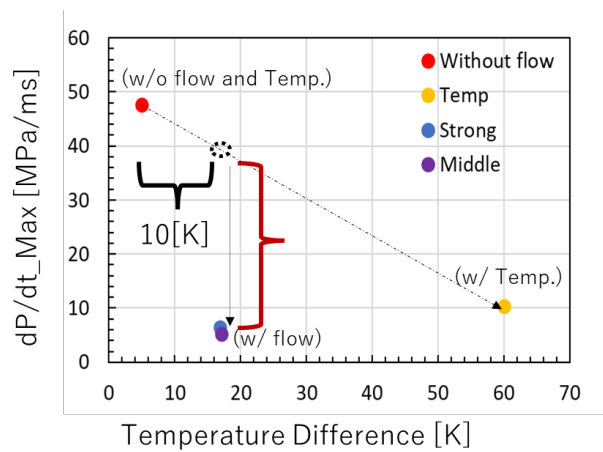Figure 4.13 Effect of temperature difference on pressure rise rate variation

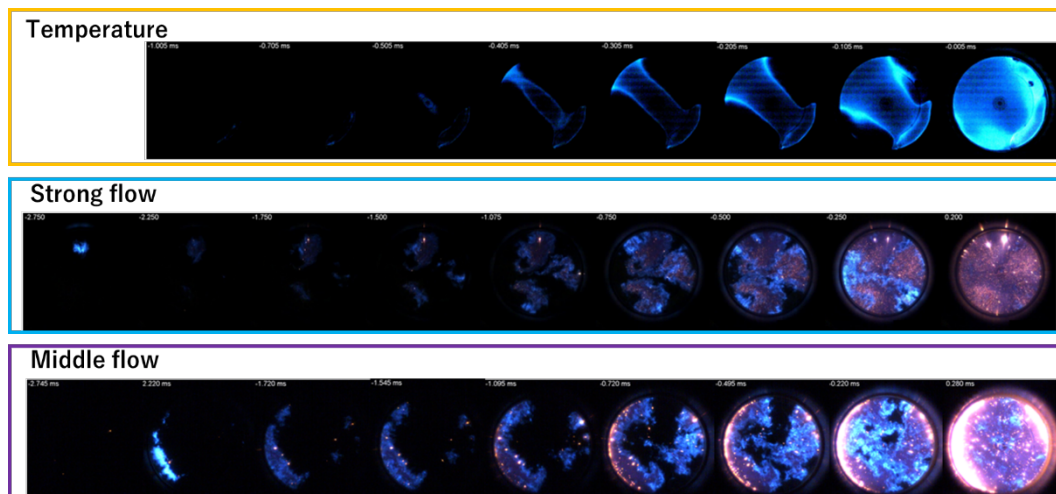Figure 4.14 Effect of in-cylinder flow (tumble) on pressure rise rate.

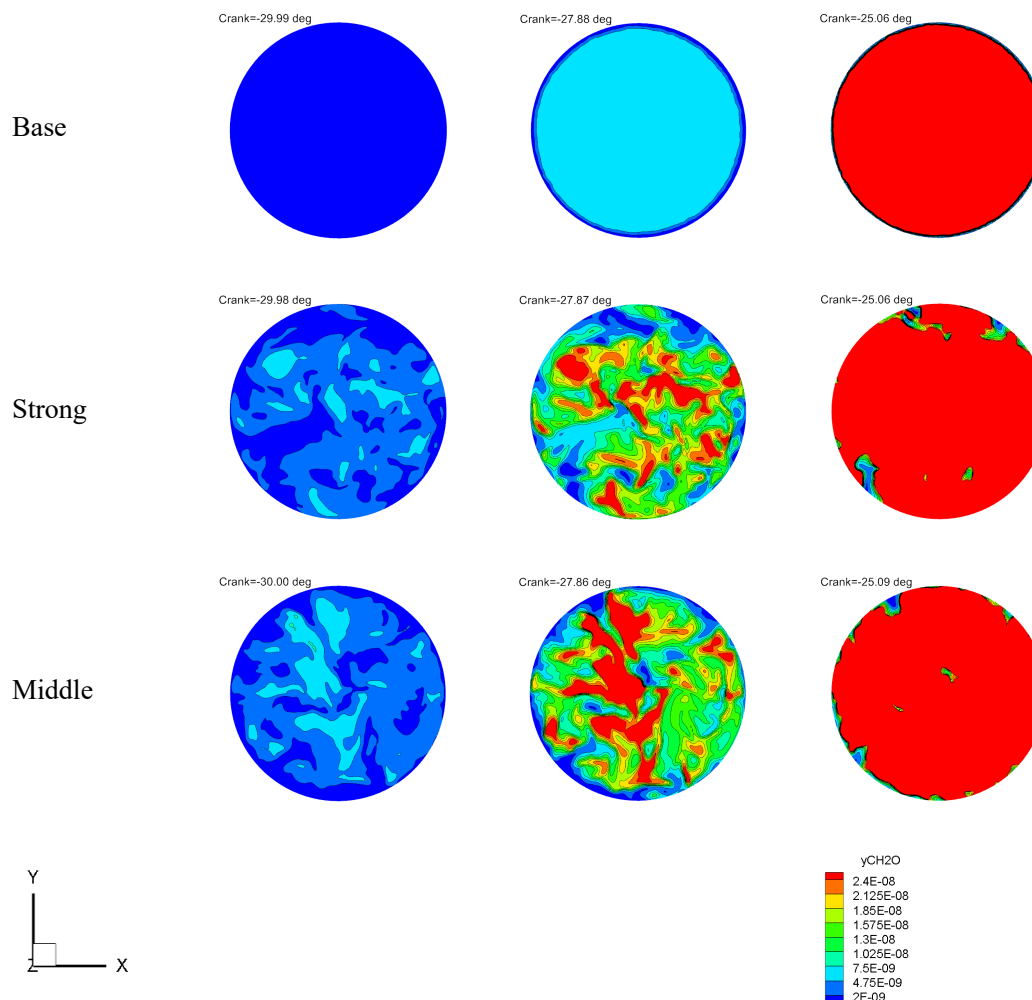Figure 4.15 The differences of combustion performance of temperature case and with in-cylinder flow cases.

Figure 4.16 The Distribution of CH2O during low-temperature oxidation

4.5 Summary

In the numerical analysis simulating the experimental conditions, the same method as in the experiment was reproduced to generate the initial flow and combustion calculations were performed.

The findings obtained in this chapter and the conclusions are presented below.

1. The numerical results shows that combustion duration and initial heat release as well as the pressure reduction effect under enhanced flow conditions showed the same trends in simulation results, which has consistent trend with experimental results.

2. Combining the optical results in Chapter 3 with the numerical calculations in Chapter 4 shows that the in-cylinder flow leads to a more dispersed ignition and, thus, to a different combustion appearance than the case without flow. This is due to the wider initial temperature distribution and greater temperature differences created by in-cylinder flow.

3. Enhanced in-cylinder flow also affects the local distribution of key chemical species, which leads to lower pressure rise rate and longer combustion. And excessive flow may have negative effects. The stirring effect of the strong flow leads to a greater dispersion of the active radicals.

Reference

https://convergecfd.com/

[1]. T. Tsurushima. A new skeletal PRF kinetic model for HCCI combustion. Proceedings of the Combustion Institute, Vol.32 (2009), pp. 2835-2841.

[2]. T. Ishihara. al.: A DNS study of the effects of temperature non-uniformity and turbulence on an auto-ignition process in a homogeneous n-heptane/air mixture. Transactions of the JSME (in Japanese), Vol.80, No.820, (2014).

[3]. K. Saijyo, K. Nishiwaki et al. A Numerical Prediction Method for the Auto-Ignition Process in a Homogeneous Charge Compression Ignition Engine. SAE 2003-01-1818

[4]. M. Hunzinger, S. Merkel et al. Turbulent Flame Propagation with Cold Walls during Lean Combustion in SI-Engines. SAE 2005-01-0238

[5]. Watanabe Y. et al., Evaluation of Homogeneous Charge Compression Ignition at High Engine Speeds using a Super Rapid Compression Machine, SAE paper 2008-01-2403

[6]. Katsumata M. et al., Behavior of Shock Wave and Pressure Wave of SI Knocking with Super Rapid Compression Machine, JSAE: 20119310

[7]. Hasegawa T et al. Characteristics of HCCI Combustion in Homogenized Temperature Fields using a Super Rapid compression Machine. JSAE 20119334

[8]. Robert S et al., On the High Load Limit of Boosted Gasoline HCCI Engine Operating in NVO Mode. SAE 2010-010162

[9]. Hibi T et al. Study on Knocking Intensity under In-Cylinder Flow Field in SI Engines Using a Rapid Compression Machine. Journal of Thermal Science and Technology, Vol.8, No.3, 2013, pp.460-475

[10]. S. G. Chumakov et al., Dynamic structure subgrid-scale models for large eddy simulation. INTERNATIONAL JOURNAL FOR NUMERICAL METHODS IN FLUIDS Int. J. Numer. Meth. Fluids 2005; 47:911–923

[11]. Shunsuke et al., Improvement of Thermal Efficiency in a Gasoline HCCI Engine with Blow-down Supercharge System by Increasing Compression Ratio, PhD thesis, Department of Population and Systems Science, Graduate School of Engineering, Chiba University, 2013.

[12]. Ushida et al., Suppression of Knocking in a SI engine by fuel and temperature stratification of mixture inside cylinder, Master's thesis, Department of Population and Systems Science, Graduate School of Engineering, Chiba University, 2012.

[13]. Takeyuki Kamimoto et al., Transactions of the Japan Society of Mechanical Engineers, The Japan Society of Mechanical Engineer, (Vol. B) 53, No. 492, Paper No. 86-0541A

[14]. Yasuhiro Okura et al., Analysis of In-Cylinder Flow for a Boosted GDI Engine Using High Speed Particle Image Velocimetry, Proceedings of The Society of Automotive Engineers of Japan, Vol.46 No.1(2015) 20154023 pp.27-33.

[15]. Takashi ISHIHARA et al., A DNS study of the effects of temperature non-uniformity and turbulence on an auto-ignition process in a homogeneous n-heptane/air mixture, Proceedings of

The Japan Society of Mechanical Engineer,Vol. 80, No. 820, Paper No. 14-00176

[16]. Watanabe et al.   The effects of in-cylinder flow and stratification on HCCI combustion characteristics, Master's thesis, Department of Population and Systems Science, Graduate School of Engineering, Chiba University, 2018.

Chapter 5 Conclusions and Future Works

5.1 Conclusions

In this study, we constructed an experimental system that can generate various temperature distributions and airflow patterns in the cylinder (based on a fast compression expansion device). The combustion process, ignition mechanism, and pressure rise rate of HCCI with normal no-flow and no temperature distribution condition, with temperature distribution only condition and with different in-cylinder flow (three different turbulence intensities) are investigated through a series of experiments and direct visualization conducted on this RCEM. This paper also combined with CFD numerical simulations to verify the results of enhanced in-cylinder flow on extending the HCCI combustion time, reducing the pressure rise rate, etc.

Numerical analysis simulating the experiment reproduced the experimental results and investigated the effect of in-cylinder flow on reducing the pressure rise rate and prolonging the HCCI combustion period.

The following are the findings obtained in this study and the conclusions of this paper.

1. This research examined the impact of varying turbulence levels on HCCI combustion using a newly developed rapid compression expansion method. It found that in-cylinder turbulence generated by the flow generation plate significantly mitigates pressure oscillations and decreases the combustion pressure rise rate, suggesting a potential method for extending the high load limit of HCCI combustion through in-cylinder flow enhancement. Moreover, increasing the in-cylinder flow, irrespective of its intensity, reduced the pressure rise rate, similar to the temperature stratification case from previous research. Interestingly, lower flow intensities in the in-cylinder flow field had a more pronounced effect on reducing the pressure increase rate within the scope of this study.

2. Visualization experiments confirmed that combustion trends with temperature distribution follow a pattern where ignition begins in the high-temperature region and subsequently spreads toward the low-temperature region. Enhancing in-cylinder flow, as evidenced by direct

photography, results in multiple ignition points in the combustion chamber, reduce the heat release rate, and suppresses the increase in the pressure rise rate. Different levels of in-cylinder flow significantly influence the location of the initial ignition nucleus. Medium-intensity in-cylinder flow also delays ignition time compared to strong flow conditions, which, coupled with the more delayed CA50, results in a lower pressure rise rate. Consequently, this leads to a relatively lower pressure rise rate than strong flow conditions.

3. The numerical analysis reproduces the experimental trends. The combustion duration and initial heat generation showed the same trends as the experiments. From the results obtained, it was concluded that one of the reasons for the reduced pressure rise rate was the temperature distribution caused by the flow.

4. One reason of the effect of in-cylinder flow on reduction of pressure rise is the temperature distribution due to the in-cylinder flow (according to the numerical calculation results). Another factor of the effect of in-cylinder flow on reduction of pressure rise was identified. It is the local distribution of key chemical species caused by the enhanced in-cylinder flow.

5.2 Future Works

This paper investigates the effect of tumbling flow on the rise rate of HCCI combustion through combustion analysis and visual observation, as well as numerical, experimental, and computational calculations. Combining the visualization results in Chapter 3 with the numerical calculations in Chapter 4 shows that the in-cylinder flow leads to a more dispersed ignition and thus to a different combustion appearance compared to the case without flow. The pressure rise rate is correspondingly reduced. One reason for this is the effect of the temperature distribution due to the in-cylinder flow (according to the numerical calculation results). The effect of in-cylinder flow on reducing pressure rise rate, however, seems to be greater than the effect of temperature distribution discussed in chapter 2. Therefore, there may be other factors that need to be confirmed in future experiments as well as in numerical calculations.

However, further research work is needed in the following areas:

Visual observation of HCCI combustion at in-cylinder flow intensity (Infrared self-luminescence shooting and PIV)

To compare how well the actual in-cylinder temperature distribution agrees with the calculated results and experimental extraction of characteristic parameters of turbulent flow.

Experimental and numerical analysis of combustion when using fuels with different ignition characteristics.

To get more detailed study of the mechanism of HCCI combustion retardation under bespoke tumble flow.

Appendix Information About the In-Cylinder Flow Generation Mechanism

1. Meaning of In-Cylinder Flow -Tumble

As a flow within the cylinder, the axial swirling flow known as "tumble" is used in petrol engines. As Figure 1.1 indicates, tumble is charging rotation about an axis orthogonal to the cylinder axis. Tumble is generated by straightening the intake port and increasing the air flowing in from the top of the intake port. Some manufacturers, even fit a tumble control valve inside the intake port. Essentially, the tumble can be adjusted by optimizing the shape of the intake port.

The tumble flow is crucial to the combustion process in spark-ignition engines. The primary goal of this process is to mix the air and fuel more efficiently to achieve better combustion and, subsequently, higher engine efficiency. Overall, the tumble flow increases the homogeneity of the air-fuel mixture, improves combustion efficiency, and reduces emissions. These are all crucial factors for an engine's performance and environmental impact [1].
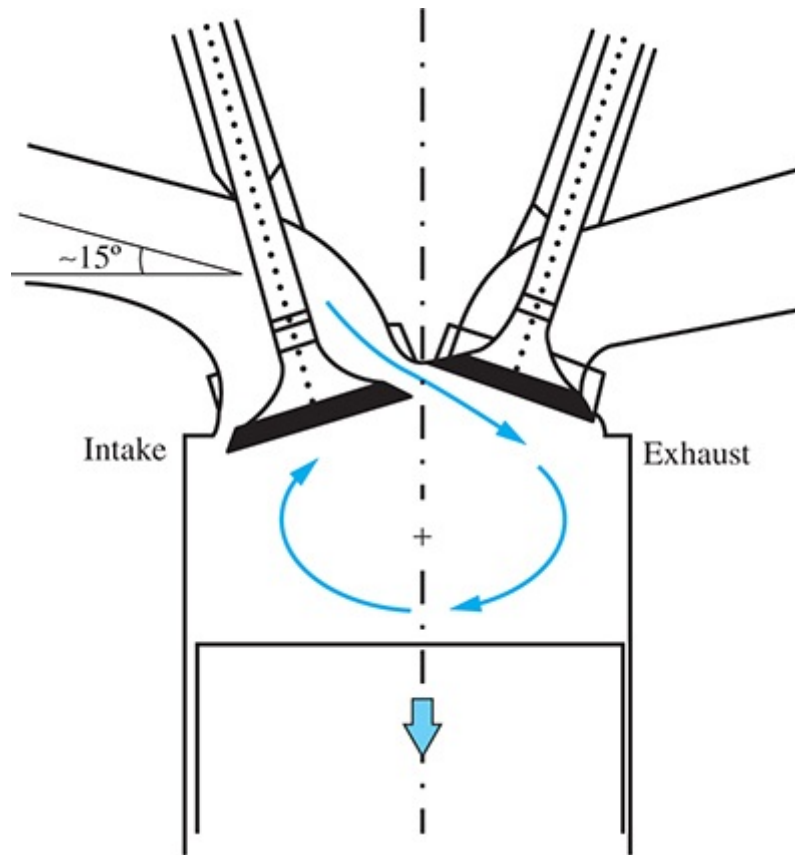
Figure 1.1 Schematic showing how the intake ports and valves (in a four-valveper-cylinder

engine), and piston motion down the cylinder, generate tumble.[1]

2 The Idea of Achieving Tumbling Flow in RCEM

An in-cylinder tumble flow formation system that can be implemented in the RCEM is needed. A literature survey was conducted with this aim. The idea of a turbulence generator, documented in [2], was suitable for this study. By additionally integrating a turbulence generator, it's possible to create a defined turbulence field in the combustion chamber of an RCM.

2.1 Introduction to The Methods of The Turbulence Generation

The turbulence generator is integrated into the main piston, as shown in Figure 2.1, and is composed of a turbulence generator plate and a ground plate, which is located on the top of the piston. At the beginning of the experiment, the turbulence generator is hauled through the

combustion chamber with a defined velocity, so that the air-fuel mixture flows through the holes of the turbulence generator plate. The structure of the turbulent field can be adjusted by changing the turbulence generator plate.
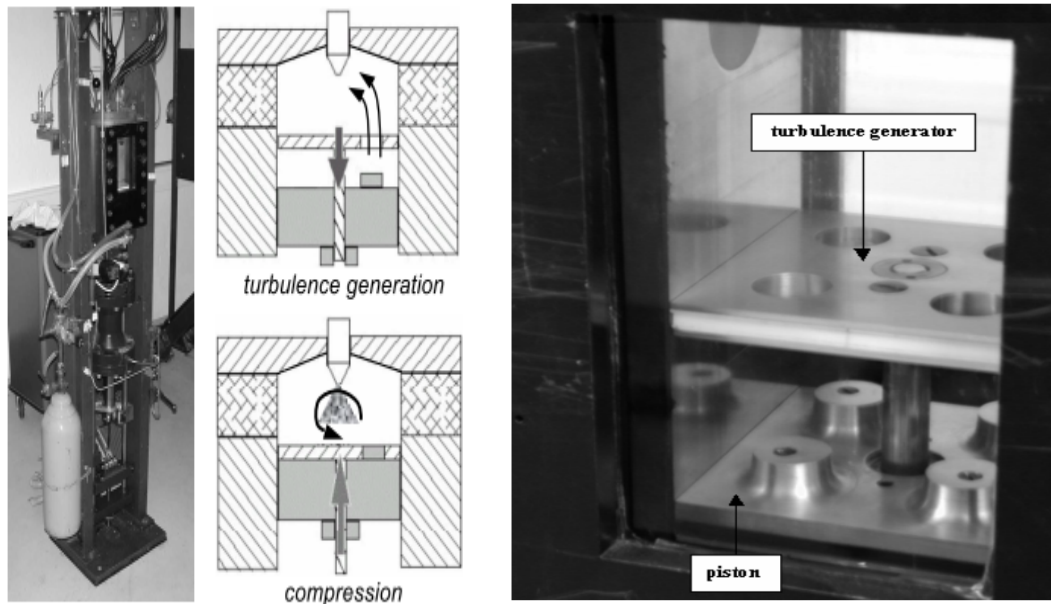
Figure 2.1 The rapid compression machine and Turbulence generator (TG) and piston [2]

3.2 Method of Generating Flow by In-Cylinder Flow Generation Plate in RCEM

The in-cylinder tumble flow is generated by pulling down from the top of the cylinder to the piston, using the method described in '[2]'. The concept diagram is shown in figure 2.2.A plate is placed inside the cylinder, and the compressed mixture passes through a hole in the plate to generate flow.
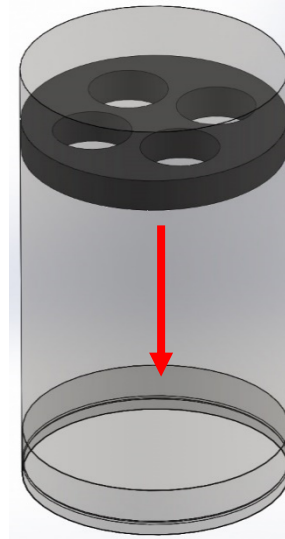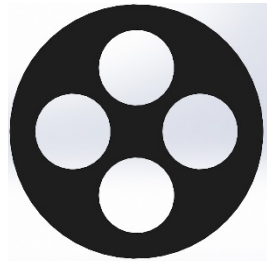
Figure 2.2 A plate with holes is dropped above the cylinder to generate flow before compression stoke.

3. Numerical Analysis of Flow Generation Plate Design

During the design of the RCEM, computational studies were carried out to determine feasible experimental conditions for the in-cylinder flow generated by the flat-type plate. The numerical analysis was conducted using CONVERGE, a thermal fluid analysis software developed specifically for engine applications.

3.1. Calculation Conditions

The engine model used was a cylindrical geometry simulating the combustion chamber geometry of the RCEM. The analysis conditions are shown in Table 3.1. Considering the analysis time, the RANS RNG k-ε turbulence model was used; Table 3.2 summarizes the various constants of the RNG k-ε model.

Table 3.1 Calculation conditions

Turbulent model	RANS RNG k-ε
Wall model	O'Rourke and Amsden
Heat transfer model	Law of wall
Chemical reaction solver	SAGE
Fuel	PRF90
Reaction mechanism	33 species, 38 reactions
Compression time	25 ms (Equivalent engine speed is 1200 rpm)
Base grid size	1.0 mm
Equivalent ratio [-]	0.5
Fuel mass [mg]	17.1
Initial average in-cylinder temperature	Adjusted to set CA50
Initial in-cylinder pressure	Adjusted with initial in-cylinder temperature to maintain fuel mass

Table 3.2 RNGk-ε Turbulence model constant

C_μ	0.845
$c_{\varepsilon 1}$	1.42
$c_{\varepsilon 2}$	1.68
$c_{\varepsilon 3}$	0.381
$1/Pr_k$	1.39
$1/Pr_\varepsilon$	1.39
B	0.012
η_0	4.38

3.2 Numerical study of in-cylinder flow generation plate

The idea of using a flow-generating plate to produce flow by dropping it inside the RCEM combustion chamber was investigated through numerical simulations of the flow variations resulting from different flat plate bore geometries. The geometry file for the plate drop is shown in Figure 3.1, where the plate was placed inside a cylinder representing the simulated RCEM combustion chamber. The plate geometry used in the study is depicted in Figure 3.2. Three types of plates were utilized: (a), (b), and (c). The geometry file for plate (a) was designed to approximate the shape of an actual engine inlet. The shapefiles were created for plates (b) and (c)

to generate tumble flow by positioning the hole on one side. The falling time and displacement of the plate were assumed to be approximately 12 ms, considering the external forces generated by the spring set in the extension piston. The displacements obtained from the plate equations of motion and elastic forces were used. Once the map data of the simulated flow (e.g., the flow inside the cylinder after the plate drop) is obtained, it is mapped to a geometry file simulating the RCEM combustion chamber geometry. Subsequently, the compression and expansion processes of the piston are calculated to determine the flow formed inside the cylinder.
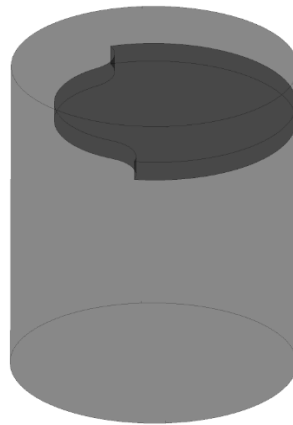
Figure 3.1 Surface model for plate fall calculation

(a)　　　　　　　　　　(b)　　　　　　　　　　(c)
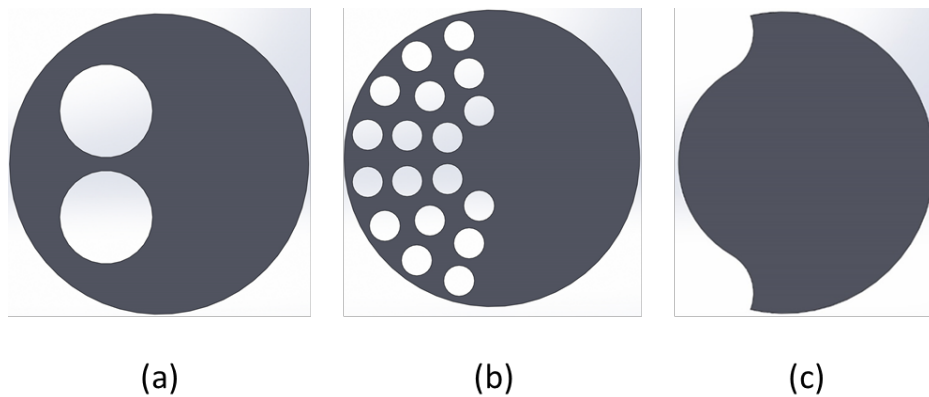
Figure 3.2 Plate shape

Figure 3.3 depicts the path lines and velocity distribution of the flow inside the cylinder during the compression-expansion process, following the calculation of the plate fall process. Figure 1.4 presents the Turbulence kinetic energy produced by each plate during the same process. Upon examining the trajectory lines for each case in Fig. 1.3, it is evident that the flow generated by plate (a) follows a complex trajectory line and fails to form a tumbling flow.

Conversely, the flow generated by plates (b) and (c) showcases a longitudinal vortex trajectory line centered at the cylinder's core. This pattern suggests the generation of a tumbling flow similar to that in an actual engine cylinder. Additionally, the flow distribution within the cylinder confirms that plate (a) does not generate a tumbling flow, while plates (b) and (c) do at -16.7 ms.ATDC, the in-cylinder mixture velocity for the flow produced by plate (a) is less than 12.5 m/s, whereas the flows produced by plates (b) and (c) maintain a velocity of 25 m/s. The turbulence in both cases is at -8.4 ms.ATDC. As per the turbulent energy presented in Figure 2.19, the turbulent energy in case (a) decays rapidly and monotonically, while in the other two cases, the energy decays more slowly and increases around -7.5 ms.ATDC due to the tumbling flow collapsing from compression.

According to the aforementioned calculations, plates (b) and (c) are capable of maintaining the flow during the compression process. Considering that the gaps in the plate section are filled by the piston crown after the plate descends, plate (c) was selected due to its ease of machining during production.
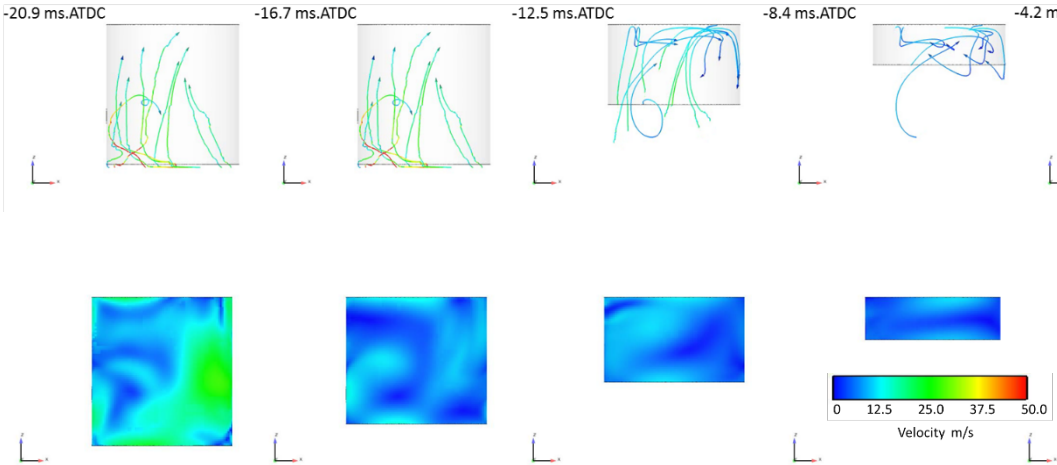
(a)
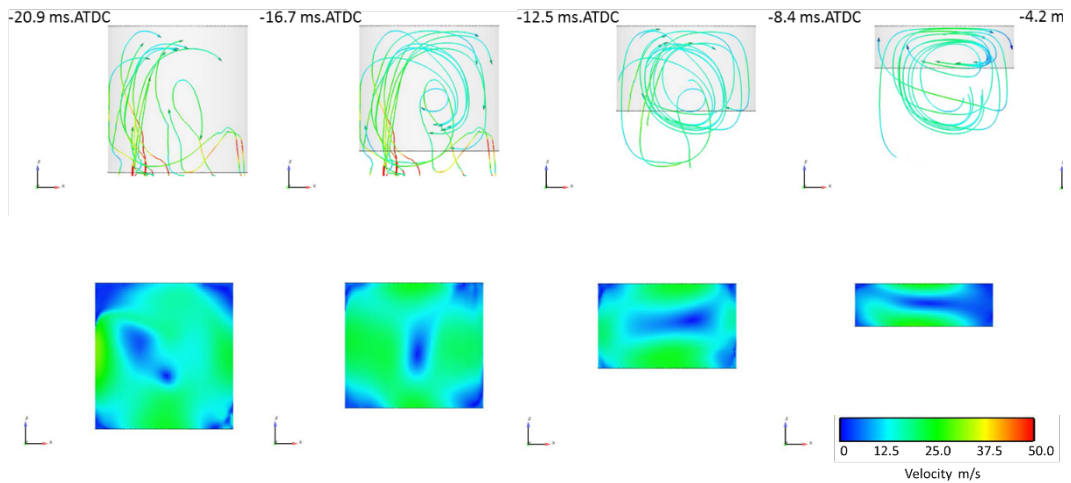
(b)
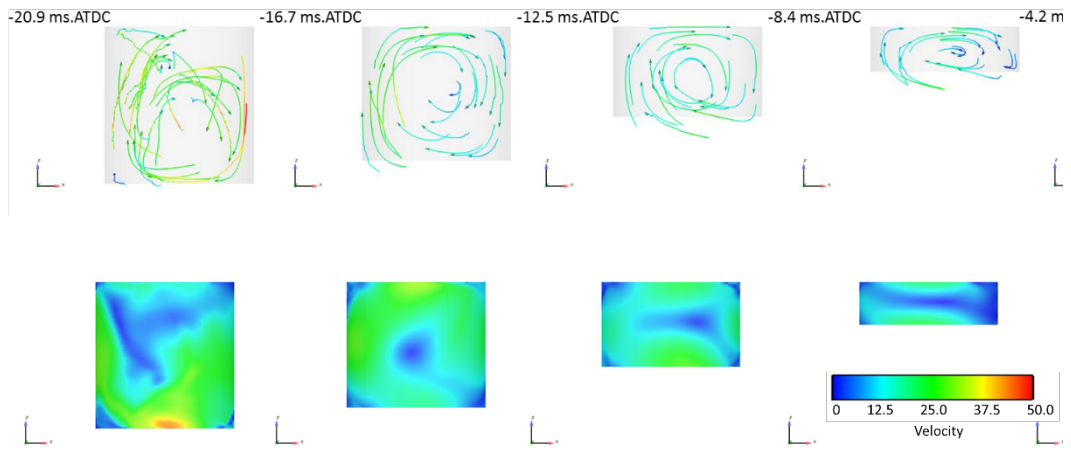
(c)

Figure 3.3 Pathline and flow speed of In-cylinder flow
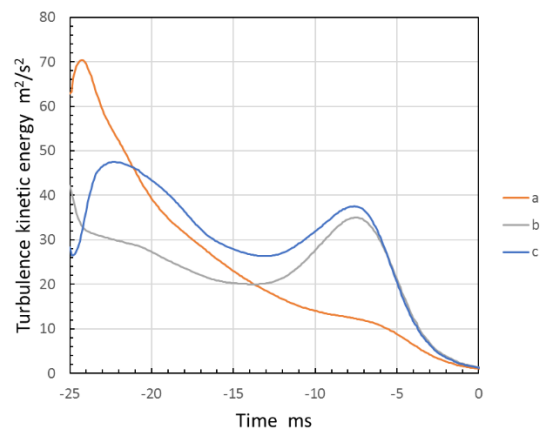
Figure 3.4 Turbulence kinetic energy of plate flow

Reference

[1] Heywood, J. B. (2018). Internal Combustion Engine Fundamentals. Internal Combustion Engine Fundamentals Second Edition.

[2]. Hunzinger, M., Merkel, S., Nauwerck, A., Velji, A. et al., "Turbulent Flame Propagation with Cold Walls during Lean Combustion in SI-Engines," SAE Technical Paper 2005-01-0238, 2005, https://doi.org/10.4271/2005-01-0238.

ACKNOWLEDGEMENT